Neural Biosensor Probes for Simultaneous Electrophysiological Recordings, Neurochemical Measurements, and Drug Delivery with High Spatial and Temporal Resolution

by

Matthew Donivan Gibson

A dissertation submitted in partial fulfillment
of the requirements for the degree of
Doctor of Philosophy
(Biomedical Engineering)
in The University of Michigan
2011

Doctoral Committee:

Professor Daryl R. Kipke, Chair
Professor Robert T. Kennedy
Professor Ralph Lydic
Assistant Professor Parag G. Patil
Assistant Professor William C. Stacey

For my family–my wife Kirsten, and my children Eden, Samuel, Claire, and Owen–who provide endless support and love in all our journeys, including this one.

ACKNOWLEDGEMENTS

More than any other aspect of my education, I value the people that I have been privileged to work with. I have been fortunate to have my path intersect with amazing, brilliant, and supportive people who have enable me to achieve more than I could on my own. I hesitate to name specific individuals for fear of forgetting others, but I feel a need to express my gratitude, and apologize if I inadvertently miss the names of others.

I would like to thank my advisor, Daryl Kipke. Daryl has been encouraging, supportive, and patient. More than projects, Daryl cares about people. He has always encouraged me to pursue my own personal path to success. Together we have weathered storms, developed mutual understanding, and made meaningful progress in research.

I have appreciated the help of other faculty members, particularly my committee. Bob Kennedy has been extremely supportive with a level of excitement for my work that nearly matched my own. I have appreciated his technical expertise, which he willingly offered as I tried to understand and apply principles of electrochemistry, biosensors, and neurochemistry. Ralph Lydic provided tremendous encouragement throughout my work. He helped me to think about and plan experiments, and allowed me to spend time in his lab to learn experimental techniques. I have appreciated working with Parag Patil, who offered insights into meaningful clinical applications. Bill Stacey willingly listened to explanations of my research progress, read my work, and provided meaningful feedback on my work. I would also like to thank Martin

Sarter, who offered critical insights to aspects of this research and allowed me to observe work in his lab.

Aileen Huang-Saad has been an extremely important and influential mentor. Aileen is a trailblazer who helped me to pursue excellence with relentless passion. Her impact is immeasurable. Thank you.

I have greatly appreciated being a member of the Neural Engineering Laboratory. There have been so many people who have helped me. Matt Johnson was my primary lab mentor. He provided the essential foundation that enabled me to pursue my research. John Seymour has been a true friend, with whom I could share and develop ideas. I have also developed a deep friendship with Paras Patel. Paras has a never ending willingness to help. He gives much more than he receives. I have appreciated his encouragement, assistance, sharing of ideas, discussions, and friendship. Kip Ludwig has always been willing to listen to ideas, offer assistance, share wisdom, and provide feedback. Nick Langhals has helped tremendously with thinking about ideas and applications, and has provided significant assistance in experimental setup and data analysis. He has answered my desperate mid-experiment phone calls on numerous occasions. I am very grateful for the assistance and encouragement of Karen Schroeder. From day one, Karen has proven to be exceptionally capable. She provided critical assistance to my work that enabled us to make rapid progress. Takashi Kozai and I entered the lab together. He has been an admirable colleague, and I have appreciated our work together, discussions, and friendship. Many thanks to other members of the lab over these years, including Erin Purcell, Azadeh Yazdan, Hirak Parikh, Eugene Daneshvar, Usha Ramkrishna, Mohammad Abidian, Tim Marzullo, Greg Gage, Pratik Rohatgi, Jey Subbaroyan, Rachel Miriani, Taegyun Moon, and Karen Coulter.

I would also like to thank my undergraduate advisor, Sterling Sudweeks. I am grateful that Sterling let me work in his lab, even though I had no experience or

training. He encouraged, taught, and inspired me. He was patient through my mistakes. My experience in his lab proved to be the most important aspect of my undergraduate education.

Most of all I would like to thank my family. My parents, Chester and Vicki Gibson, provided me with a foundation in life that I could build upon. They taught me to work hard, be persistent, expand my abilities, strive for excellence, and be my best. They have been loving and supportive. I will forever owe them more than I can possibly return.

I am particularly grateful to my wife, Kirsten, and to my children, Eden, Samuel, Claire, and Owen. They have endured this difficult journey patiently and lovingly. They have sacrificed time, energy, and effort. In return, they have given hugs, kisses, love, and smiles. Truly, there is no place like home. Most of all, I owe the world to Kirsten. She has been immensely supportive and loving. She has exceeded all that has been asked of her, set aside personal gratification, and made this whole process possible. I love you. Thank you so much.

TABLE OF CONTENTS

LIST OF FIGURES

Figure

LIST OF TABLES

Table

ABSTRACT

Neural Biosensor Probes for Simultaneous Electrophysiological Recordings, Neurochemical Measurements, and Drug Delivery with High Spatial and Temporal Resolution

by

Matthew Donivan Gibson

Chair: Daryl R. Kipke

The aim of this work is to develop and validate novel neural biosensor probes for simultaneous electrophysiological and neurochemical measurements with precise, localized drug delivery. This technology has been developed to interface with the complex environment of the brain for more advanced experimental investigations at the intersections of neurophysiology, neuropathology, and neuropharmacology. The validation experiments have been conducted using relevant *in vivo* testbeds as a foundation for future work to more fully understand and treat neurological disorders.

Chapter II presents a multimodal probe that enables concurrent detection of choline, recording of electrophysiology, and localized drug delivery. Central to this work is the development of selective electrodeposition methods for enzyme immobilization and polymerization on individual microelectrode sites that more closely approach the scale of neurons than currently reported neural biosensors.

Multiple neurotransmitter systems are implicated in the pathophysiology of schizophrenia, Alzheimer's disease, Parkinson's disease, and other neurological disorders, yet the direct relationships remain unclear. The ability to simultaneously monitor multiple

chemical signals concurrently with electrophysiology and integrated pharmacological manipulation can serve as a useful tool to further these investigations. Chapter III further extends the probe capabilities to include glutamate sensing concurrent with choline sensing, electrophysiology recordings, and drug delivery.

Electrochemical biosensors are commonly used to record neurotransmitter dynamics, yet there remains no standard calibration media or procedure. Differences in calibration procedures can impact reported performance making the interpretation of *in vivo* difficult. Chapter IV aims to improve our ability to interpret *in vivo* neurochemical recordings by investigating the influence of calibration media on performance characteristics of amperometric biosensors.

Bridging the electrophysiological and neurochemical domains with sufficient fidelity, resolution, sensitivity, and selectivity can provide novel insights into neurophysiology that lead to improved therapeutic approaches for treating neurological disorders.

CHAPTER I

Introduction

The brain is one of the most complex and remarkable systems known to mankind. It consists of an estimated 100 billion neurons, each with hundreds to thousands of synaptic connections to other neurons (Damasio, 2001). The cortex alone has 20 billion neurons with 1.5×10^{14} synapses (Pakkenberg and Gundersen, 1997; Pakkenberg et al., 2003). The brain interacts with other physiological systems through a myriad of electrical pulses, neurotransmitters, hormones, proteins, and dynamic interconnections. With its central role in physiology, the brain has been the focus of scientific research for many centuries. Yet due to its inherent complexity, our understanding of neurophysiology and our ability to treat neurological disorders has remained limited. In many ways, the brain remains the final frontier of human physiology. Debilitating and costly disorders such as Alzheimer's disease, Parkinson's disease, schizophrenia, depression, and multiple sclerosis remain prevalent throughout society.

The past century, and particularly the past several decades, have witnessed remarkable developments in neural interfaces from novel neuroscience tools to promising clinical treatments. One of the most significant challenges in neuroscience technology is to bridge the electrophysiological and neurochemical domains with sufficient fidelity, resolution, sensitivity, and selectivity to enable thorough investigation of the complex interplay between chemical signals and electrical signals, and their resulting

influence on memory, perception, sensation, and behavior. Various methods provide insight to individual components of these signals, yet few tools exist for simultaneously recording neurochemical and electrophysiological activity with high spatial and temporal resolution. The ability to simultaneously integrate multiple neurophysiological signals is an unmet need that can strengthen the current investigational and therapeutic strategies for neuropathologies.

The work embodied in this dissertation aims to further expand upon this growing toolset through the development and validation of high density neural biosensor arrays that enable simultaneous monitoring of choline, glutamate, and electrophysiology combined with localized drug delivery. Multi-modal neural biosensor probes will enable more advanced experimental investigations at the intersections of neurophysiology, neuropathology, and neuropharmacology through the integration of these fundamental neural signals.

1.1 Fundamentals of Neurophysiology

Neurons are the fundamental unit of the nervous system. The connections between neurons form marvelous networks that provide the human body with all its function. Since detailed discussion of neurons can be found in many textbooks, only a brief overview for introducing the context of this work will be provided here (see also Kandel et al., 2000; Squire, 2003; Purves, 2008).

Neurons consist of several important regions. The cell body, or soma, is the core of the cell. Two types of branches extend from the soma for sending and receiving signals to and from other neurons. Neurons have a single axon, which is the pathway for signal conduction away from the soma to other neurons. The point at which an axon connects to another cell is called a synapse. The axon may branch many times and form multiple connections to other neurons. For example, in the cortex of humans, each neuron has an average of 7000 synapses (Pakkenberg et al., 2003).

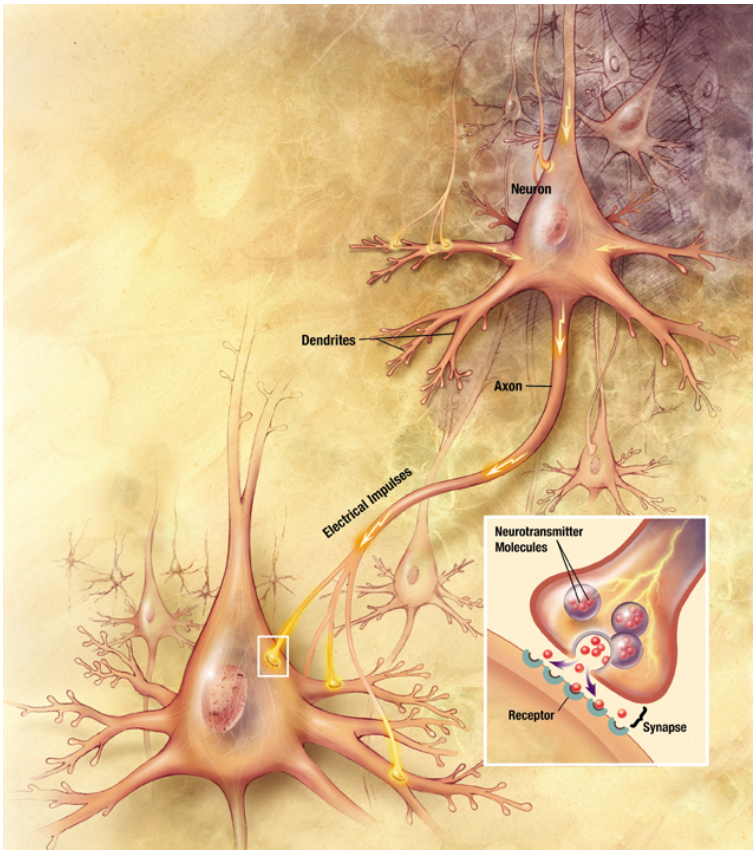

Figure 1.1: Neuron Structure and Communication. Neurons consist of the soma (cell body), axon (for transmitting signals to other neurons), dendrites (for receiving signals), and synapses (the connections between neurons). Action potentials travel through the axon to the synapses where neurotransmitters are released to excite or inhibit the activity of other neurons. Figure courtesy of www.nia.nih.gov and used in accordance with reproduction policies.

Neurons typically have receiving branches called dendrites, from which a neuron receives inputs from other neurons. Synaptic terminals can form at dendrites, somas, and occasionally on other axons.

Neurons communicate through both electrical and chemical signals. The electrical signals travel through the axon and dendrites. Neurons have an electric potential across the cell membrane due to a concentration difference of various ions, including K^+, Na^+, and Cl^-. This concentration gradient is maintained through selective ion channels and pumps. In the resting state, the membrane potential is typically around -70mV (intracellular vs. extracellular). This potential can be calculated by using the

Goldman equation (Goldman, 1943), which is a generalization and extension of the Nernst equation (see also Hille, 2001; Bard and Faulkner, 2001; Kandel et al., 2000):

$$E_m = \frac{RT}{zF} \ln \frac{[\text{ion}]_{out}}{[\text{ion}]_{in}} \qquad \text{Nernst equation} \qquad (1.1)$$

$$E_m = \frac{RT}{F} \ln \left(\frac{\sum_i^N P_{C_i^+} [C_i^+]_{\text{out}} + \sum_j^M P_{A_j^-} [A_j^-]_{\text{in}}}{\sum_i^N P_{C_i^+} [C_i^+]_{\text{in}} + \sum_j^M P_{A_j^-} [A_j^-]_{\text{out}}} \right) \qquad \text{Goldman equation} \qquad (1.2)$$

Where E_m is the membrane potential, R is the gas constant, T is the temperature in Kelvin, z is the ion valence, F is the Faraday constant, $[\text{ion}]_{out}$ and $[\text{ion}]_{in}$ are ion concentrations outside and inside the neuron, P is membrane permeability (cm/s), C represents cations, and A represents anions.

In the specific case of Na^+, K^+, and Cl^-, the three primary ions in the cytoplasm and extracellular cerebrospinal fluid, the Goldman equation goes to:

$$E_m = \frac{RT}{F} \ln \left(\frac{P_{Na^+}[Na^+]_{\text{out}} + P_{K^+}[K^+]_{\text{out}} + P_{Cl^-}[Cl^-]_{\text{in}}}{P_{Na^+}[Na^+]_{\text{in}} + P_{K^+}[K^+]_{\text{in}} + P_{Cl^-}[Cl^-]_{\text{out}}} \right) \qquad (1.3)$$

In the pioneering work of Hodgkin and Katz (1949), it was determined that the permeability ratios of these ions in the resting state were $P_K : P_{Na} : P_{Cl} = 1.0 : 0.04 : 0.45$, in the action potential peak $P_K : P_{Na} : P_{Cl} = 1.0 : 20 : 0.45$, and in the refractory period $P_K : P_{Na} : P_{Cl} = 1.8 : 0 : 0.45$.

The resting potential of a neuron is primarily due to the difference in K^+ concentrations, which has high permeability in the resting state (see Table 1.1 as well as Hodgkin and Katz, 1949 and Hille, 2001). The permeability of other ions, and Na^+ particularly, changes dramatically as voltage-gated ion channels open and close at the membrane to allow ionic flow to propagate the action potential. Small changes in the K^+ concentration can cause depolarization or hyperpolarization. This property is particularly leveraged in the current work to drive transient neural activity

Ions	Intracellular (mM)	Extracellular (mM)	Nernst E (mV)	Resting Permeability	Peak Potential Permeability	Refractory Permeability
K^+	150	5.5	-86	1.0	1.0	1.8
Na^+	15	150	+60	0.01-0.04	20	0
Cl^-	10	125	-66	0.1-0.45	0.45	0.45
Ca^+	0.0001	2	+180			

Table 1.1: Ionic Concentrations, Nernst Potential, and Permeability in Mammalian Neurons
Adapted from Hille (2001), Pritchard and Alloway (1999), Hodgkin and Katz (1949), and Wright (2004).

for validating the function of biosensor arrays. Since the concentrations of ions are tightly modulated by physiological systems, a portion of the work in this dissertation also focuses on understanding how the ionic concentrations affect the biosensor performance to improve the correlation between measured responses and physiological levels of various neurotransmitters.

Excitatory and inhibitory inputs summate at a point of the soma called the axon hillock. When a depolarization threshold is crossed (approximately -55mV), a rapid electrical pulse, or action potential, propagates through the axon to the synapses as voltage-gated ion channels allow an influx of Na^+. At the synaptic cleft, the action potential causes the release of synaptic vesicles containing neurotransmitters. The neurotransmitters transverse the synaptic cleft by diffusion and bind to postsynaptic receptors to enable communication between neurons across the network. These receptors may be excitatory or inhibitory, and may directly modulate ion channels (ionotropic) or activate other signaling cascades (metabotropic). Neurotransmitters include dopamine, acetylcholine, glutamate, serotonin, and various neuropeptides.

1.2 Fundamentals of Electrochemistry

Electrochemistry utilizes electrodes and electrical properties of molecules to investigate experimental systems. While the broad set of electrochemical techniques

utilize and measure virtually every electrical property of a system (potential, current, impedance, capacitance, frequency response, analyte concentration, geometry, electrode material, reaction kinetics, mass transfer, etc.), this discussion will focus on two primary branches of electrochemistry that are particularly useful for developing tools for investigating neurophysiology: potentiometry and voltammetry. In-depth discussion on additional electrochemical techniques, theory, and instrumentation can be found in the texts of Kissinger and Heineman (1996), Bard and Faulkner (2001), and Zoski (2007). For a text specifically on electrochemical methods in neuroscience, refer to Michael and Borland (2007).

Potentiometry is an electrochemical method which uses potential as the measured variable during a zero current flow condition. The potential between two electrodes (working electrode and reference electrode) is monitored.

$$E_{measured} = E_{working} - E_{reference} \tag{1.4}$$

In electrochemical experiments, the working electrode is made selective for a particular molecule (such as H^+ for a pH sensor) such that the measured potential reflects the concentration of the analyte of interest.

Voltammetry differs from potentiometry in that potential of the working electrodes is controlled by external instrumentation (potentiostat), and the current at the electrode is measured (Figure 1.2). The resulting faradaic (oxidation or reduction) current can be related to the analyte concentration. This current is also dependent on the shape and magnitude of the voltage waveform. Three common forms of voltammetry are cyclic voltammetry (triangle wave), chronoamperometry (square wave), and constant potential amperometry (O'Neill, 1994; Phillips and Wightman, 2003).

Cyclic voltammetry results in oxidation and reduction peaks that can provide a

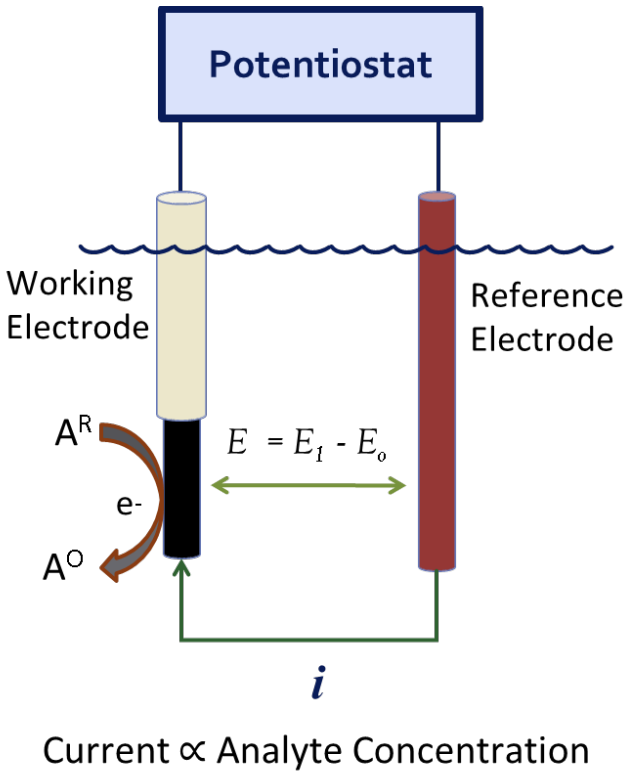

Figure 1.2: Diagram of an Electrochemical Cell. A bias applied at the working electrode versus the reference electrode can drive the oxidation or reduction of analytes. The resulting current from electron release can be related to the concentration of the analyte. In potentiometry no bias is applied, but rather the potential at the working electrode is measured.

chemical signature for identifying specific molecules with greater selectivity. Similarly, chronoamperometry can offer a measure of selectivity through the ratio of oxidation to reduction currents. Both cyclic voltammetry and chronoamperometry are limited in temporal resolution by the period of the waveform, which is typically around 10Hz with carbon fiber electrodes for *in vivo* voltammetry for neural recordings.

Applying a constant potential ("constant potential amperometry") can further improve temporal resolution, because the limiting factors are diffusion and the sampling rate of the potentiostat, not the period of the waveform. Since constant potential amperometry oxidizes or reduces all molecules at the surface that have a formal potential of lesser magnitude than the applied potential, this technique has no inherent selectivity. Permselective membranes can be used to increase selectivity by limiting the molecules that can diffuse to the electrode surface.

1.2.1 Microelectrodes

Microelectrodes are of particular interest for studying neurophysiological dynamics to enable spatial resolution on the order of neuron sizes (approximately 10μm diameter). Microelectrodes with dimensions in the micron range (typically considered $< 25\mu$m) perform differently than their macro counterparts in regard to electrochemical processes (Bard and Faulkner, 2001; Kissinger and Heineman, 1996). First, the redox reactions of the analyte at the electrode interface will not affect the bulk concentration of the analyte, which can increase the accuracy of concentration measurements. Second, the current at the electrodes are typically in the picoamp or nanoamp range. As a result, the ohmic iR voltage drop across the electrolyte solution is trivial and the applied potential more closely matches the true bias at the electrode. In most cases, a two electrode system can be used as illustrated in Figure 1.2. Finally, at the microelectrode interface, radial or convergent diffusion (as opposed to planar diffusion) is the dominant mode of mass transfer, which results in

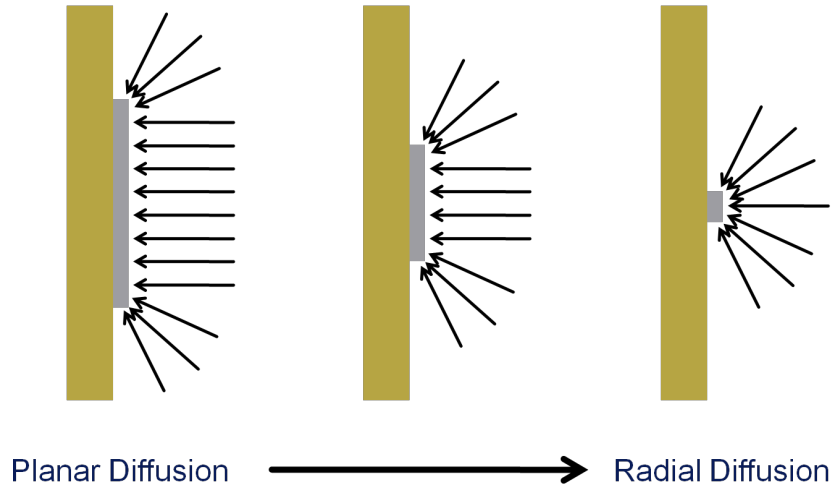

Figure 1.3: Planar Diffusion and Radial Diffusion. As the electrode dimensions are reduced, radial diffusion plays an increasingly large role at the electrode interface, thus altering the way microelectrodes perform compared to their macroelectrode counterparts.

higher charge density and greater relative sensitivity (Figure 1.3).

While advantageous in many regards, these functional differences of microelectrodes mean that moving from the macroelectrode scale, where most electranalytial sensors have been developed, to the microelectrode realm, is not a straight-line process. For example, electrodeposited polymers exhibit different behaviors as the electrode size goes smaller, which is likely due to the increased role of radial diffusion, resulting in higher charge densities and edge effects (McMahon et al., 2004; Rothwell et al., 2009). Rothwell et al. (2009) used electrodes of various geometries (disks and cylinders) and sizes to investigate the relationship between electrode dimensions and polymer deposition characteristics. They found that as electrodes are made smaller and, more specifically, the ratio of the edge to the area (edge density) grows, the permselectivity of phenylenediamine for H_2O_2 over ascorbic acid degraded (Figure 1.4). One significant challenge of the work presented in this dissertation involves the development of selective functionalization strategies for microelectrodes.

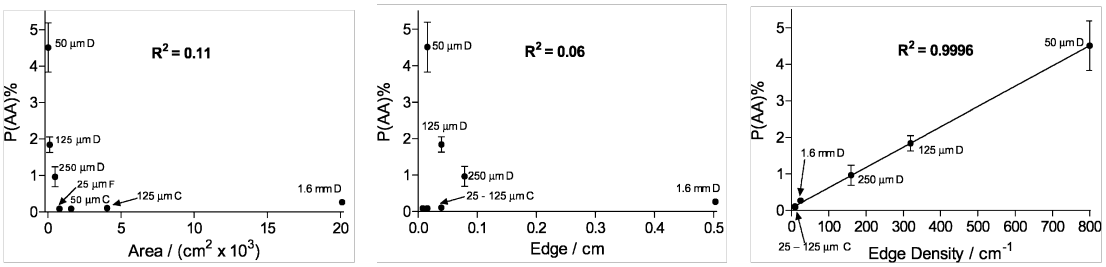

Figure 1.4: Relationship between Probe Geometry and the Performance of the Permselective Membrane Phenylenediamine (Originally published in Rothwell et al. (2009).) Plots of averaged values of ascorbic acid permeability (P(AA)%) for seven variations of Pt electrode geometry and size versus working electrode area (left), edge length (middle), and edge density (right). R^2 values were calculated using linear regression. For the bottom plot (edge density), the results were significant, indicating that as edge density increases, the performance of phenylenediamine degrades. For planar electrodes, edge density increases as size decreases.

1.3 Recording *in vivo* Neurophysiology

1.3.1 Recording Electrophysiology

Bioelectric potentials generated by neurons and other excitable cells, such as muscle, can be measured through a form of potentiometry. If an electrode is placed in the changing biopotential field, small currents will flow across the electrode-electrolyte interface. In this case, instead of measuring a molecular concentration (e.g. pH), the potential changes at the electrode reflect the local biopotentials (Webster and Clark, 1998).

Several established experimental methods, including patch-clamp techniques, microdialysis, and microelectrodes, have provided a wealth of information to neuroscientists and clinicians about the function of the brain. Choice of technique is application-driven as each of these methods is primarily used to directly observe either neurochemical or electrophysiological activity, but typically not both.

Foundational work by pioneers such as Hodgkin, Huxley, Katz, Neher, Sakmann, and others paved the way for advanced *in vivo* investigations of the brain (Hodgkin

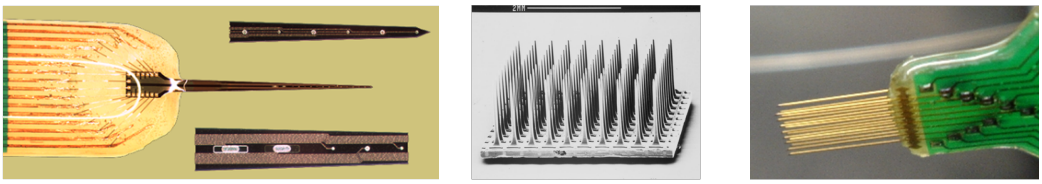

Figure 1.5: Neural Probes. Three common neural probes include the Michigan Probe, Utah Array (Rousche and Normann, 1998), and microwire array. Image of microwire array is from the public domain and courtesy of Steve M. Potter.

and Huxley, 1939; Hodgkin and Katz, 1949; Neher and Sakmann, 1976; Kipke et al., 2008). Numerous microelectrodes have been developed for monitoring *in vivo* extracellular electrophysiology, including platinum microwires (Schwartz, 2004), the Utah array (Maynard et al., 1997), and the Michigan probe (Wise et al., 2004), (Figure 1.5). Microwire electrodes, which typically consist of 1–4 insulated microwires with exposed tips, are simple, but have proven to be quite effective in recording unit activity and local field potentials in many experiments. The Utah array offers high electrode density with 100 electrode sites for recording or stimulation.

Michigan probes, which are fabricated with photolithography and microfabrication techniques, have a large range of design parameters for electrode size, shape, and material (Wise et al., 2004). While originally based on silicon technology, recent designs have used polymers, such as parylene, as a substrate (Pellinen et al., 2005; Seymour and Kipke, 2007; Purcell et al., 2009; Seymour et al., 2011). These probes were developed for recording electrophysiological signals *in vivo* for neural prosthetic devices. They have also been used for electrical stimulation (Weiland and Anderson, 2000). Work from van Horne et al. (1992) showed some success in using the Michigan probe technology for neurochemical sensing, but these early attempts were not fully developed. More recently, the Michigan probe has been used *in vivo* to monitor the activity single neurotransmitters such as dopamine (Johnson et al., 2008) and choline (Gibson and Kipke, 2008).

1.3.2 Recording Neurochemistry

Various methods are used to explore neurochemical dynamics of the brain. The two most common methods today are microdialysis and voltammetry (Figure 1.6). Microdialysis has become an indispensable tool for monitoring and modulating neurochemical activity in the brain (Watson et al., 2006). Microdialysis probes typically consist of a semi-permeable membrane, an inlet tube for perfusing fluids such as extracellular fluid or pharmacological agents, and an outlet tube for sampling the fluid within the probe, called the dialysate. The dialysate is analyzed by high pressure liquid chromatography or capillary electrophoresis to determine the molecules present. A notable advantage of microdialysis is its high selectivity and sensitivity. Microdialysis methods allow for accurate identification of multiple chemical species at nanomolar concentrations.

Microdialysis has traditionally suffered from low spatial and temporal resolution. Typical microdialysis probes have a diameter of several hundred microns and sampling rates of 10-20 minutes, which stands in contrast to synaptic events occurring on a millisecond timescale. Recent work using capillary electrophoresis, laser-induced fluorescence detection, and segmented dialysate flow in Robert Kennedy's lab at the University of Michigan have improved the temporal resolution to the order of seconds for several neurotransmitters (Bowser and Kennedy, 2001; Kennedy et al., 2002; Shou et al., 2004, 2006; Shackman et al., 2007; Wang et al., 2008).

In vivo voltammetry with carbon and platinum electrodes (Figure 1.6) is an established method for sensing various neurotransmitters including dopamine (Wiedemann et al., 1991; Wightman et al., 1988; Phillips and Wightman, 2004; Cheer et al., 2005), acetylcholine or choline (Burmeister and Gerhardt, 2003; Mitchell, 2004; Parikh et al., 2004; Bruno et al., 2006; Burmeister et al., 2008), and glutamate (Burmeister and Gerhardt, 2001; Hascup et al., 2008) with sub-micromolar sensitivity and subsecond temporal resolution (O'Neill, 1994). One advantage of voltammetry is its high tem-

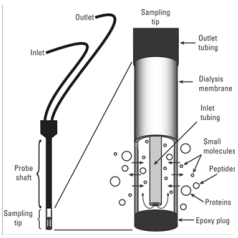

Microdialysis Probe

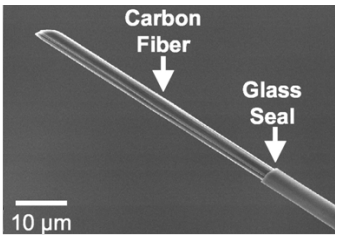

Carbon Fiber Electrode

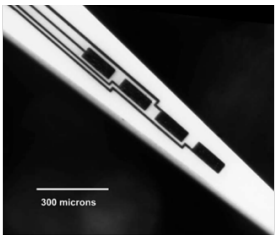

Ceramic Substrate, Platinum Electrode Array

Figure 1.6: Neurochemical Probes. Three common neurochemical probes include microdialysis probes (Watson et al., 2006), carbon fiber electrodes (Robinson et al., 2003), and ceramic substrate platinum electrode arrays (Burmeister et al., 2005).

poral resolution, which enables the differentiation of phasic signals from slower tonic changes. Monitoring these faster dynamics has recently impacted our understanding of various neurochemical systems, including dopamine, glutamate, and acetylcholine (Parikh et al., 2007; Sarter et al., 2009; Parikh et al., 2008; Parikh and Sarter, 2008). Histological analysis of neuronal density, gliosis, and microglia activation have indicated that microelectrodes cause less tissue damage than microdialysis probes, which has been hypothesized to increase signal integrity (Khan and Michael, 2003; Borland et al., 2005; Hascup et al., 2009; Yang et al., 1998).

Carbon fibers are commonly used in conjuction with cyclic voltammetry and chronoamperometry for the measurement of electroactive molecules, such as catecholamines (e.g. dopamine) and serotonin. Other neurotransmitters, such as acetylcholine and glutamate, are not electroactive and cannot be measured directly with voltammetric methods. The most common approach for electrochemically detecting these molecules is to enzymatically convert them to an electroactive reporter molecule (e.g. Hydrogen Peroxide or H_2O_2) with an appropriate oxidase enzyme immobilized on the surface of the electrode (Burmeister and Gerhardt, 2001; Mitchell, 2004; Rothwell et al., 2009). The H_2O_2 is then oxidized at the electrode with an applied electrical potential (typically +700mV vs. Ag/AgCl). The following generalized reactions describe these processes ("Ox" represents an oxidase enzyme and "FAD" represents

flavin adenine dinucleotide, which becomes $FADH_2$ when oxidized) (Rothwell et al., 2009):

$$\text{Substrate} + \text{Ox/FAD} \rightarrow \text{Products} + \text{Ox/FADH}_2 \tag{1.5}$$

$$\text{Ox/FADH}_2 + \text{O}_2 \rightarrow \text{Ox/FAD} + \text{H}_2\text{O}_2 \tag{1.6}$$

$$\text{H}_2\text{O}_2 \rightarrow \text{O}_2 + 2\text{H}^+ + 2e^- \tag{1.7}$$

Platinum electrodes have high catalytic activity for the oxidation of H_2O_2 and thus are frequently used for the amperometric detection of molecules through the above mechanism (Burmeister et al., 2000; Burmeister and Gerhardt, 2003; Burmeister et al., 2005; Mitchell, 2004; Rothwell et al., 2009).

The selectivity of the amperometric biosensors is improved through permselective membranes to inhibit the molecules that can diffuse to the electrode surface, while maintaining permeability to the molecule of interest (H_2O_2 in this case). Common permselective membranes include Nafion (Gerhardt et al., 1984; Parikh et al., 2004) and phenylenediamine (Mitchell, 2004; Rothwell et al., 2008; Parikh et al., 2008). Additionally, multi-site biosesnor arrays can further increase specificity through "self-referencing," a technique in which a proximate reference electrode site is coated without the enzyme (Burmeister and Gerhardt, 2001; Phillips and Wightman, 2003). The signal from this reference site includes similar non-specific currents that can be subtracted from the sensing site to reduce or eliminate interference signals from the recordings. An example of this form of referencing is diagrammed in Figure 1.7

1.4 Previous Work from our Lab

As a foundation for this work, our lab has recently demonstrated the utility of multi-electrode neural probes in recording neurochemical field dynamics with mi-

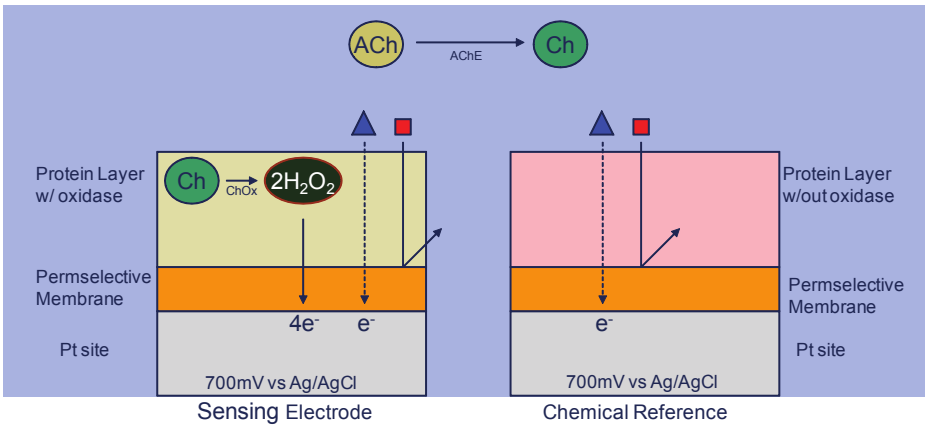

Figure 1.7: Diagram of Neurochemical Referencing on a Single Array. The left site represents a choline sensitive site and the right site represents a chemical reference site without choline oxidase. Acetylcholinesterase converts acetylcholine to choline, which then can diffuse to the electrode. On the sensing site, the choline is converted to H_2O_2 and oxidized at the surface. A permselective membrane prevents potential interferents (depicted by the triangle and square) from reaching the surface. In the case that an interferent reaches the electrode surface (triangle), it will do so on both sites, thus can be subtracted from the signal.

croelectrode arrays. Specifically, we have conducted experiments, led by Matthew Johnson, in recording pH dynamics through potentiometric methods and dopamine through constant potential amperometry (Johnson et al., 2007, 2008).

1.4.1 pH

Neural probes with 16 iridium microelectrode sites on a single shank were modified by electrochemically growing pH-sensitive hydrous iridium oxide on individual electrode sites (Johnson et al., 2007). These probes, which showed selective linear sensitivity to pH, were used to record local pH changes during probe insertion at various speeds as a measure of local tissue trauma (Figure 1.8). The electrochemical modification of individual electrode sites is a fundamental concept shared with aspects of the current body of work.

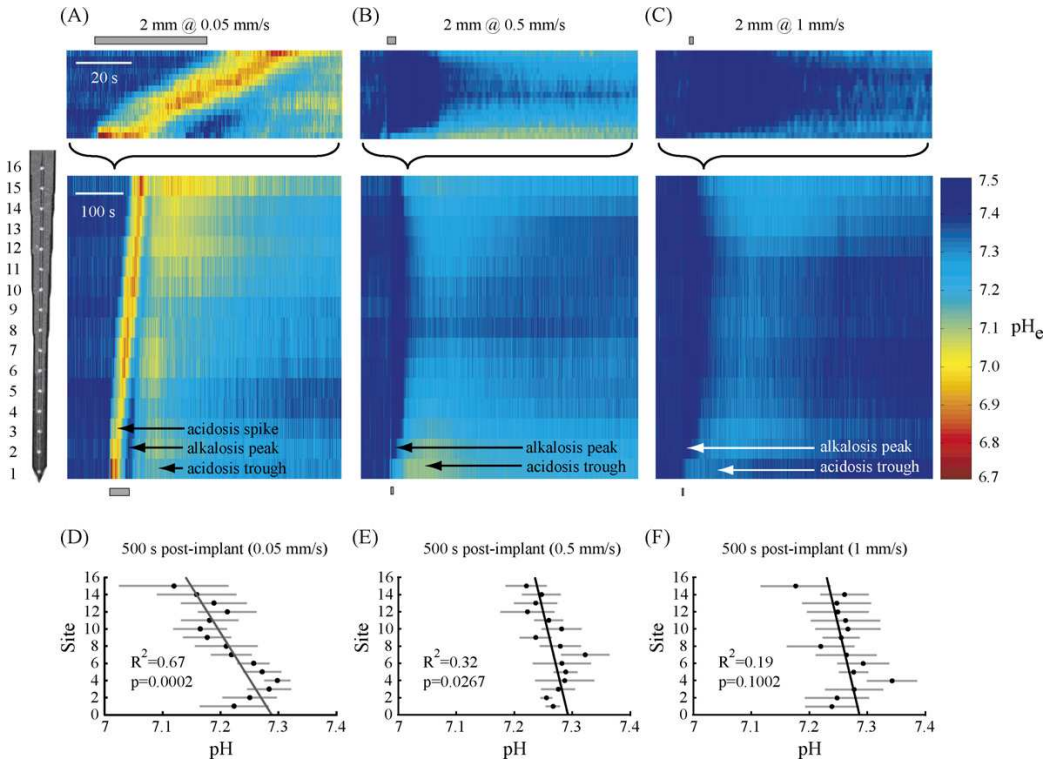

Figure 1.8: Spatiotemporal pH dynamics during probe insertion. Originally published in Johnson et al. (2007). Spatiotemporal pH plots revealed more robust long-term acidosis across the array for slower insertion speeds as well as variability in the response along the probe shank. Shown are representative 2mm–deep insertions at (A) 0.05mm/s, (B) 0.50mm/s, and (C) 1.0 mm/s. Upper plots (AC) illustrate a detailed picture of the pH response during the act of insertion (gray bars), while the lower plots show a 10 min response window. A triphasic acidicalkalineacidic waveform, which included substantial long-term acidosis, was evident following the slowest insertions. Speeds of 0.50 and 1.00mm/s typically elicited a biphasic alkalineacidic waveform with a muted acidosis trough. The average pH at each contact site 500s after insertion had a significant spatial component for (D) the 0.05mm/s insertions (R^2= 0.67, n = 11 implants) and to a lesser extent for (E) the 0.50mm/s insertions (R^2= 0.32, n = 5 implants) and (F) the 1.00mm/s insertions (R^2 = 0.19, n = 8 implants). Consistent across these implants, however, was a general trend of superficial contact sites recording more long-term acidosis than sites located near the tip. Error bars correspond to standard errors.

1.4.2 Dopamine

We recently demonstrated concurrent recordings of local field potentials, unit activity, and dopamine efflux in the striatum of anesthetized rats using silicon neural probes with interdigitated platinum and iridium sites spaced at 200μm (Johnson et al., 2008). Dopamine was monitored amperometrically at either +350mV or +500mV vs. Ag/AgCl at four platinum electrode sites, which were dip-coated with Nafion to reduce possible signal interference from ascorbic acid and other interferents. Electrical stimulation of the medial forebrain bundle (MFB) produced spatially heterogeneous, but reproducible, dopamine efflux, and measurable changes in unit activity and local field potentials (Figure 1.9).

The dopamine-electrophysiology work served as an initial foundation for multi-modal sensors. The current work builds upon this fundamental multi-modal recording work by extending sensing capabilities to nonelectroactive molecules (choline/acetylcholine and glutamate), adding chemical reference sites for improved signal integrity, and adding localized drug delivery capabilities.

1.5 Dissertation Organization

The aim of this work is to develop and validate novel neural biosensor probes for simultaneous electrophysiological and neurochemical measurements with precise, localized drug delivery. This technology has been developed to interface with the complex environment of the brain for more advanced experimental investigations at the intersections of neurophysiology, neuropathology, and neuropharmacology. The validation experiments have been conducted using relevant *in vivo* testbeds as a foundation for future work to more fully understand and treat neurological disorders.

Chapter II presents a multimodal probe that enables concurrent detection of choline, recording of electrophysiology, and localized drug delivery. Central to this

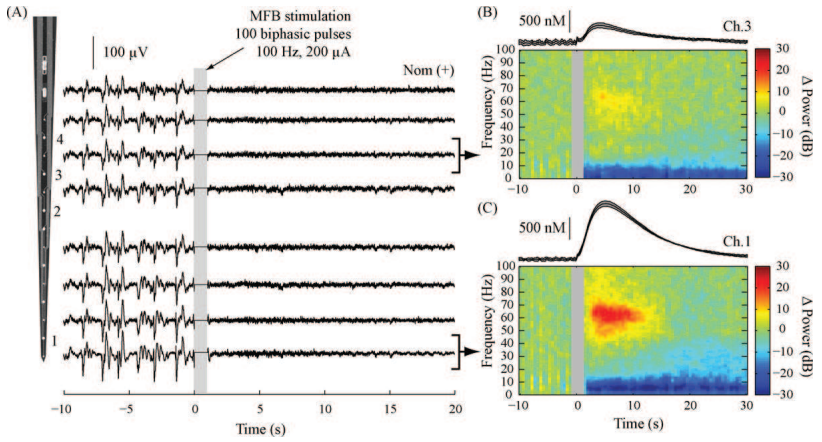

Figure 1.9: MFB stimulation elicited local field potential modulation and dopamine release in striatum. Originally published in Johnson et al. (2008). MFB stimulation elicited local field potential modulation and dopamine release in striatum. (A) The figure shows an example recording session sampled continuously during electrochemical recordings for dopamine on adjacent sites (indicated by numbers 1-4 next to the probe). Following MFB stimulation (indicated by the gray bar), slow-wave activity was suppressed considerably and coincided with the emergence of higher frequency activity. (B and C) Event-averaged spectrograms showed significant modulation in the 0–20 and 40–90 Hz bands following stimulation (n = 5 trials). Above each plot is the event-averaged dopamine response recorded on an adjacent site. Recordings reflect the presence of nomifensine (10mg/kg).

work is the development of selective electrodeposition methods for enzyme immobilization and polymerization on individual microelectrode sites that more closely approach the scale of neurons than currently reported neural biosensors.

Multiple neurotransmitter systems are implicated in the pathophysiology of schizophrenia, Alzheimer's disease, Parkinson's disease, and other neurological disorders, yet the direct relationships remain unclear. The ability to simultaneously monitor multiple chemical signals concurrently with electrophysiology and integrated pharmacological manipulation can serve as a useful tool to further these investigations. Chapter III further extends the probe capabilities to include glutamate sensing concurrent with choline sensing, electrophysiology recordings, and drug delivery.

Electrochemical biosensors are commonly used to record neurotransmitter dynamics, yet there remains no standard calibration media or procedure. Differences in calibration procedures can impact reported performance making the interpretation of *in vivo* difficult. Chapter IV aims to improve our ability to interpret *in vivo* neurochemical recordings by investigating the influence of calibration media on performance characteristics of amperometric biosensors.

Finally, Chapter V provides a conclusion for this work and suggestions for future directions. Bridging the electrophysiological and neurochemical domains with sufficient fidelity, resolution, sensitivity, and selectivity can provide novel insights into neurophysiology that lead to improved therapeutic approaches for treating neurological disorders.

References

Bard, A. and Faulkner, L. (2001). *Electrochemical methods: fundamentals and applications*. Wiley, 2nd edition.

Borland, L. M., Shi, G., Yang, H., and Michael, A. C. (2005). Voltammetric study of extracellular dopamine near microdialysis probes acutely implanted in the striatum of the anesthetized rat. *J Neurosci Methods*, 146(2):149–158.

Bowser, M. T. and Kennedy, R. T. (2001). In vivo monitoring of amine neurotransmitters using microdialysis with on-line capillary electrophoresis. *Electrophoresis*, 22(17):3668–3676.

Bruno, J. P., Gash, C., Martin, B., Zmarowski, A., Pomerleau, F., Burmeister, J., Huettl, P., and Gerhardt, G. A. (2006). Second-by-second measurement of acetylcholine release in prefrontal cortex. *Eur J Neurosci*, 24(10):2749–2757.

Burmeister, J. J. and Gerhardt, G. A. (2001). Self-referencing ceramic-based multisite microelectrodes for the detection and elimination of interferences from the measurement of l-glutamate and other analytes. *Anal. Chem.*, 73(5):1037–1042.

Burmeister, J. J. and Gerhardt, G. A. (2003). Ceramic-based multisite microelectrode arrays for in vivo electrochemical recordings of glutamate and other neurochemicals. *TrAC Trends in Analytical Chemistry*, 22(8):498–502.

Burmeister, J. J., Moxon, K., and Gerhardt, G. A. (2000). Ceramic-based multisite microelectrodes for electrochemical recordings. *Anal. Chem.*, 72(1):187–192.

Burmeister, J. J., Palmer, M., and Gerhardt, G. A. (2005). L-lactate measures in brain tissue with ceramic-based multisite microelectrodes. *Biosensors & bioelectronics*, 20(9):1772–1779.

Burmeister, J. J., Pomerleau, F., Huettl, P., Gash, C. R., Werner, C. E., Bruno, J. P., and Gerhardt, G. A. (2008). Ceramic-based multisite microelectrode arrays for simultaneous measures of choline and acetylcholine in cns. *Biosensors & bioelectronics*, 23(9):1382–1389.

Cheer, J. F., Heien, M. L. A. V., Garris, P. A., Carelli, R. M., and Wightman, R. M. (2005). Simultaneous dopamine and single-unit recordings reveal accumbens gabaergic responses: implications for intracranial self-stimulation. *Proc. Natl. Acad. Sci. U. S. A.*, 102(52):19150–19155.

Damasio, A. (2001). *The Scientific American book of the brain*. Lyons Press.

Gerhardt, G. A., Oke, A. F., Nagy, G., Moghaddam, B., and Adams, R. N. (1984). Nafion-coated electrodes with high selectivity for cns electrochemistry. *Brain Res.*, 290(2):390–395.

Gibson, M. D. and Kipke, D. R. (2008). Neural probes for simultaneous recordings of in vivo neurochemical and electrophysiological activity. In Phillips, P., Sandberg, S., Ahn, S., and Phillips, A., editors, *Monitoring Molecules in Neuroscience*, pages 117–119. University of British Columbia Institute of Mental Health.

Goldman, D. E. (1943). Potential, impedance, and rectification in membranes. *J Gen Physiol*, 27(1):37–60.

Hascup, E. R., af Bjerkn, S., Hascup, K. N., Pomerleau, F., Huettl, P., Strmberg, I., and Gerhardt, G. A. (2009). Histological studies of the effects of chronic implantation of ceramic-based microelectrode arrays and microdialysis probes in rat prefrontal cortex. *Brain Res*, 1291:12–20.

Hascup, K. N., Hascup, E. R., Pomerleau, F., Huettl, P., and Gerhardt, G. A. (2008). Second-by-second measures of l-glutamate in the prefrontal cortex and striatum of freely moving mice. *The Journal of pharmacology and experimental therapeutics*, 324(2):725–731.

Hille, B. (2001). *Ion channels of excitable membranes*. Sinauer.

Hodgkin, A. L. and Huxley, A. (1939). Action potentials recorded from inside a nerve fibre. *Nature*, 144:710–711.

Hodgkin, A. L. and Katz, B. (1949). The effect of sodium ions on the electrical activity of giant axon of the squid. *J Physiol*, 108(1):37–77.

Johnson, M. D., Franklin, R. K., Gibson, M. D., Brown, R. B., and Kipke, D. R. (2008). Implantable microelectrode arrays for simultaneous electrophysiological and neurochemical recordings. *J Neurosci Methods*, 174(1):62–70.

Johnson, M. D., Kao, O. E., and Kipke, D. R. (2007). Spatiotemporal ph dynamics following insertion of neural microelectrode arrays. *J Neurosci Methods*, 160(2):276–287.

Kandel, E., Schwartz, J., and Jessell, T. (2000). *Principles of neural science*. McGraw-Hill, Health Professions Division.

Kennedy, R. T., Thompson, J. E., and Vickroy, T. W. (2002). In vivo monitoring of amino acids by direct sampling of brain extracellular fluid at ultralow flow rates and capillary electrophoresis. *J Neurosci Methods*, 114(1):39–49.

Khan, A. S. and Michael, A. C. (2003). Invasive consequences of using microelectrodes and microdialysis probes in the brain. *Trends in Analytical Chemistry*, 22(8):503–508.

Kipke, D. R., Shain, W., Buzski, G., Fetz, E., Henderson, J. M., Hetke, J. F., and Schalk, G. (2008). Advanced neurotechnologies for chronic neural interfaces: new horizons and clinical opportunities. *J Neurosci*, 28(46):11830–11838.

Kissinger, P. and Heineman, W. (1996). *Laboratory techniques in electroanalytical chemistry*. Marcel Dekker, Inc.

Maynard, E. M., Nordhausen, C. T., and Normann, R. A. (1997). The utah intracortical electrode array: a recording structure for potential brain-computer interfaces. *Electroencephalogr Clin Neurophysiol*, 102(3):228–239.

McMahon, C. P., Killoran, S. J., Kirwan, S. M., and O'Neill, R. D. (2004). The selectivity of electrosynthesised polymer membranes depends on the electrode dimensions: implications for biosensor applications. *Chem Commun (Camb)*, 40(18):2128–2130.

Michael, A. and Borland, L. (2007). *Electrochemical methods for neuroscience*. CRC Press/Taylor & Francis.

Mitchell, K. M. (2004). Acetylcholine and choline amperometric enzyme sensors characterized in vitro and in vivo. *Anal. Chem.*, 76(4):1098–1106.

Neher, E. and Sakmann, B. (1976). Single-channel currents recorded from membrane of denervated frog muscle fibres. *Nature*, 260(5554):799–802.

O'Neill, R. D. (1994). Microvoltammetric techniques and sensors for monitoring neurochemical dynamics in vivo. a review. *Analyst*, 119(5):767–779.

Pakkenberg, B. and Gundersen, H. J. G. (1997). Neocortical neuron number in humans: Effect of sex and age. *J. Comp. Neurol.*, 384(2):312–320.

Pakkenberg, B., Pelvig, D., Marner, L., Bundgaard, M. J., Gundersen, H. J. G., Nyengaard, J. R., and Regeur, L. (2003). Aging and the human neocortex. *Experimental Gerontology*, 38(1-2):95–99.

Parikh, V., Kozak, R., Martinez, V., and Sarter, M. (2007). Prefrontal acetylcholine release controls cue detection on multiple timescales. *Neuron*, 56(1):141–154.

Parikh, V., Man, K., Decker, M. W., and Sarter, M. (2008). Glutamatergic contributions to nicotinic acetylcholine receptor agonist-evoked cholinergic transients in the prefrontal cortex. *J Neurosci*, 28(14):3769–3780.

Parikh, V., Pomerleau, F., Huettl, P., Gerhardt, G. A., Sarter, M., and Bruno, J. P. (2004). Rapid assessment of in vivo cholinergic transmission by amperometric detection of changes in extracellular choline levels. *Eur. J. Neurosci.*, 20(6):1545–1554.

Parikh, V. and Sarter, M. (2008). Cholinergic mediation of attention: contributions of phasic and tonic increases in prefrontal cholinergic activity. *Ann N Y Acad Sci*, 1129:225–235.

Pellinen, D. S., Moon, T., Vetter, R. J., Miriani, R., and Kipke, D. R. (2005). Multifunctional flexible parylene-based intracortical microelectrodes. In *Proc. 27th Annual International Conference of the Engineering in Medicine and Biology Society IEEE-EMBS 2005*, pages 5272–5275.

Phillips, P. E. M. and Wightman, R. M. (2003). Critical guidelines for validation of the selectivity of in-vivo chemical microsensors. *TrAC Trends in Analytical Chemistry*, 22(8):509–514.

Phillips, P. E. M. and Wightman, R. M. (2004). Extrasynaptic dopamine and phasic neuronal activity. *Nat. Neurosci.*, 7(3):199; author reply 199.

Pritchard, T. and Alloway, K. (1999). *Medical neuroscience*. Fence Creek Pub.

Purcell, E. K., Seymour, J. P., Yandamuri, S., and Kipke, D. R. (2009). In vivo evaluation of a neural stem cell-seeded prosthesis. *J Neural Eng*, 6(2):26005.

Purves, D. (2008). *Neuroscience*. Sinauer.

Robinson, D. L., Venton, B. J., Heien, M. L., and Wightman, R. M. (2003). Detecting subsecond dopamine release with fast-scan cyclic voltammetry in vivo. *Clin Chem*, 49(10):1763–1773.

Rothwell, S. A., Killoran, S. J., Neville, E. M., Crotty, A. M., and O'Neill, R. D. (2008). Poly(o-phenylenediamine) electrosynthesized in the absence of added background electrolyte provides a new permselectivity benchmark for biosensor applications. *Electrochem. Commun.*, 10(7):1078–1081.

Rothwell, S. A., Kinsella, M. E., Zain, Z. M., Serra, P. A., Rocchitta, G., Lowry, J. P., and O'Neill, R. D. (2009). Contributions by a novel edge effect to the permselectivity of an electrosynthesized polymer for microbiosensor applications. *Anal. Chem.*, 81(10):3911–3918.

Rousche, P. J. and Normann, R. A. (1998). Chronic recording capability of the utah intracortical electrode array in cat sensory cortex. *J Neurosci Methods*, 82(1):1–15.

Sarter, M., Parikh, V., and Howe, W. M. (2009). Phasic acetylcholine release and the volume transmission hypothesis: time to move on. *Nat Rev Neurosci*, 10(5):383–390.

Schwartz, A. B. (2004). Cortical neural prosthetics. *Annu Rev Neurosci*, 27:487–507.

Seymour, J. P. and Kipke, D. R. (2007). Neural probe design for reduced tissue encapsulation in cns. *Biomaterials*, 28(25):3594–3607.

Seymour, J. P., Langhals, N. B., Anderson, D. J., and Kipke, D. R. (2011). Novel multi-sided, microelectrode arrays for implantable neural applications. *Biomed Microdevices*.

Shackman, H. M., Shou, M., Cellar, N. A., Watson, C. J., and Kennedy, R. T. (2007). Microdialysis coupled on-line to capillary liquid chromatography with tandem mass spectrometry for monitoring acetylcholine in vivo. *J Neurosci Methods*, 159(1):86–92.

Shou, M., Ferrario, C. R., Schultz, K. N., Robinson, T. E., and Kennedy, R. T. (2006). Monitoring dopamine in vivo by microdialysis sampling and on-line ce-laser-induced fluorescence. *Anal Chem*, 78(19):6717–6725.

Shou, M., Smith, A. D., Shackman, J. G., Peris, J., and Kennedy, R. T. (2004). In vivo monitoring of amino acids by microdialysis sampling with on-line derivatization by naphthalene-2,3-dicarboxyaldehyde and rapid micellar electrokinetic capillary chromatography. *J Neurosci Methods*, 138(1-2):189–197.

Squire, L. (2003). *Fundamental neuroscience*. Academic Press.

van Horne, C., Hoffer, B., Stromberg, I., and Gerhardt, G. (1992). Clearance and diffusion of locally applied dopamine in normal and 6- hydroxydopamine-lesioned rat striatum. *J Pharmacol Exp Ther*, 263(3):1285–1292.

Wang, M., Roman, G. T., Schultz, K., Jennings, C., and Kennedy, R. T. (2008). Improved temporal resolution for in vivo microdialysis by using segmented flow. *Anal Chem*, 80(14):5607–5615.

Watson, C. J., Venton, B. J., and Kennedy, R. T. (2006). In vivo measurements of neurotransmitters by microdialysis sampling. *Anal. Chem.*, 78(5):1391–1399.

Webster, J. and Clark, J. (1998). *Medical instrumentation: application and design*. Wiley.

Weiland, J. D. and Anderson, D. J. (2000). Chronic neural stimulation with thin-film, iridium oxide electrodes. *IEEE Transactions on Biomedical Engineering*, 47(7):911–918.

Wiedemann, D. J., Kawagoe, K. T., Kennedy, R. T., Ciolkowski, E. L., and Wightman, R. M. (1991). Strategies for low detection limit measurements with cyclic voltammetry. *Anal Chem*, 63(24):2965–2970.

Wightman, R. M., May, L. J., and Michael, A. C. (1988). Detection of dopamine dynamics in the brain. *Anal. Chem.*, 60(13):769A–779A.

Wise, K., Anderson, D., Hetke, J., Kipke, D., and Najafi, K. (2004). Wireless implantable microsystems: high-density electronic interfaces to the nervous system. *Proc. IEEE*, 92(1):76–97.

Wright, S. H. (2004). Generation of resting membrane potential. *Adv Physiol Educ*, 28(1-4):139–142.

Yang, H., Peters, J. L., and Michael, A. C. (1998). Coupled effects of mass transfer and uptake kinetics on in vivo microdialysis of dopamine. *J. Neurochem.*, 71(2):684–692.

Zoski, C., editor (2007). *Handbook of Electrochemistry*. Elsevier.

CHAPTER II

Neural Biosensor Arrays for Simultaneous Recordings of Cholinergic Activity and Electrophysiology with Integrated Drug Delivery

2.1 Introduction

Neural systems communicate through coordinated synaptic neurotransmitter release and electrophysiological signals, yet few tools exist for simultaneously recording these multimodal neural signals with high spatial and temporal resolution. Bridging the electrophysiological and neurochemical domains with sufficient fidelity, resolution, sensitivity, and selectivity can provide novel insights into neurophysiology that lead to improved therapeutic approaches for treating neurological disorders (Villa et al., 2000; Hammond et al., 2007; Agid et al., 2007; Kipke et al., 2008; Johnson et al., 2008; Rohatgi et al., 2009; Howe et al., 2010; Frey et al., 2010; Agnesi et al., 2010). For example, real-time monitoring of multimodal neural activity during drug delivery may have significant implications for improving drug development processes, disease diagnosis, and therapy (Agid et al., 2007; Rohatgi et al., 2009; Seidl et al., 2010). Combining electrophysiology, biosensing, and drug delivery capabilities has the potential to greatly expand investigations of neural systems.

Microelectrodes are commonly used for high-density recording of electrophysio-

logical activity from individual neurons and neuronal ensembles (Vetter et al., 2004; Chapin, 2004; Patil et al., 2004; Moxon et al., 2004; Buzski, 2004; Zhang et al., 2009; Ludwig et al., 2011). Additionally, *in vivo* voltammetry with carbon and platinum microelectrodes is an established method for electrochemically sensing various neurochemicals including dopamine, serotonin, acetylcholine, choline, and glutamate with sub-micromolar (μM) sensitivity and sub-second temporal resolution (Garguilo and Michael, 1995; Burmeister et al., 2002, 2003; Mitchell, 2004; Parikh et al., 2007; Hascup et al., 2008; Kile et al., 2010; Zachek et al., 2010; Flagel et al., 2011). In some cases, these modalities have been combined by alternating between electrophysiology and neurochemical recordings at a single electrode (Cheer et al., 2005) or by extracting low frequency local field potentials from amperometric neurochemical recordings (Zhang et al., 2009).

In vivo voltammetry utilizes a potentiostat to apply a voltage waveform at a microelectrode implanted in the brain to produce a current from the oxidation and/or reduction of analytes at the electrode surface (O'Neill, 1994; Robinson et al., 2008). The resulting faradaic current is proportional to the analyte concentration within the sensor's linear range. Some neurochemicals, such as dopamine and serotonin, are electroactive molecules that undergo oxidation or reduction directly at the electrode surface. Non-electroactive neurotransmitters, such as acetylcholine and glutamate, cannot be measured directly with voltammetric methods. The most common approach for electrochemically detecting these molecules is to enzymatically convert them to an electroactive reporter molecule (e.g. Hydrogen Peroxide or H_2O_2) with an appropriate oxidase enzyme (choline oxidase, glutamate oxidase, etc.) immobilized on the surface of the electrode (Burmeister and Gerhardt, 2001; Mitchell, 2004; O'Neill et al., 2008; Frey et al., 2010). The H_2O_2 is then oxidized at the electrode, which has a typical bias of +0.7V versus Ag/AgCl. With constant potential amperometry, the electrode bias is fixed, and thus the temporal resolution is limited only

by diffusion and the sampling rate of the potentiostat. In the case of acetylcholine, endogenous acetylcholinesterase rapidly converts free acetylcholine to choline. Immobilized choline oxidase at the electrode surface catalyzes the reaction of choline to H_2O_2, which is measured by its faradaic oxidation current, as described below:

$$\mathrm{ACh} + \mathrm{H_2O} \xrightarrow{AChE} \mathrm{Ch} + \text{Acetic Acid} \tag{2.1}$$

$$\mathrm{Ch} + \mathrm{O_2} \xrightarrow{ChOx} 2\mathrm{H_2O_2} + \text{Betaine Aldehyde} \tag{2.2}$$

$$\mathrm{H_2O_2} \xrightarrow[+0.7V]{} \mathrm{O_2} + 2\mathsf{H}^+ + 2e^- \tag{2.3}$$

Microelectrode arrays provide an excellent platform for multimodal neural probes because the electrodes can be spaced closely together for high spatial resolution with dimensions that approach those of the neurons (Buzski, 2004; Johnson et al., 2008; Seymour et al., 2011). In this work, we present a multimodal probe that enables concurrent detection of choline, recording of electrophysiology, and localized drug delivery. We utilized an electrochemically–aided adsorption protocol (Johnson, 1991; Strike et al., 1995; Frey et al., 2010) modified for extremely small microelectrode sizes (area = $625\mu\mathrm{m}^2$) to selectively functionalize individual sites with immobilized choline oxidase and a permselective membrane for choline recording, while allowing neighboring sites to remain unmodified for electrophysiology recordings. We validated the multimodal neural biosensor arrays in anesthetized rat cortex by using the integrated fluidic channel for precise, localized drug delivery. These results confirm the *in vivo* function of the high-density sensing array and highlight the potential for continued *in vivo* investigations of neural systems and diseases.

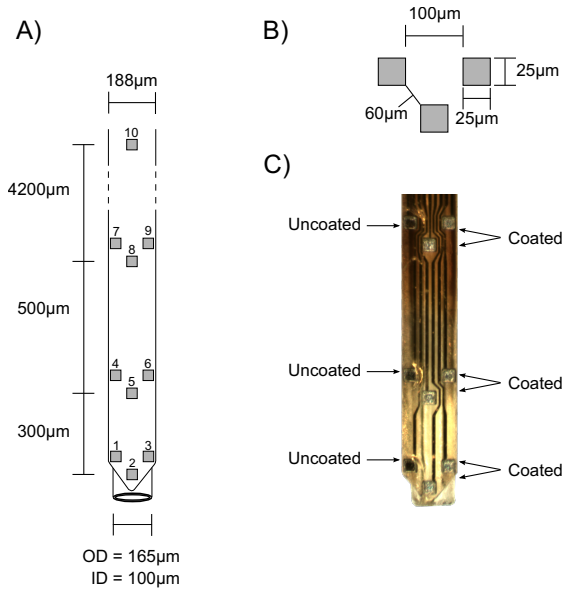

Figure 2.1: Microelectrode Arrays (A) Schematic of biosensors array with dimensions. Each sites is independently addressable, and can be used for either choline through enzyme modification or electrophysiological recordings. The site numbering is used in subsequent figures. (B) Diagram of electrode clusters with dimensions. The sizes and spaces are the same for each cluster. (C) Image of an electrode with enzyme coatings on sites 2,3,5,6, 8, and 9.

2.2 Materials and methods

2.2.1 Fabrication of microsensors

This work utilized custom designed polyimide substrate microelectrode arrays with 10 independently addressable platinum electrode sites (Neuronexus Technologies, Inc., Ann Arbor, MI). The electrode configuration comprised three clusters of three sites placed at the tip, 300μm from the tip and 800μm from the tip with one additional site placed 5mm from the probe tip (see Figure 2.1). Each site was 25μm $\times$ 25μm (area = 625μm^2).

The microelectrode arrays were fabricated on silicon wafers, which served as carriers for the microprocessing steps. Silicon oxide (SiO_2) was deposited on the wafer as a sacrificial layer. A base polyimde layer was deposited, followed by platinum deposition. The platinum was patterned to form the sites, leads, and bond pads. A top

layer of polyimide was deposited and patterned to define the device shape and expose the electrode sites and bond pads. This process produced sites slightly recessed (2μm) from the surface. The arrays were released from the wafer by dissolving the sacrificial oxide layer. After device release, the arrays were epoxied to a fused silica capillary (outer diameter = 165μm, inner diameter = 100μm), which served as an integrated microinjection port for *in vivo* injections of nanoliter fluid volumes. The arrays were bonded to a printed circuit board connector that enabled the independent interfacing of individual microelectrode sites with external instrumentation.

2.2.2 Chemicals

Choline oxidase (ChOx) (EC 1.1.3.17) from arthrobacter globiformis, bovine serum albumin (BSA), glutaraldehyde, m-phenylenediamine, hydrogen peroxide (H_2O_2), choline, ascorbic acid (AA), dopamine (DA), potassium, calcium chloride, sodium chloride, and neostigmine were purchased from Sigma-Aldrich (St. Louis, MO). A 10X concentrate of phosphate buffered saline (PBS) was obtained from Fisher Scientific (Pittsburgh, PA) and used to make 0.01M PBS. All chemicals were prepared in ultra pure filtered water (Millipore, Billerica, MA).

2.2.3 Preparation of biosensor arrays

Initial functionality of each site on an array was confirmed through a two-step process. First, a 1 kHz impedance measurement was conducted using an electrochemical potentiostat/galvanostat (Autolab PGSTAT12, Eco Chemie, Utrecht, The Netherlands). The impedance measurement provides verification that the site has conductivity and serves as one measure of the site's ability to record electrophysiological activity (Humphrey and Schmidt, 1990; Kovacs, 1994; Ludwig et al., 2011). Second, the biosensor arrays were calibrated to H_2O_2. The electrode sites were immersed in a stirred solution of 0.01M PBS at 37°C. Electrode sites were biased with

a constant potential of +0.7V versus an Ag/AgCl reference electrode (Bioanalytical Systems, Inc., West Lafayette, IN) using multichannel potentiostat systems (BioStat, Discovery Technology International, LLLP, Sarasota FL) and sampled at 60Hz, the maximum rate of the potentiostat system. After reaching a stable baseline, H_2O_2 was added to the solution in two 10μM steps. Only sites that had an H_2O_2 sensitivity greater than 10pA/μM (1600 pA/μM/mm^2) were used for electrochemical sensing purposes. The sensitivity, limit of detection, and linearity were calculated using custom automated MATLAB software (The MathWorks, Inc., Natick, MA).

Choline oxidase was immobilized to the electrode surface through electrochemically–aided adsorption optimized for the electrode sites. Previously published electrochemical enzyme immobilization procedures (Frey et al., 2010; Strike et al., 1995; Johnson, 1991) used electrodes an order of magnitude or more larger than the current microelectrode sites (Area = 625μm^2). This important difference in size creates functional differences that affect electrochemical behavior of the electrode. Specifically, as the electrode becomes smaller, radial diffusion becomes the dominate form of mass transport to the electrode surface, which results in higher edge current densities (see also Bard and Faulkner, 2001). One effect of increased relative current densities at the electrode edge can be non-uniform electrodeposition and decreased polymer performance. Rothwell et al. (2009) reported that phenylenediamine loses selectivity for H_2O_2 over ascorbic acid for electrodes with an edge-to-area ratio exceeding 50cm^{-1}. The current electrodes have an edge-to-area ratio of 1600cm^{-1}. Thus, electrochemical functionalization procedures, while not entirely new, were optimized with the current technologies to further decrease electrode size and provide increased spatial resolution within microenvironments of neural systems.

The electrode surface was prepared for deposition with 10 cyclic voltammetry scans between -0.2V and 1.0V versus Ag/AgCl at 50mV per second in 0.01M PBS. For choline oxidase deposition, the array was placed in a 100μL solution of 0.075U/μL

choline oxidase, 1% (w/v) BSA, and 1% (v/v) glutaraldehyde within a custom microchamber with a stainless steel wire as a counter electrode and Ag/AgCl wire as a reference. Electrochemically–aided adsorption at the electrode sites proceeded by a series of 50 current pulses with a magnitude of 31.5nA per electrode site and duration of 5 seconds, followed by a 5-second open circuit relaxation period between pulses. Multiple electrode sites on a single array were coated simultaneously. The electrodeposition is represented schematically in Figure 2.2.

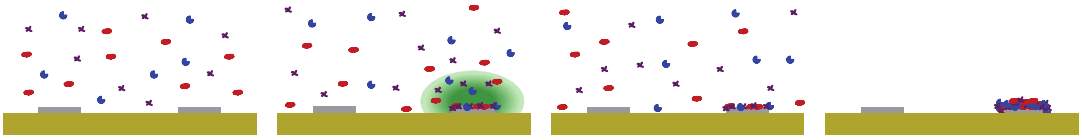

Figure 2.2: Illustration of Electrodeposition Procedure. Electrode sites are selectively coated with immobilized enzyme, while adjacent sites remain uncoated. Electrodepoited sites are cycled between current pulses (step b) and relaxation periods (step c). The pulses attract the charged enzyme to the electrode at a high enough concentration to crosslink with the glutaraldehyde (represented in purple). The relaxation period (steps c) allows for normal mass transfer and more controlled deposition. The process results in selective deposition of the enzyme onto specificied sites (site d). The solution consists of the enzyme (blue), BSA (red), and glutaraldehyde (purple).

A minimum of one site on each array was selected for use as a sentinel or chemical reference site to enable differential measurements for interference rejection and for verifying choline signals *in vivo* (Burmeister and Gerhardt, 2001; Parikh et al., 2004; Frey et al., 2010). The functionalization procedure used a modified solution composition of 1.5% BSA (w/v) and 1% (v/v) glutaraldehyde, with no enzyme. The number (50), magnitude (31.5nA/site), and duration (5 sec pulses, 5 sec open) of the current pulses remained the same. The fluidic channels of the devices were flushed with ultra-purified water to avoid possible clogging from the solutions following the enzyme and sentinel coating procedures.

After coating the electrode sites, a bias of -200mV versus Ag/AgCl was applied in 30 second intervals with a 60 second pause up to 3 times in 0.01M PBS to re-

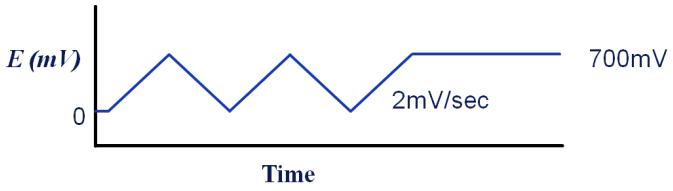

Figure 2.3: m-Phenylenediamine Deposition Procedure. The electrode bias was cycled between 0.0V and 0.7V versus Ag/AgCl at 2mV/sec twice followed by a ramp back up to 0.7V where the potential was held for 15 minutes.

duce oxides that formed during electrochemically–aided adsorption procedures. All choline sensing and sentinel sites, but not sites used for electrophysiology, were then coated with a permselective anti-interference membrane of m-phenylenediamine and resorcinol to provide selectivity over ascorbic acid, dopamine, and other potential interferents (Geise et al., 1991; Mitchell, 2004; Burmeister et al., 2008; Frey et al., 2010). A solution of 5mM m-phenylenediamine and 5mM resorcinol in 0.01M PBS was mixed and immediately purged of oxygen by bubbling N_2 for 30 minutes. After placement in the mPD/resorcinol solution, the electrode bias was cycled between 0.0V and 0.7V versus Ag/AgCl at 2mV/sec twice followed by a ramp back up to 0.7V where the potential was held for 15 minutes.

2.2.4 *In vitro* calibration

Electrode sites functionalized for choline sensing and referencing were calibrated in a stirred solution of 0.01M PBS at 37°C with a constant bias of 0.7V versus Ag/AgCl (as described above for H_2O_2 before functionalization). Functionalized sites were calibrated to ascorbic acid (0-500μM), dopamine (0-10μM), and choline (0-40μM) in succession within the same solution. The sensitivity, limit of detection, linearity, and selectivity for choline over ascorbic acid and dopamine were calculated for each electrode as described previously (Burmeister and Gerhardt, 2001). For selectivity calculations, if no change was detected or the ratio was greater than 1000:1, a value of 1000:1 was used for averaging purposes.

2.2.5 *In vivo* recordings

All animal procedures were approved by the University of Michigan Committee on Use and Care of Animals and complied with the NIH guidelines for the care and use of laboratory animals. Male Sprague-Dawley rats (250-450g, n = 13) were anesthetized with an intraperitoneal injection of urethane (1500mg/kg) and secured to a stereotaxic frame. Body temperature was maintained with a heating pad. Craniotomies (2-3mm in diameter) were made over the prelimbic cortex (AP: +3.0mm, ML: +0.7mm, from bregma) for implanting the microelectrode array and on the contralateral hemisphere (AP: 3.0mm, ML: +2.0mm, from bregma) for implanting an Ag/AgCl wire reference electrode (Paxinos and Watson, 2007). In one group of animals (n = 2), an injection cannula (Plastics One, Roanoke, VA) was implanted into the right lateral ventricle (AP: -0.8mm, ML: 1.5mm, DV: -4.3mm) for injection of neostigmine. One bone screw was placed in each hemisphere for stabilization and grounding for electrophysiology recordings. The biosensor arrays were connected to a custom multi-channel headstage with independently configurable channels that enabled each electrode site to be accessed by either a potentiostat system for electrochemical recordings or an electrophysiology recording system. During *in vivo* recording sessions, the sites designated for electrochemical recording were biased at 0.7V versus the implanted Ag/AgCl wire and sampled at 60Hz with a BioStat multichannel potentiostat (Discovery Technology International, LLLP, Sarasota FL). Sites were allowed to reach a stable baseline for a minimum of 30 minutes after implantation. Electrophysiology recordings were obtained using a Pentusa neural recording system (Tucker-Davis Technologies, Alachua, FL). Local field potentials (LFPs) were filtered from 0.1Hz to 100Hz. Probes were inserted through the craniotomy to target prelimbic cortex (AP: +2.5-350mm, ML: +0.5-1.5mm; DV: -2.5-3.5; from bregma).

Animals received a series of cortical injections of either choline (10mM), KCl (70mM KCl, 2.5mM $CaCl_2$, 75mM NaCl), or high KCl (120mM KCl, 2.5mM $CaCl_2$,

29mM NaCl) through the integrated drug delivery channel. Injections were controlled using a pressure injection system (Ultra 2415 Workstation, Nordson EFD, East Providence, RI). Typical injection volumes ranged from 50nL to 500nL and were monitored by graduated markings on the tubing. Ventricle injections of neostigmine were conducted with a 5μL precision syringe (Hamilton Company, Reno, NV). Neostigmine was used to verify *in vivo* that the recordings at choline-sensitive sites represented choline derived from acetylcholine (Parikh et al., 2004). Neostigmine inhibits the hydrolysis of acetylcholine to choline by acetylcholinesterase (see equation 2.1), which in turn reduces the acetylcholine/choline response at the electrode (see equation 2.3).

After completion of the experiment, probes were removed from the brain and calibrated to verify functionality; however, only pre-experiment calibrations are used for sensitivity reporting.

2.3 Results and Discussion

2.3.1 *In vitro* performance

In this work, we utilized electrodeposition techniques for enzyme immobilization and polymer deposition to develop microelectrode sites sensitive to and selective for choline (Table 2.1). Electrodeposition techniques offer the distinct advantage of discrete functionalization of individual electrode sites, while allowing other electrodes on the same device to remain unmodified, thus it has direct applicability in the development of microscale biosensor arrays.

Forms of electrochemically–aided adsorption for enzyme immobilization have been previously reported using electrodes at least an order of magnitude larger in area than sites on the current microelectrode arrays (Johnson, 1991; Strike et al., 1995; Frey et al., 2010). In the present work, we successfully developed electrochemically–aided enzyme immobilization procedures for choline oxidase deposition on microelectrode

sites with dimensions of 25μm $\times$ 25μm (see Figure 2.1 and Table 2.1).

We successfully polymerized m-phenylenediamine with high selectivity for H_2O_2 on the microelectrode sites using a combination of slow cycling of the applied bias, followed by a constant holding potential. The slow cycling eliminates the initial current surge at the electrode when applying a large bias and results in a stable, uniform polymer layer. This process was used to minimize detrimental edge effects during deposition at micreoelectrodes. The final holding potential improves overall selectivity (Geise et al., 1991; McMahon et al., 2004; Dai et al., 2006; Kirwan et al., 2007; Rothwell et al., 2009). Previous reports showed that the standard constant potential technique for phenylenediamine results in poor selectivity for H_2O_2 over ascorbic acid on electrodes with edge-to-area ratios exceeding 50cm^{-1} (Rothwell et al., 2009). Our modified procedure resulted in high selectivity for electrodes with an edge-to-area ratio of 1600cm^{-1} and an area of 625μm^2, which is an order of magnitude smaller than other reported electrodes (Frey et al., 2010; Burmeister et al., 2003). These procedures, in combination, resulted in differentially functionalized electrode sites with high levels of performance for choline sensing.

Sensitivity pA/μM	**Normalized Sensitivity pA/μM/mm^2**	**Limit of Detection μM**	**Linearity R^2**	**AA Selectivity (Ch:AA)**	**DA Selectivity (Ch:DA)**	**Impedance MΩ**
2.1±0.7	3291±108	0.08±0.09	0.9992±0.0018	896±207	743±432	1.11±0.49

Table 2.1: Probe Performance Specifications for Choline-Electrophysiology Probes
n = 49 for all measurements except impedance where n = 116
Range is ± Standard Deviation

Figure 2.4 shows a typical calibration for three sites modified with ChOx deposition and one chemical reference site. Table 2.1 summarizes the performance data for all sensors. The average sensitivity (n = 49) was 2.1 ± 0.7 pA/μM or 3291 ± 108 pA/μM/mm^2 with a limit of detection of 0.08 ± 0.09μM and linearity (R^2=0.9992 ± 0.0018) across the physiological range (n = 49, reported error is standard deviation).

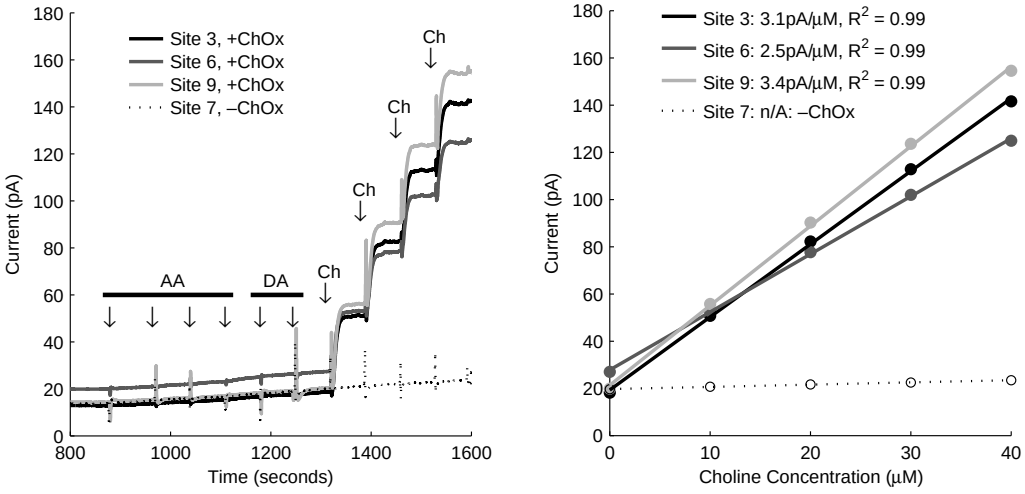

(A) (B)

Figure 2.4: Choline Sensor Calibration (A) Representative calibration data for a set of electrode sites on a single biosensor array. Sites 3,6, and 9 were functionalized with choline oxidase (+ChOx), while site 7 served as a reference site with no choline oxidase (-ChOx). Arrows show injections to adjust the concentration of ascorbic acid (AA: 20μM, 100μM, 200μM, 500μM), dopamine (DA: 2μM, 10μM), and choline (Ch: 10μM, 20μM, 30μM, 40μM). (B) The sensitivity plot for choline of the electrode sites.

The biosensors also exhibited high selectivity over ascorbic acid (896:1) and dopamine (743:1). The sensitivity, when adjusted for area, compares favorably to other amperometric biosensors for choline, which have a reported range of 1200-4000 pA/μM/mm^2 (Parikh et al., 2004; Burmeister et al., 2003; Frey et al., 2010). Electrode sites also had impedance measurements (avg = 1.11MΩ) appropriate for electrophysiology (Table 2.1).

2.3.2 *In vivo*, concurrent choline and electrophysiology recordings

Biosensor arrays were implanted into the prelimbic cortex and validated through local injections of choline, KCl (70mM), or high molarity KCl (120mM). Figure 2.5 shows the response of three choline sensitive sites (Sites 9, 6, and 3) and a sentinel site (Site 1) spatially distributed across the array during a series of 200nL and 400nL injections of 10mM choline. The sensing sites show responses that are both volume-

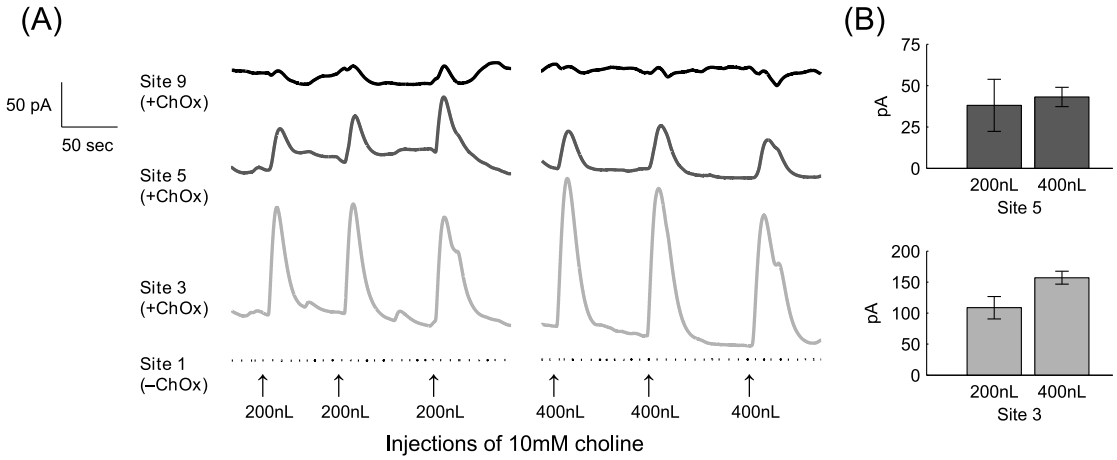

Figure 2.5: Choline–Induced Choline Responses (A) Local injections of choline indicate that the electrodes maintain sensitivity *in vivo*. The responses are dependent on both injection volume and proximity to the injection port. (B) The average responses of each injection volume for site 3 and site 5. Site 3 has better resolution of choline injection volume than site 5 due to its proximity to the choline injection.

and spatially-dependent, while the sentinel site shows no appreciable response. The choline responses show a spatial dependence with stronger responses near the delivery port. Immediately at the injection site, the different volumes are distinguishable by response magnitude. The reasons for nonlinear *in vivo* responses may include signal saturation, reuptake parameters, and/or induced signal cascades (Frey et al., 2010). At 300μm (Site 5) from the injection port, the injections induce measurable responses from both the 200nL and 400nL injections, but factors such as reuptake and diffusion, affect the local concentration such that the volumes become indistinguishable. At 800μm (Site 9), the effects of the choline injections are essentially immeasurable, although other signal cascades may be, and likely are, induced by such injections.

In addition to validating *in vivo* sensitivity, these measurements provide a measure of the spatial 'footprint' of injections through the delivery port. While this pattern of spatially dependent responses is not unexpected, it is an important consideration for localized drug delivery studies. Small changes in the placement of an injection cannula in relation to a sensor can have significant effects on measured responses due

to physical (diffusion) and biological (reuptake, signal cascades) effects, even with highly responsive sensors.

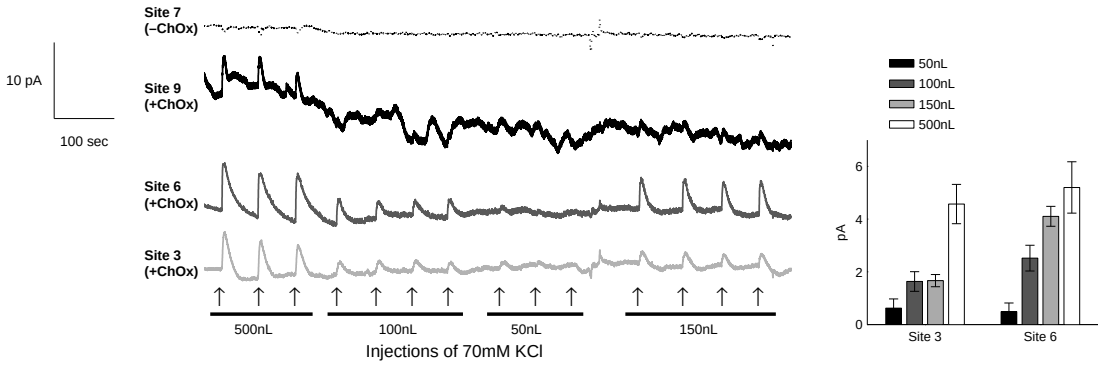

(A) (B)

Figure 2.6: K^+–Induced Depolarization Responses (A) Injections of various volumes of 70mM KCl cause local ACh release, which is recorded at the sensor sites. Response magnitudes are effected by spatial proximity to the injection site and injection volume. (B) The average magnitude of the responses at sites 3 and 6 for the data in (A).

Biosensor function was further verified through controlled injections of KCl to elicit acetylcholine release through depolarization. K^+–evoked responses were robust and repeatable (Figure 2.6). As seen with choline–induced responses, the K^+-induced ACh responses were dependent on spatial relationships and injection volumes. Interestingly, and in contrast to choline injections, the responses of the sites nearest the injection site frequently have a smaller magnitude than those slightly further away (see also Figure 2.7). One plausible explanation for this effect is that the injection dilutes the local chemical concentrations in the immediate vicinity of the injection port. As it diffuses, the dilution effect is reduced, but the concentration of K^+ remains high enough to cause ACh release through depolarization.

In Figure 2.6, the recording sensor site nearest the drug delivery port (Site 3) and the one separated by 300μm (Site 6) both show a response to injections of 70mM KCl. The more distal recording site (800μm from the point of injection) has a distinct response to KCl injections only at the highest volume (500nL) injections. The site appears noisy during the injection period, yet pre- and post-implant calibration reflect

high, stable sensitivity at the site (pre-implant = 2.55pA/μM, baseline = 16pA, post-implant = 2.38pA/μM, baseline = 17pA). Additionally, baseline data collected before initial injections were stable (data not shown). These distal cholinergic responses indicate that this site resided at the edge of the immediate response field of the injections. The dynamics recorded at this site may reflect slower diffusion of KCl and/or compensatory feedback mechanisms more distal from the immediate injection site.

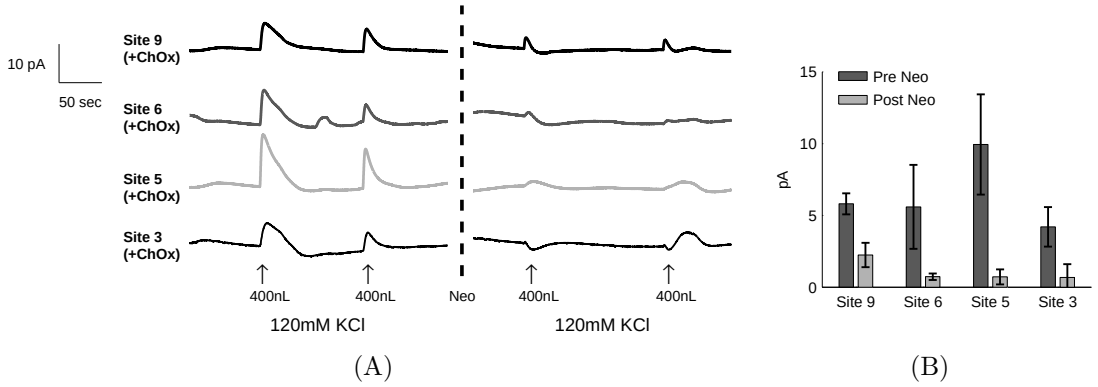

Figure 2.7: K^+-Induced Depolarization Responses with Neostigmine Injections (A) Injections of 120mM KCl cause local ACh release, but neostigmine reduces that response, indicating that the measured response is due to endogenous acetylcholine release (B) The average magnitude of the responses at sites 3,5,6, and 9 for the data in (A).

In order to verify that the choline measurements were attributable to endogenously released acetylcholine, 120mM KCl injections were followed by ventricle injections of 100mM neostigmine to inhibit the hydrolysis of acetylcholine by acetylcholinesterase (Figure 2.7). The neostigmine attenuated the K^+–induced response by 81 $\pm$ 14% (n = 4), which indicates that the recordings are a reflection of acetylcholine release. This attenuation is similar in magnitude to that seen in validating other choline biosensors (Parikh et al., 2004; Frey et al., 2010). In the data represented in Figure 2.7, a cholinergic response was recorded even at the most distal site 800μM from the injection. This may be attributed to the higher KCl concentration (120mM) utilized

for this experiment, which causes depolarization through a larger diffusion sphere that included the more distal sites. We most commonly observed responses at the two sets of sites near the tip, but responses at distal sites varied. While this can be attributed in part to variations in experimental parameters such as injection volume or concentration, it may also be affected by differences in probe location, local tissue damage, reuptake dynamics, neural projections, signal cascades, or other feedback mechanisms.

The precise, confined deposition of the biosensor coatings allows neighboring sites to remain unmodified, which is a benefit for multi-modal sensing applications, including electrophysiology, where a bare surface is commonly used for recording purposes. In this work, we were particularly interested in recording local field potentials (LFPs) as a starting point for combined electrophysiology recordings. LFPs represent the synchronized activity of neural systems, and have been shown to relate to neurochemical dynamics (Johnson et al., 2008; Zhang et al., 2009). The microelectrode arrays were able to obtain electrophysiology recordings on a subset of electrode sites, while concurrently recording cholinergic activity on neighboring sites. Figure 2.8 shows traces for LFP data (0.1-100Hz) with choline responses during injections of 70mM KCl.

While we were able to record field potentials, we did not typically record unit activity. The most likely cause of reduced unit activity is the urethane anesthesia, which has been noted to significantly reduce or eliminate electrophysiology in deep anesthetic states(Friedberg et al., 1999; Devonshire et al., 2010; Sceniak and Maciver, 2006); however, urethane is commonly used for recording neurochemical responses in anesthetized animals (Parikh et al., 2004; Burmeister et al., 2003). The ability to record is a positive sign of the proper function of these electrodes for recording electrophysiology. Additionally, they have appropriate performance characteristics to expect unit activity in other experimental setups, which will include behavioral paradigms in the future.

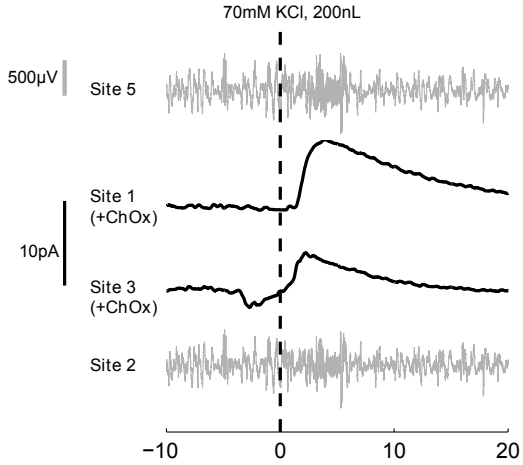

Figure 2.8: Simultaneous Electrophysiology, Cholinergic Recording, and Drug Delivery. Sites 2 and 5 recorded local field potentials, while sites 1 and 3 simultaneously recorded cholinergic activity

2.4 Conclusion

In this work, we validated a neural biosensor probe that establishes a multimodal neural interface through choline recordings, electrophysiology recordings, and localized drug delivery. We utilized electrodeposition procedures for choline oxidase immobilization and membrane polymerization to selectively functionalize electrode sites within a high-density array to provide high spatial and temporal resolution for recording and modulating neural dynamics.

These neural biosensor arrays can provide novel investigation in neurophysiology and neuropathologies. While the current work focuses on the validation of these techniques in an acute preparation, future work will investigate the neurochemical and electrophysiological dynamics within disease models and behavioral experiments. Furthermore, many other neurotransmitters including, dopamine, serotonin, glutamate, and GABA, play important roles in neurophysiology and neuropathologies and suggest a strong need for multi-analyte, multimodal neural interfaces. The ability to record neurochemical and electrophysiology interactions is important for advancing our understanding of Parkinson's disease, Alzheimer's disease, and other neurological

disorders.

Acknowledgements

I would like to thank Karen Schroeder, Paras Patel, Usha Ramkrishna, Nick Langhals, Matt Johnson, Ralph Lydic, Vinay Parikh, Martin Sarter, Matt Howe, and Howard Gritton for assistance with this work. This work was supported by a National Science Foundation Graduate Fellowship, the Coulter Foundation, and the Center for Neural Communication Technology. The Center for Neural Communication Technology is a P41 Resource Center funded by the National Institute of Biomedical Imaging and Bioengineering (NIBIB, P41 EB002030) and supported by the National Institutes of Health (NIH).

References

Agid, Y., Buzsaki, G., Diamond, D. M., Frackowiak, R., Giedd, J., Girault, J.-A., Grace, A., Lambert, J. J., Manji, H., Mayberg, H., Popoli, M., Prochiantz, A., Richter-Levin, G., Somogyi, P., Spedding, M., Svenningsson, P., and Weinberger, D. (2007). How can drug discovery for psychiatric disorders be improved? *Nat. Rev. Drug Discovery*, 6(3):189–201.

Agnesi, F., Blaha, C. D., Lin, J., and Lee, K. H. (2010). Local glutamate release in the rat ventral lateral thalamus evoked by high-frequency stimulation. *J Neural Eng*, 7(2):26009.

Bard, A. and Faulkner, L. (2001). *Electrochemical methods: fundamentals and applications*. Wiley, 2nd edition.

Burmeister, J. J. and Gerhardt, G. A. (2001). Self-referencing ceramic-based multisite microelectrodes for the detection and elimination of interferences from the measurement of l-glutamate and other analytes. *Anal. Chem.*, 73(5):1037–1042.

Burmeister, J. J., Palmer, M., and Gerhardt, G. A. (2003). Ceramic-based multisite microelectrode array for rapid choline measures in brain tissue. *Anal. Chim. Acta*, 481(1):65–74.

Burmeister, J. J., Pomerleau, F., Huettl, P., Gash, C. R., Werner, C. E., Bruno, J. P., and Gerhardt, G. A. (2008). Ceramic-based multisite microelectrode arrays for simultaneous measures of choline and acetylcholine in cns. *Biosensors & bioelectronics*, 23(9):1382–1389.

Burmeister, J. J., Pomerleau, F., Palmer, M., Day, B. K., Huettl, P., and Gerhardt, G. A. (2002). Improved ceramic-based multisite microelectrode for rapid measurements of -glutamate in the cns. *J Neurosci Methods*, 119(2):163–171.

Buzski, G. (2004). Large-scale recording of neuronal ensembles. *Nat Neurosci*, 7(5):446–451.

Chapin, J. K. (2004). Using multi-neuron population recordings for neural prosthetics. *Nat Neurosci*, 7(5):452–455.

Cheer, J. F., Heien, M. L. A. V., Garris, P. A., Carelli, R. M., and Wightman, R. M. (2005). Simultaneous dopamine and single-unit recordings reveal accumbens gabaergic responses: implications for intracranial self-stimulation. *Proc. Natl. Acad. Sci. U. S. A.*, 102(52):19150–19155.

Dai, Y.-Q., Zhou, D.-M., and Shiu, K.-K. (2006). Permeability and permselectivity of polyphenylenediamine films synthesized at a palladium disk electrode. *Electrochimica Acta*, 52(1):297–303.

Devonshire, I. M., Grandy, T. H., Dommett, E. J., and Greenfield, S. A. (2010). Effects of urethane anaesthesia on sensory processing in the rat barrel cortex revealed by combined optical imaging and electrophysiology. *European Journal of Neuroscience*, 32(5):786–797.

Flagel, S. B., Clark, J. J., Robinson, T. E., Mayo, L., Czuj, A., Willuhn, I., Akers, C. A., Clinton, S. M., Phillips, P. E. M., and Akil, H. (2011). A selective role for dopamine in stimulus-reward learning. *Nature*, 469(7328):53–57.

Frey, O., Holtzman, T., McNamara, R. M., Theobald, D. E. H., van der Wal, P. D., de Rooij, N. F., Dalley, J. W., and Koudelka-Hep, M. (2010). Enzyme-based choline and l-glutamate biosensor electrodes on silicon microprobe arrays. *Biosensors & Bioelectronics*, 26(2):477–484.

Friedberg, M. H., Lee, S. M., and Ebner, F. F. (1999). Modulation of receptive field properties of thalamic somatosensory neurons by the depth of anesthesia. *J Neurophysiol*, 81(5):2243–2252.

Garguilo, M. G. and Michael, A. C. (1995). Enzyme-modified electrodes for peroxide, choline, and acetylcholine. *TrAC Trends in Analytical Chemistry*, 14(4):164–169.

Geise, R. J., Adams, J. M., Barone, N. J., and Yacynych, A. M. (1991). Electropolymerized films to prevent interferences and electrode fouling in biosensors. *Biosensors and Bioelectronics*, 6(2):151–160.

Hammond, C., Bergman, H., and Brown, P. (2007). Pathological synchronization in parkinson's disease: networks, models and treatments. *Trends in Neurosciences*, 30(7):357–364.

Hascup, K. N., Hascup, E. R., Pomerleau, F., Huettl, P., and Gerhardt, G. A. (2008). Second-by-second measures of l-glutamate in the prefrontal cortex and striatum of freely moving mice. *The Journal of pharmacology and experimental therapeutics*, 324(2):725–731.

Howe, W. M., Ji, J., Parikh, V., Williams, S., Mocar, E., Trocm-Thibierge, C., and Sarter, M. (2010). Enhancement of attentional performance by selective stimulation of alpha4beta2(*) nachrs: underlying cholinergic mechanisms. *Neuropsychopharmacology*, 35(6):1391–1401.

Humphrey, D. R. and Schmidt, E. M. (1990). Extracellular single-unit recording methods. In *Neuromethods*, volume 15, pages 1–64. Humana Press, Clifton, NJ.

Johnson, K. W. (1991). Reproducible electrodeposition of biomolecules for the fabrication of miniature electroenzymatic biosensors. *Sensors and Actuators B: Chemical*, 5(1-4):85–89.

Johnson, M. D., Franklin, R. K., Gibson, M. D., Brown, R. B., and Kipke, D. R. (2008). Implantable microelectrode arrays for simultaneous electrophysiological and neurochemical recordings. *J Neurosci Methods*, 174(1):62–70.

Kile, B. M., Guillot, T. S., Venton, B. J., Wetsel, W. C., Augustine, G. J., and Wightman, R. M. (2010). Synapsins differentially control dopamine and serotonin release. *J Neurosci*, 30(29):9762–9770.

Kipke, D. R., Shain, W., Buzski, G., Fetz, E., Henderson, J. M., Hetke, J. F., and Schalk, G. (2008). Advanced neurotechnologies for chronic neural interfaces: new horizons and clinical opportunities. *J Neurosci*, 28(46):11830–11838.

Kirwan, S., Rocchitta, G., McMahon, C., Craig, J., Killoran, S., O'Brien, K., Serra, P., Lowry, J., and O'Neill, R. (2007). Modifications of poly(o-phenylenediamine) permselective layer on pt-ir for biosensor application in neurochemical monitoring. *Sensors*, 7(4):420–437.

Kovacs, G. T. A. (1994). Introduction to the theory, design and modeling of thin-film microelectrodes for neural interfaces. In Stenger, D. and McKenna, T., editors, *Enabling Technologies for Cultured Neural Networks*, pages 121–166. Academic Press, New York.

Ludwig, K. A., Langhals, N. B., Joseph, M. D., Richardson-Burns, S. M., Hendricks, J. L., and Kipke, D. R. (2011). Poly(3,4-ethylenedioxythiophene) (pedot) polymer coatings facilitate smaller neural recording electrodes. *Journal of neural engineering*, 8(1):014001.

McMahon, C. P., Killoran, S. J., Kirwan, S. M., and O'Neill, R. D. (2004). The selectivity of electrosynthesised polymer membranes depends on the electrode dimensions: implications for biosensor applications. *Chem Commun (Camb)*, 40(18):2128–2130.

Mitchell, K. M. (2004). Acetylcholine and choline amperometric enzyme sensors characterized in vitro and in vivo. *Anal. Chem.*, 76(4):1098–1106.

Moxon, K. A., Kalkhoran, N. M., Markert, M., Sambito, M. A., McKenzie, J. L., and Webster, J. T. (2004). Nanostructured surface modification of ceramic-based microelectrodes to enhance biocompatibility for a direct brain-machine interface. *IEEE Trans Biomed Eng*, 51(6):881–889.

O'Neill, R. D. (1994). Microvoltammetric techniques and sensors for monitoring neurochemical dynamics in vivo. a review. *Analyst*, 119(5):767–779.

O'Neill, R. D., Rocchitta, G., McMahon, C. P., Serra, P. A., and Lowry, J. P. (2008). Designing sensitive and selective polymer/enzyme composite biosensors for brain monitoring in vivo. *TrAC Trends in Analytical Chemistry*, 27(1):78–88.

Parikh, V., Kozak, R., Martinez, V., and Sarter, M. (2007). Prefrontal acetylcholine release controls cue detection on multiple timescales. *Neuron*, 56(1):141–154.

Parikh, V., Pomerleau, F., Huettl, P., Gerhardt, G. A., Sarter, M., and Bruno, J. P. (2004). Rapid assessment of in vivo cholinergic transmission by amperometric

detection of changes in extracellular choline levels. *Eur. J. Neurosci.*, 20(6):1545–1554.

Patil, P. G., Carmena, J. M., Nicolelis, M. A. L., and Turner, D. A. (2004). Ensemble recordings of human subcortical neurons as a source of motor control signals for a brain-machine interface. *Neurosurgery*, 55(1):27–35; discussion 35–8.

Paxinos, G. and Watson, C. (2007). *The Rat Brain in Stereotaxic Coordinates, Sixth Edition*. Academic Press, London, UK, 6th edition.

Robinson, D. L., Hermans, A., Seipel, A. T., and Wightman, R. M. (2008). Monitoring rapid chemical communication in the brain. *Chem Rev*, 108(7):2554–2584.

Rohatgi, P., Langhals, N. B., Kipke, D. R., and Patil, P. G. (2009). In vivo performance of a microelectrode neural probe with integrated drug delivery. *Neurosurgical focus*, 27(1):E8.

Rothwell, S. A., Kinsella, M. E., Zain, Z. M., Serra, P. A., Rocchitta, G., Lowry, J. P., and O'Neill, R. D. (2009). Contributions by a novel edge effect to the permselectivity of an electrosynthesized polymer for microbiosensor applications. *Anal. Chem.*, 81(10):3911–3918.

Sceniak, M. P. and Maciver, M. B. (2006). Cellular actions of urethane on rat visual cortical neurons in vitro. *J Neurophysiol*, 95(6):3865–3874.

Seidl, K., Spieth, S., Herwik, S., Steigert, J., Zengerle, R., Paul, O., and Ruther, P. (2010). In-plane silicon probes for simultaneous neural recording and drug delivery. *Journal of Micromechanics and Microengineering*, 20(10):105006–.

Seymour, J. P., Langhals, N. B., Anderson, D. J., and Kipke, D. R. (2011). Novel multi-sided, microelectrode arrays for implantable neural applications. *Biomed Microdevices*.

Strike, D. J., de Rooij, N. F., and Koudelka-Hep, M. (1995). Electrochemical techniques for the modification of microelectrodes. *Biosens. Bioelectron.*, 10(1-2):61–66.

Vetter, R. J., Williams, J. C., Hetke, J. F., Nunamaker, E. A., and Kipke, D. R. (2004). Chronic neural recording using silicon-substrate microelectrode arrays implanted in cerebral cortex. *IEEE Transactions on Biomedical Engineering*, 51(6):896–904.

Villa, A. E. P., Tetko, I. V., Dutoit, P., and Vantini, G. (2000). Non-linear cortico-cortical interactions modulated by cholinergic afferences from the rat basal forebrain. *Biosystems*, 58(1-3):219–228.

Zachek, M. K., Takmakov, P., Park, J., Wightman, R. M., and McCarty, G. S. (2010). Simultaneous monitoring of dopamine concentration at spatially different brain locations in vivo. *Biosens Bioelectron*, 25(5):1179–1185.

Zhang, H., Lin, S.-C., and Nicolelis, M. A. L. (2009). Acquiring local field potential information from amperometric neurochemical recordings. *J Neurosci Methods*, 179(2):191–200.

CHAPTER III

Multi-modal Neural Biosensors for Choline, Glutamate, and Electrophysiology Recordings with Localized Drug Delivery

3.1 Introduction

Recent advances in neural microelectrode technologies have greatly expanded investigations of neural systems from both an electrophysiology perspective (Ward et al., 2009; Kipke et al., 2008) and neurochemical perspective (Michael and Borland, 2007). Carbon fiber electrodes are well established for recording dopamine signals, while amperometric biosensors for monitoring choline/acetylcholine, glutamate, and other non-electroactive biomolecules have gained increased use (Burmeister and Gerhardt, 2001; Burmeister et al., 2002, 2003, 2005; Michael and Borland, 2007; Parikh et al., 2004, 2007; Hashemi and Wightman, 2007; Walker et al., 2007; Wassum et al., 2008). Many electrochemical neural sensors function on a subsecond timescale making them particularly appropriate for studying fast neurochemical dynamics. Other techniques, such as microdialysis and radioactive labeling, are unable to monitor these events (Sarter et al., 2007). This important ability has revealed new information regarding neurochemical dynamics (Sabeti et al., 2002; Daws et al., 2005; Parikh et al., 2004; Binns et al., 2005; Bruno et al., 2006; Parikh and Sarter, 2006; Oldenziel et al., 2006),

and notable differences in the regulation of basal versus phasic dopamine, glutamate, acetylcholine release (Phillips et al., 2003; Wightman and Robinson, 2002; Day et al., 2006; Owesson-White et al., 2008; Parikh et al., 2008; Aragona et al., 2009; Agnesi et al., 2010). These findings may play important roles in the development of disease therapies.

Virtually all neural function utilizes multiple neurotransmitter systems with complex dynamics at multiple levels. For example, Parikh et al. investigated the roles of various cortical nicotinic acetylcholine receptor subtypes in the regulation of cholinergic and glutamatergic dynamics in the context of cue detection and attentional performance (Parikh et al., 2010, 2008). In these studies, the researchers utilized multiple sets of animals each recording a single neurotransmitter, either choline or glutamate. While the researchers were effective in these studies, between animal variations can cloud important aspects of these systems, including comparisons of concentration levels and precise timing aspects of the involved neurotransmitters and electrophysiological changes.

This work presents the development and validation of multimodal neural biosensor arrays for recording and modulating multimodal neural dynamics. We utilize multiple electrochemical methods for site-selective functionlization coatings of enzymes (choline oxidase and glutamate oxidase) and polymers (p-3,4-ethylenedioxythiophene or PEDOT, and poly-m-phenylenediamine) to individual, high-density microelectrode sites to enable simultaneous recordings of choline, glutamate, and electrophysiology. The devices also allow for localized drug delivery of precise nanoliter volumes through an integrated drug delivery channel, which is used for the validation of sensing modalities.

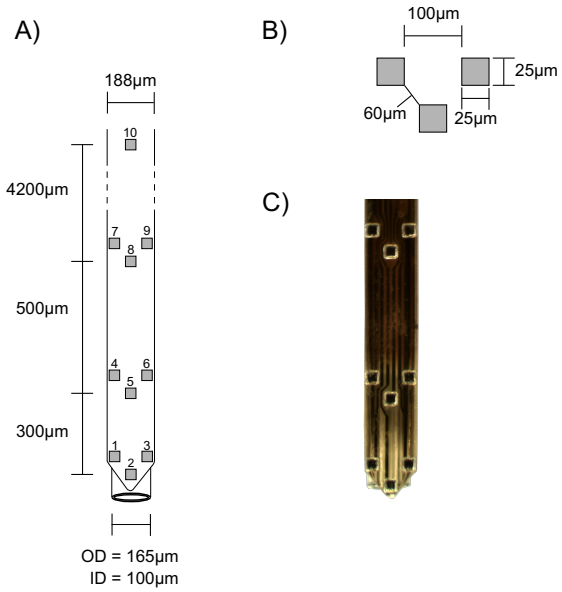

Figure 3.1: Microelectrode Arrays (A) Schematic of biosensors array with dimensions. Each sites is independently addressable, and can be used for either choline through enzyme modification or electrophysiological recordings. The numbering used to identify the sites is used in subsequent figures. A typical functionalization configuration for this work was to deposit PEDOT on sites 2 and 5, choline oxidase on sites 3,6, and 9, glutamate oxidase on sites 1,4 and 7, and neurochemical reference coatings on sites 8 and 10. (B) Diagram of electrode clusters with dimensions. The sizes and spaces are the same for each cluster. (C) Image of an electrode

3.2 Materials and methods

3.2.1 Fabrication of microsensors

This work utilized custom designed polyimide substrate microelectrode arrays with 10 independently addressable platinum electrode sites (Neuronexus Technologies, Inc., Ann Arbor, MI). The electrode configuration comprised three clusters of three sites placed at the tip, 300μm from the tip and 800μm from the tip with one additional site placed 5mm from the probe tip (see Figure 3.1). Each site was 25μm $\times$ 25μm (area = 625μm^2).

The microelectrode arrays were fabricated on silicon wafers, which served as carriers for the microprocessing steps. Silicon oxide (SiO_2) was deposited on the wafer as a sacrificial layer. A base polyimde layer was deposited, followed by platinum de-

position. The platinum was patterned to form the sites, leads, and bond pads. A top layer of polyimide was deposited and patterned to define the device shape and expose the electrode sites and bond pads. This process produced sites slightly recessed (2μm) from the surface. The arrays were released from the wafer by dissolving the sacrificial oxide layer. After device release, the arrays were epoxied to a fused silica capillary (outer diameter = 165μm, inner diameter = 100μm), which served as an integrated microinjection port for *in vivo* injections of nanoliter fluid volumes. The arrays were bonded to a printed circuit board connector that enabled the independent interfacing of individual microelectrode sites with external instrumentation.

3.2.2 Chemicals

Choline oxidase (ChOx) (EC 1.1.3.17) from arthrobacter globiformis, bovine serum albumin (BSA), glutaraldehyde, m-phenylenediamine, hydrogen peroxide (H_2O_2), choline, L-Glutamic acid (glutamate), ascorbic acid (AA), dopamine (DA), potassium, calcium chloride, sodium chloride, 3,4-ethylenedioxythiophene (EDOT), polystyrene sulfonate (PSS), and nicotine were purchased from Sigma-Aldrich (St. Louis, MO). L-Glutamate oxidase (EC 1.4.3.11)) was purchased from U.S. Biological (Swampscott, MA). A 10X concentrate of phosphate buffered saline (PBS) was obtained from Fisher Scientific (Pittsburgh, PA) and used to make 0.01M PBS. All chemicals were prepared in ultra pure filtered water (Millipore, Billerica, MA).

3.2.3 Preparation of biosensor arrays

Initial functionality of each site on an array was confirmed through a two-step process. First, a 1 kHz impedance measurement was conducted using an electrochemical potentiostat/galvanostat (Autolab PGSTAT12, Eco Chemie, Utrecht, The Netherlands). The impedance measurement provides verification that the site has conductivity and serves as one measure of the site's ability to record electrophysio-

logical activity (Humphrey and Schmidt, 1990; Kovacs, 1994; Ludwig et al., 2011). Second, the biosensor arrays were calibrated to H_2O_2. The electrode sites were immersed in a stirred solution of 0.01M PBS at 37°C. Electrode sites were biased with a constant potential of +0.7V versus an Ag/AgCl reference electrode (Bioanalytical Systems, Inc., West Lafayette, IN) using multichannel potentiostat systems (BioStat, Discovery Technology International, LLLP, Sarasota FL) and sampled at 60Hz, the maximum rate of the potentiostat system. After reaching a stable baseline, H_2O_2 was added to the solution in two 10μM steps. Only sites that had an H_2O_2 sensitivity greater than 10pA/μM (1600 pA/μM/mm^2) were used for electrochemical sensing purposes. The sensitivity, limit of detection, and linearity were calculated using custom automated MATLAB software (The MathWorks, Inc., Natick, MA).

The first functionalization procedure was deposition of PEDOT. PEDOT has been shown to improve electrophysiology recordings of microelectrodes (Ludwig et al., 2006, 2011; Seymour et al., 2011). Polymerization of PEDOT was conducted in a solution of 0.01M EDOT and 0.1M PSS in purified water. A constant current of 3nA per sites applied for 9 minutes for a total charge density of 2.6nC/μm^2. Impedance measurements were taken before and after PEDOT deposition.

Electrode sites were modified for choline and glutamate sensing by immobilization of choline oxidase and glutamate oxidase, respectively. These enzymes convert choline and glutamate to H_2O_2, which can be measured by biasing the electrode to 700mV versus an Ag/AgCl reference electrode. The oxidation of H_2O_2 produces a current proportional to the concentration of the analyte of interest.

Choline oxidase and glutamate oxidase were immobilized to the electrode surface through electrochemically–aided adsorption optimized for the electrode sites. Previously published electrochemical enzyme immobilization procedures (Frey et al., 2010; Strike et al., 1995; Johnson, 1991) used electrodes an order of magnitude or more larger than the current microelectrode sites (Area = 625μm^2). This important differ-

ence in size creates functional differences that affect electrochemical behavior of the electrode. Specifically, as the electrode becomes smaller, radial diffusion becomes the dominate form of mass transport to the electrode surface, which results in higher edge current densities (see also Bard and Faulkner (2001)). One effect of increased relative current densities at the electrode edge can be non-uniform electrodeposition and decreased polymer performance. Rothwell et al. (2009) reported that phenylenediamine loses selectivity for H_2O_2 over ascorbic acid for electrodes with an edge-to-area ratio exceeding 50cm^{-1}. The current electrodes have an edge-to-area ratio of 1600cm^{-1}. Thus, electrochemical functionalization procedures, while not entirely new, were optimized with the current technologies to further decrease electrode size and provide increased spatial resolution within microenvironments of neural systems.

The electrode surface was prepared for deposition with 10 cyclic voltammetry scans between -0.2V and 1.0V versus Ag/AgCl at 50mV per second in 0.01M PBS. For choline oxidase deposition, the array was placed in a 100μL solution of $0.075\text{U}/\mu\text{L}$ choline oxidase, 1% (w/v) BSA, and 1% (v/v) glutaraldehyde within a custom microchamber with a stainless steel wire as a counter electrode and Ag/AgCl wire as a reference. electrochemically–aided adsorption at the electrode sites proceeded by a series of 50 current pulses with a magnitude of 31.5nA per electrode site and duration of 5 seconds, followed by a 5-second open circuit relaxation period between pulses. Multiple electrode sites on a single array were coated simultaneously.

For glutamate oxidase deposition, the array was placed in a 26μL solution of $0.075\text{U}/\mu\text{L}$ glutamate oxidase, 1% (w/v) BSA, and 1% (v/v) glutaraldehyde within a custom microchamber with a stainless steel wire as a counter electrode and Ag/AgCl wire as a reference. electrochemically–aided adsorption at the electrode sites proceeded by a series of 25 voltage pulses with a magnitude of 1.8V vs. Ag/AgCl per electrode site and duration of 5 seconds, followed by a 5-second open circuit relaxation period between pulses. Multiple electrode sites on a single array were coated

simultaneously. The glutamate oxidase did not deposit effectively to the electrode site when current pulses were used. Care must be taken during various electrode deposition procedures to avoid degradation of microelectrode sites.

A minimum of one site on each array was selected for use as a sentinel or chemical reference site to enable differential measurements for interference rejection and for verifying choline signals *in vivo* (Burmeister and Gerhardt, 2001; Parikh et al., 2004; Frey et al., 2010). The functionalization procedure used a modified solution composition of 1.5% BSA (w/v) and 1% (v/v) glutaraldehyde, with no enzyme. The number (50), magnitude (31.5nA/site), and duration (5 sec pulses, 5 sec open) of the current pulses remained the same as for choline oxidase immobilization. The fluidic channels of the devices were flushed with ultra-purified water after each procdure to avoid possible clogging from the solutions.

After coating the electrode sites, a bias of -200mV versus Ag/AgCl was applied in 30 second intervals with a 60 second pause up to 3 times in 0.01M PBS to reduce oxides that formed during electrochemically–aided adsorption procedures. All choline, glutamate, and neurochemical reference sites, but not sites used for electrophysiology, were then coated with a permselective anti-interference membrane of m-phenylenediamine and resorcinol to provide selectivity over ascorbic acid, dopamine, and other potential interferents (Geise et al., 1991; Mitchell, 2004; Burmeister et al., 2008; Frey et al., 2010). A solution of 5mM m-phenylenediamine and 5mM resorcinol in 0.01M PBS was mixed and immediately purged of oxygen by bubbling N_2 for 30 minutes. After placement in the mPD/resorcinol solution, the electrode bias was cycled between 0.0V and 0.7V versus Ag/AgCl at 2mV/sec twice followed by a ramp back up to 0.7V where the potential was held for 15 minutes.

The typical order of functionalization was: PEDOT polymerization, neurochemical reference coating, choline oxidase immobilzation, glutamate oxidase immobilization, m-phenylenediamine polymerization.

3.2.4 *In vitro* calibration

Electrode sites functionalized for neurotransmitter sensing and referencing were calibrated in a stirred solution of 0.01M PBS at 37°C with a constant bias of 0.7V versus Ag/AgCl (as described above for H_2O_2 before functionalization). Functionalized sites were calibrated to ascorbic acid (0-500μM), dopamine (0-10μM), glutamate (0-20μM), and choline (0-40μM) in succession within the same solution. The sensitivity, limit of detection, linearity, and selectivity for glutamate and choline over ascorbic acid and dopamine were calculated for each electrode as described previously (Burmeister and Gerhardt, 2001). For selectivity calculations, if no change was detected or the ratio was greater than 1000:1, a value of 1000:1 was used for averaging purposes.

3.2.5 *In vivo* recordings

All animal procedures were approved by the University of Michigan Committee on Use and Care of Animals and complied with the NIH guidelines for the care and use of laboratory animals. Male Sprague-Dawley rats (275-450g, n = 7) were anesthetized with an intraperitoneal injection of urethane (1500mg/kg) and secured to a stereotaxic frame. Body temperature was maintained with a heating pad. Craniotomies (2-3mm in diameter) were made over the prelimbic cortex (AP: +3.0mm, ML: +0.7mm, from bregma) for implanting the microelectrode array and on the contralateral hemisphere (AP: 3.0mm, ML: +2.0mm, from bregma) for implanting an Ag/AgCl wire reference electrode (Paxinos and Watson, 2007). One bone screw was placed in each hemisphere for stabilization and grounding for electrophysiology recordings.

The biosensor arrays were connected to a custom multi-channel headstage with independently configurable channels that enabled each electrode site to be accessed by either a potentiostat system for electrochemical recordings or an electrophysiology recording system. During *in vivo* recording sessions, the sites designated for elec-

trochemical recording were biased at 0.7V versus the implanted Ag/AgCl wire and sampled at 60Hz with a BioStat multichannel potentiostat (Discovery Technology International, LLLP, Sarasota FL). Sites were allowed to reach a stable baseline for a minimum of 30 minutes after implantation. Electrophysiology recordings were obtained using a Pentusa neural recording system (Tucker-Davis Technologies, Alachua, FL). Local field potentials (LFPs) were filtered from 0.1Hz to 100Hz. Probes were inserted through the craniotomy to target prelimbic cortex (AP: +2.5-350mm, ML: +0.5-1.5mm; DV: -2.5-3.5; from bregma).

Animals received a series of cortical injections of either choline (10mM), glutamate (10mM), KCl (70mM KCl, 2.5mM $CaCl_2$, 75mM NaCl), or nicotine (5mM) through the integrated drug delivery channel. Injections were controlled using a pressure injection system (Ultra 2415 Workstation, Nordson EFD, East Providence, RI). Typical injection volumes ranged from 25nL to 500nL and were monitored by graduated markings on the tubing.

After completion of the experiment, probes were removed from the brain and calibrated to verify functionality.

3.3 Results

3.3.1 *In vitro* Performance

We utilized five separate electrodeposition procedures (PEDOT polymerization, neurochemical reference coating, choline oxidase immobilzation, glutamate oxidase immobilization, m-phenylenediamine polymerization) to successfully functionalize the biosensor arrays. Specified sites were independently sensitive to choline or glutamate.

Figure 3.2 demonstrates the calibration of a sensor with two sets of sites modified separately for choline and glutamate sensings, as well as a chemical reference site. Table 3.1 and Table 3.2 summarize the performance data of the sensors. The average

sensitivity of the glutamate sensors (n = 16) was 1.1 ± 0.1 pA/μM or 1763 ± 169 pA/μM/mm^2 with a limit of detection of 0.4 ± 0.09μM (reported error is standard error of the mean). The glutamte biosensors also exhibited high selectivity over ascorbic acid (822:1) and dopamine (579:1). The corresponding average sensitivity of the choline sensors (n = 21) was 3.5 ± 0.2 pA/μM or 5617 ± 399 pA/μM/mm^2 with a limit of detection of 0.1 ± 0.05μM. The choline biosensors showed similarly high selectivity over ascorbic acid (855:1) and dopamine (556:1). The high selectivity on both sensor types is indicative of an effective phenylenediamine polymerization procedure on the small microelectrode sites (Rothwell et al., 2009).

Table 3.1: Probe Performance Specifications for Glutamate Biosensors

Glutamate Sensitivity pA/μM	**Normalized Sensitivity pA/μM/mm^2**	**Limit of Detection μM**	**Selectivity Glut:AA**	**Selectivity Glut:DA**
1.1±0.1	1763±169	0.4±0.09	822±78	579±123

n = 16; Range is ± Standard Error of the Mean

Table 3.2: Probe Performance Specifications for Choline Biosensors

Choline Sensitivity pA/μM	**Normalized Sensitivity pA/μM/mm^2**	**Limit of Detection μM**	**Selectivity Ch:AA**	**Selectivity Ch:DA**
3.5±0.2	5617±399	0.1±0.05	855±61	556±105

n = 21; Range is ± Standard Error of the Mean

Notably, the sensitivity of the glutamate biosensors was approximately 30% of the sensitivity of the choline biosensors; however, reported sensitivity for amperometric glutamate sensor have frequently shown lower sensitivity than their choline counterparts. Typical reported values for glutamate sensors, when normalized area, are in the range of 900-2200 pA/μM/mm^2, while choline sensors have a reported range of 1200-4000 pA/μM/mm^2 (Burmeister et al., 2002, 2003; Parikh et al., 2004, 2010; Frey et al., 2010). Our biosensors have sensitivity that falls within that range.

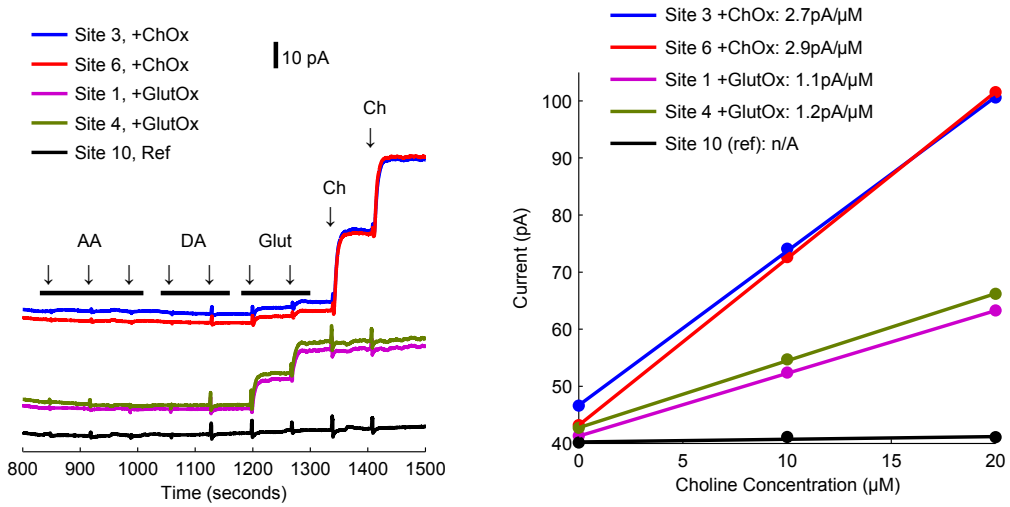

(A) (B)

Figure 3.2: Choline-Glutamate Sensor Calibration (A) Representative calibration data for a set of electrode sites on a single biosensor array. Sites 3 and 6 were functionalized with choline oxidase (+ChOx), sites 1 and 4 with glutamate oxidase (+GlutOx), and site 7 served as a neurochemical reference site with no choline enzyme (Ref). Arrows show injections to adjust the concentration of ascorbic acid (AA: 100μM, 200μM, 500μM), dopamine (DA: 2μM, 10μM), glutamate (Glut:10μM, 20μM), and choline (Ch: 10μM, 20μM). (B) The sensitivity plot for choline and glutamate of the respective biosensor sites.

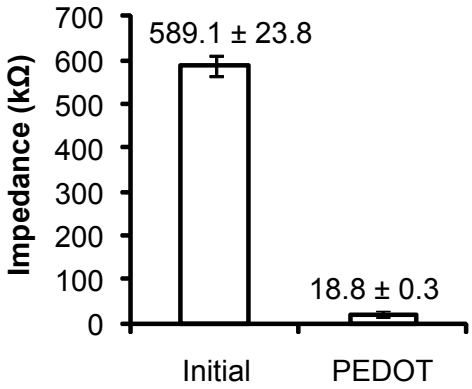

Figure 3.3: Impedance of Electrodes Before and After PEDOT. PEDOT coatings reduced the impedance from an average of 589.1kΩ to 18.8kΩ.

Electrode sites showed impedance measurements appropriate for electrophysiology both before and after PEDOT coatings. The PEDOT coatings reduced the impedance from an average of 589.1kΩ to 18.8kΩ, indicating successful polymerization on the electrode sites (Figure 3.3).

3.3.2 *In vivo* Validation and Performance

Biosensor arrays were implanted into the prelimbic cortex and validated through local injections of saline (Ringers), choline, glutamate, KCl, or nicotine. This experimental set is designed primarily to show *in vivo* function as a foundation for future neurophysiological investigations.

Saline injections were used as a control to determine the response from pressure injections. Figure 3.4 shows the data traces for these response. A typical saline injection evoked a minimal response at normal injection volumes. These responses were frequently, although not always, reflected in the reference channel as well, which indicates that the response was due to a transient disruption of the tissue-electrode interface. On occasions when the reference site did not show similar changes, the responses were small ($\leq$1–2μM) relative to measurements from KCl, choline, glutamate, or nicotine at similar volumes. The saline injections did not induce changes in LFP activity.

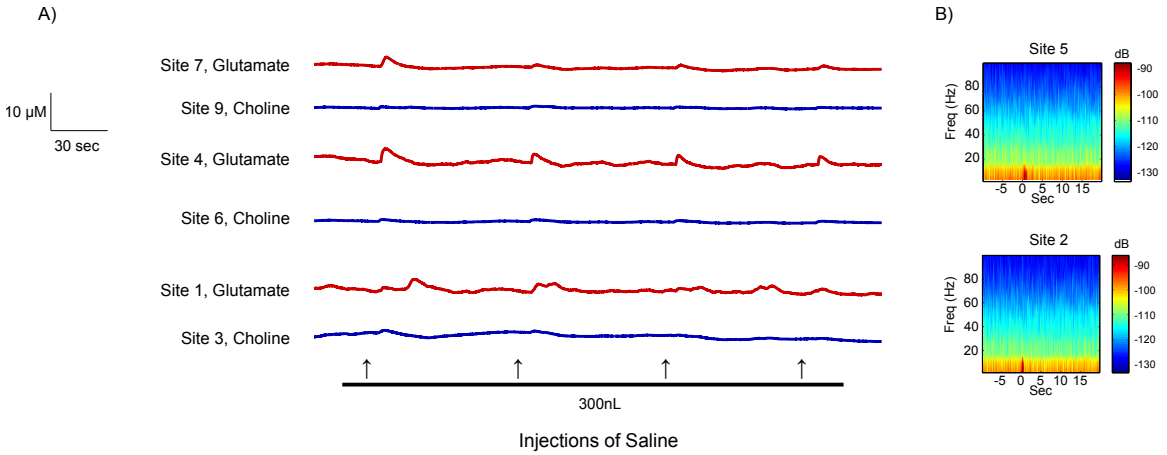

Figure 3.4: Saline Injections during recordings of Glutamate, Choline, and Electrophysiology (A) Glutamate responses are shown in red. Sites 1, 4, and 7 had benchtop sensitivity responses of 0.8, 0.7, and 1.6pA/μM glutamate, respectively. Choline responses are shown in blue. Sites 3, 6, and 9 had benchtop sensitivity responses of 2.8, 2.8, and 3.4pA/μM choline, respectively. (B) The average power spectrogram for the local field potentials also shows no appreciable change. Injection occurred at time 0.

Figure 3.5 shows the response of two choline sensitive sites (Sites 3 and 6 in blue) and two glutamate sensitive sites (Sites 1 and 4 in red) distributed across the array during a series of 150nL, 250nL, and 500nL injections of 10mM choline. Local injections of choline indicate that the choline sites maintain sensitivity *in vivo*, but also induce local release of glutamate, which is measured on parallel glutamate sensing sites. The sensing sites show responses that are volume- and spatially-dependent. In this particular case, the choline sites, although separated by 300μm, recorded similar amplitudes. Both had volume dependence distinguishable by response magnitude. The glutamate responses showed a similar volume dependence, but also had stronger spatial differences. Interestingly, the sites further from the tip recorded stronger glutamate responses. We have seen this type of relationship in several experiments, and it most frequently occurs when the injection agonist is not the analyte being measured at the electrode site (see also Section 2.3.2 in the previous chapter and the discussion below).

Glutamate injections also produced regular, repeatable responses at the sensing

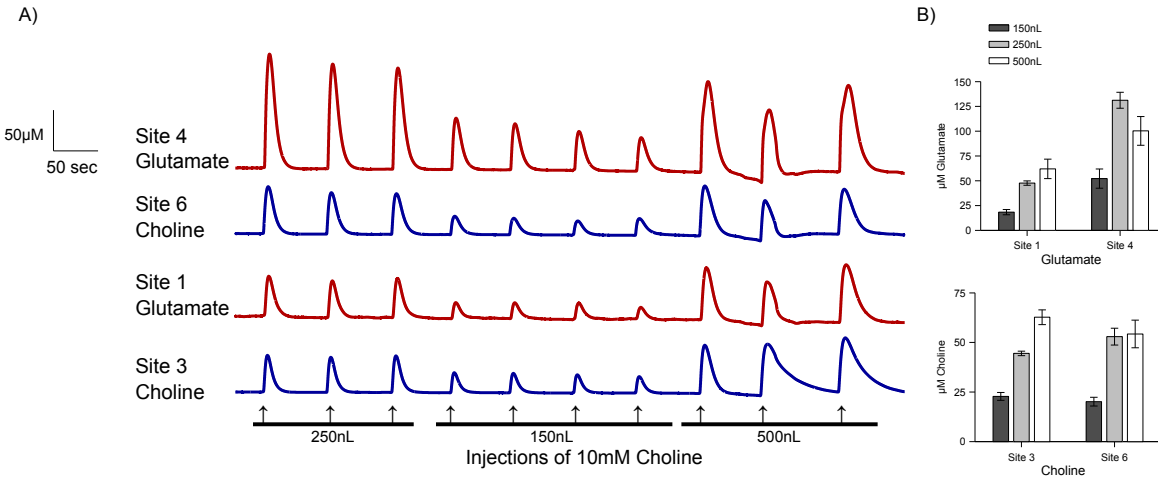

Figure 3.5: Choline–Induced Glutamate and Choline Responses (A) Glutamate responses are shown in red. Sites 1 and 4 had benchtop sensitivities of 1.5 and 0.8pA/μM glutamate, respectively. Choline responses are shown in blue. Sites 3 and 6 had benchtop sensitivities of 3.9 and 1.7pA/μM choline respectively. (B) The average glutamate and choline responses (with standard deviation) for each choline injection volume during the series.

sites as seen in Figure 3.6. Glutamate responses during glutamate injections were often 10–40X higher than corresponding choline responses at the same depth. Figure 3.6 also demonstrates the concurrent electrophysiology/LFP recordings during these injections. The responses also show volume and spatial dependence. Site 4, which is nearer to the injection site than site 7, reflects high concentrations at virtually all volumes. Site 7 shows a clearer volume dependence, indicative of the greater diffusion of glutamate concentration further from the injection site.

KCl was injected to elicit cholinergic and glutamatergic responses through direct depolarization of local neurons (Figure 3.7 and Figure 3.8). KCl–induced responses were volume dependent for both choline and glutamate. Of particular note, the magnitude of KCl–evoked choline responses were similar in magnitude to the glutamate–evoked choline responses. Additionally, the magnitude of KCl–evoked glutamate responses were similar in magnitude to the choline–evoked glutamate responses. In other words, the KCl caused neurotransmitter release at approximately the same levels as direct injection of the choline or glutamate.

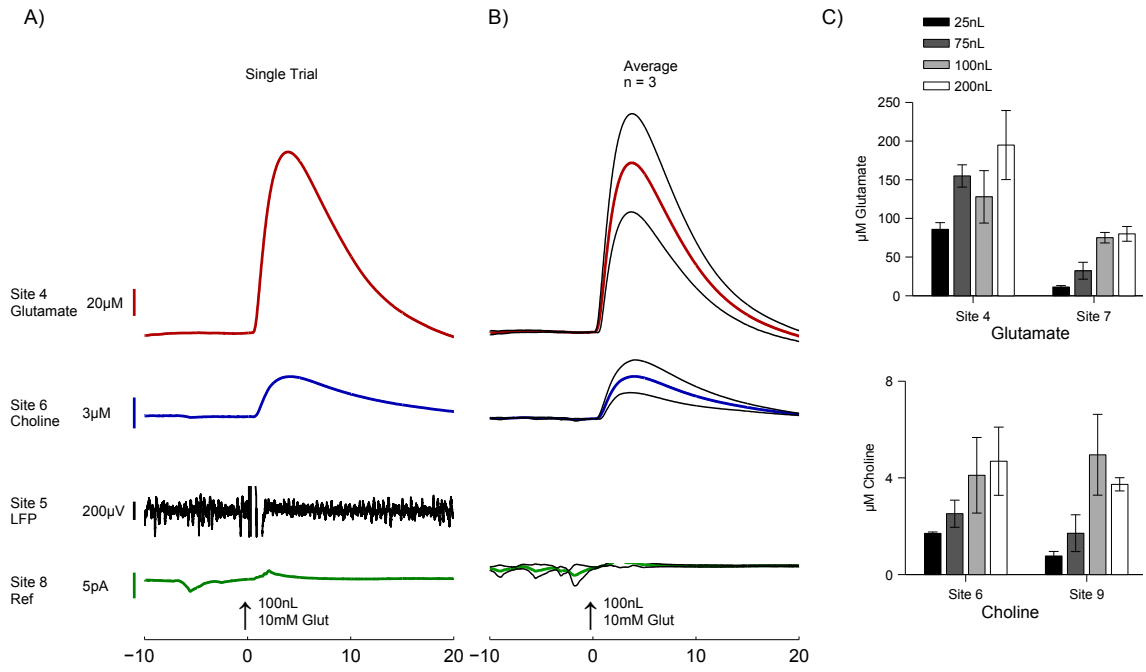

Figure 3.6: Glutamate–Induced Glutamate, Choline, and LFP Responses (A) Example of a glutamate–induced (10mM, 100nL) response for glutamate (site 4, red), choline (site 4, blue), LFPs (site 5, black), and chemical reference (site 8, green). (B) The average response (with standard deviation) of 3 injections. (C) The average peak heights (with standard deviation) for glutamate and choline sensing sites (n = 3 for each injection) for the series of injections that includes (A) and (B).

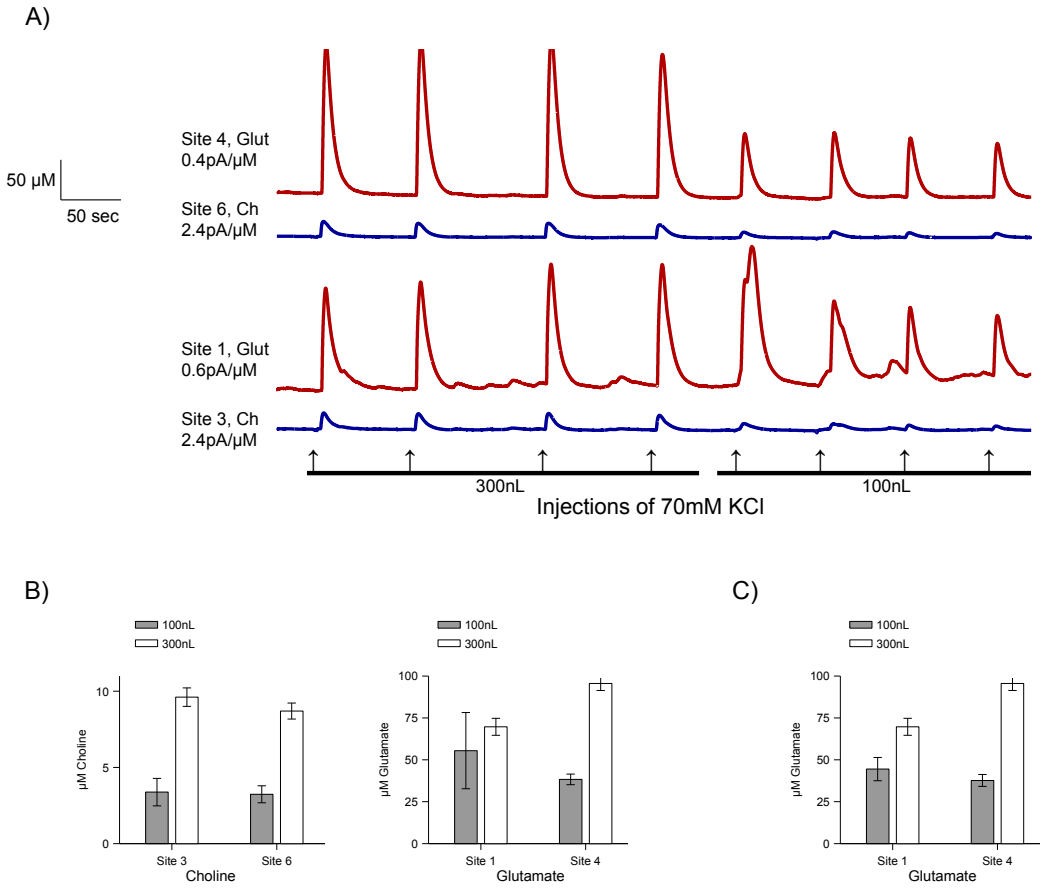

Figure 3.7: KCl–induced Glutamate and Choline Responses (A) Glutamate responses are shown in red (sites 1,4). Choline responses are shown in blue (sites 3,6). (B) The average glutamate and choline responses (with standard deviation) of each KCl injection volume during the series. (C) The average glutamate response when the first 100nL injection is removed as a potential outlier.

Local field potentials were also recorded during the KCl injections. As seen in Figure 3.7, the KCl caused only a brief, transient change in LFPs across the entire band. As saline did not induce such a change in LFPs, this transient peak reflects the rapid depolarization during the KCl injection.

As a final evoked response procedure, we injected nicotine, which has previously been shown to cause both aceteylcholine and glutamate release in the prefrontal cortex through nAChR-mediated signaling pathways Parikh et al. (2008, 2010). Both glutamate and choline were recorded at the respective biosensor sites (Figure 3.9). The electrophysiological response was a large, but brief signal similar to that seen

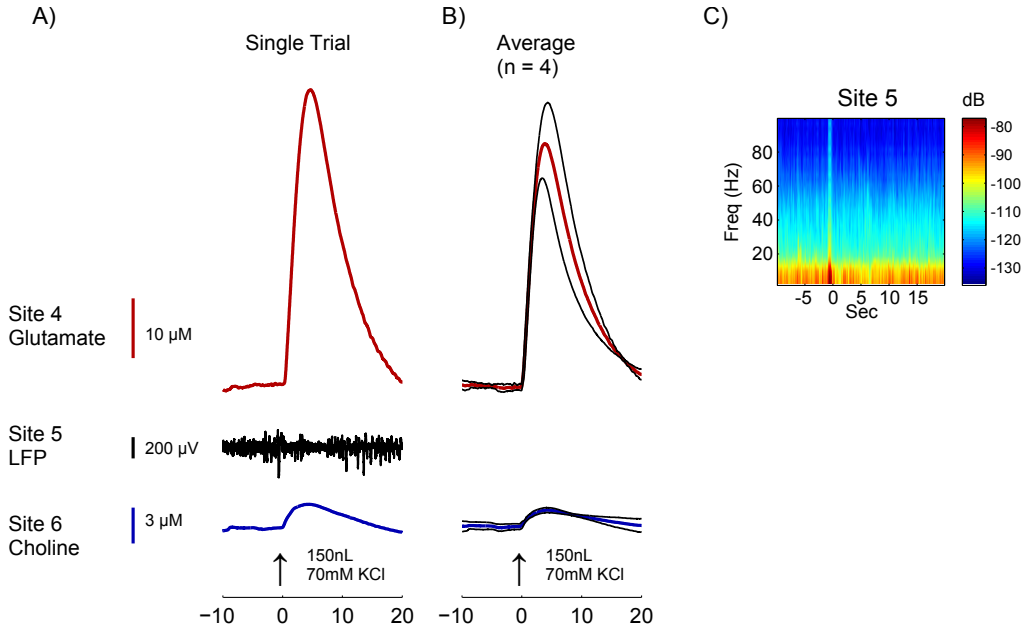

Figure 3.8: KCl–induced Glutamate, Choline, and LFP Responses (A) The glutamate response is shown in red (site 4) and the choline response is shown in blue (site 6). (B) The average glutamate and choline response for this series of 150nL KCl injections (with standard deviation). (C) The average power spectrogram for the local field potentials. Changes occurred directly at injection onset at time 0.

during KCl injections.

3.4 Discussion

In this work, we have presented and validated a multimodal neural probe for establishing multiple neurochemical, electrophysiological, and pharmacological interfaces with the brain. Our results indicate that the sensors have high performance characteristics (sensitivity, limit of detection, selectivity) that continue to function well *in vivo* to enable recordings of glutamate, choline, and electrophysiology in real time, while also providing an integrated drug delivery interface. As the results from saline injections and concurrent reference channels indicate, injections with this neural probe have minimal impact on the measurements; however, care should be taken with repeated injections or large, rapid injections. Such protocols may result in variability, tissue damage, and degradation of the electrode-tissue interface.

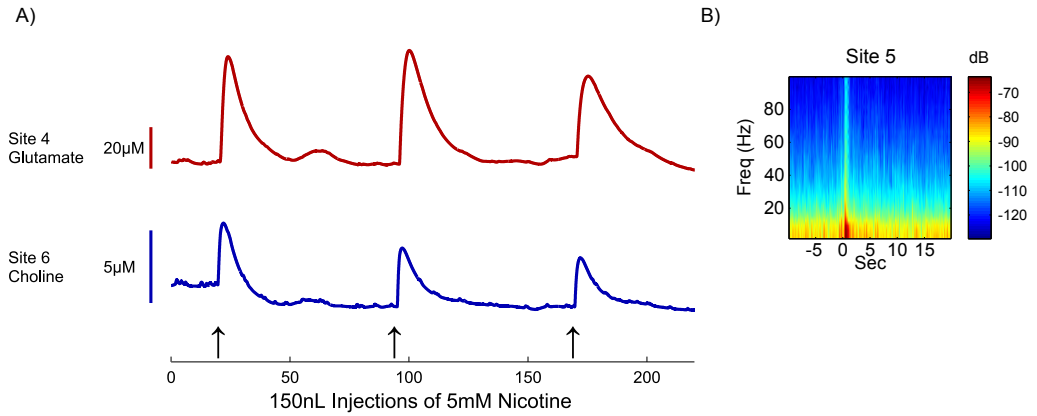

Figure 3.9: Nicotine–Induced Glutamate, Choline, and LFP Responses (A) The glutamate response is shown in red (site 4), and the choline response is shown in blue (site 6). (C) TThe average power spectrogram for the local field potentials. Changes occurred directly at injection onset at time 0.

An important outcome of this work is the ability to modify closely–spaced microelectrode sites without affecting other sites on the same array. These procedures further extended the limits of electrode size and spacing for biosensor arrays. Of particular note, the modification procedures and coatings were highly compatible, allowing for multiple different sensing elements with high performance.

Injections of KCl and nicotine resulted in amplitudes at choline sites that were approximately equivalent to those during glutamate injections. Conversely, glutamate responses during KCl and nicotine were similar to those seen during choline injections. This result indicates that the difference in magnitude from KCl– or nicotine–induced signals compared to the direct neurotransmitter injection can be primarily attributed to the injected neurotransmitters, and is a positive indicator that our sensors are continuing to function appropriately. Of additional interest, choline served as an effective activation agent for causing glutamate release through its role as a nAChR agonist (Uteshev and Knot, 2005; Gusev and Uteshev, 2010). As Figure 3.5 indicates, during choline injections, choline induces a glutamate response that is similar in magnitude to the choline response. In our set of experiments, this was the only condition where the choline and glutamate responses were similar. Typically, glutamate was much

higher.

The multisite array also demonstrates interesting aspects of injection or diffusion-based experiments. In several cases, spatially separated sites reflect similar signal amplitudes. This may be due to reaching a maximum amplitude, wicking up the device interface, neural projections that cause similar responses at different depths, and/or *in vivo* functional differences due to proximity to vasculature, protein adhesion, and tissue response. Occasionally, sites nearest the injection port show very low response magnitudes, while more distal sites respond more robustly. We have seen this type of relationship in several experiments, and it most frequently occurs when the injection agonist is not the analyte being measured at the electrode site (e.g. measuring either neurotransmitter during KCl or nicotine injections, measuring choline during a glutamate injection, or measuring glutamate during a choline injection). While this may seem counterintuitive initially, the injection can produce a "wash out" effect, or a region immediately around the injection site with lower concentration of endogenous analytes due to the injection volume and resulting diffusion. When injecting the molecule being measured, the most proximal site typically has at least as robust of a response as the more distal sites (for example, Figure 3.6). While the current study does not determine an optimal distance for sensor placement in relation to the injection point, this relationship should be considered during experimental and device design.

In the past, injection-diffusion experiments have been used to study enzyme and reuptake kinetics (Sabeti et al., 2002; Oldenziel et al., 2006). Clearly, these studies have provided new insights to neurotransmitter dynamics, but the present results with spatial differentiation indicate that aspects of these kinetics my be strongly influenced by the infusate bolus and resulting diffusion. For example, KCl injections cause depolarization by affecting the local concentration of K^+. As long as the K^+ concentration is locally high even as it diffuses, the membrane potential of local neurons will

be depolarized and neurotransmitters may be released, unless the supply is exhausted due to repeated release or high levels of release. Although separate synaptic release events would not be distinguishable, the period of this concentration threshold could extend beyond the refractory period, which is on the order of milliseconds. Distance from the electrode and local tissue differences may play a role in the recorded kinetic responses, and these factors must be considered during diffusion-based experiments. Recent work by several groups has focused on understanding characteristics of diffusion in brain tissue, which is complicated by reuptake, receptors, tissue damage, and device specifications (Gardner-Medwin, 1983; Retterer et al., 2004; Nicholson, 201; Rohatgi et al., 2009). While locally infused molecules may obscure or complicate aspects of neurophysiology when directly driving a response, such experimental systems may be very appropriate for delivery of modulators, such as antagonists, when the physiological response is drive by other means, such as behavioral experiments or upstream stimulation.

Throughout these experiments, we successfully recorded field potentials, but did not record unit activity, even with PEDOT coatings. Urethane anesthesia has been shown to reduce electrophysiology (Friedberg et al., 1999; Devonshire et al., 2010; Sceniak and Maciver, 2006), as do many anesthetic agents, particularly in deeper states of anesthesia. The purpose of this set of experiments with regard to electrophysiology was to 1) validate functionality, which was accomplished through field potential recordings, and 2) demonstrate compatibility of the various functional coating procedures, including PEDOT. Both aims were met in the current experiments. This framework lays the foundation for continued experiments.

3.5 Conclusion

The biosensor arrays presented in this work provide a multimodal neural interface with the ability to record rapid dynamics of choline, glutamate, and electrophysiology

combined with local drug delivery. The arrays consist of 10 independent microelectrode sites (area = 625 μm^2) that enable high-density, spatially distributed recordings. We utilize multiple electrochemical methods for site-selective functional coatings of enzymes and polymers to selectively modify multiple electrode sites in various functional configurations on a single electrode array. The *in vivo* experiments validated proper function and urge further investigations of neurophysiology and neuropathologies with this multimodal interface.

Acknowledgements

I would like to thank Karen Schroeder, Paras Patel, and Nick Langhals for assistance with this work. This work was supported by a National Science Foundation Graduate Fellowship, the Coulter Foundation, and the Center for Neural Communication Technology. The Center for Neural Communication Technology is a P41 Resource Center funded by the National Institute of Biomedical Imaging and Bioengineering (NIBIB, P41 EB002030) and supported by the National Institutes of Health (NIH).

References

Agnesi, F., Blaha, C. D., Lin, J., and Lee, K. H. (2010). Local glutamate release in the rat ventral lateral thalamus evoked by high-frequency stimulation. *J Neural Eng*, 7(2):26009.

Aragona, B. J., Day, J. J., Roitman, M. F., Cleaveland, N. A., Wightman, R. M., and Carelli, R. M. (2009). Regional specificity in the real-time development of phasic dopamine transmission patterns during acquisition of a cue-cocaine association in rats. *Eur J Neurosci*, 30(10):1889–1899.

Bard, A. and Faulkner, L. (2001). *Electrochemical methods: fundamentals and applications*. Wiley, 2nd edition.

Binns, B. C., Huang, Y., Goettl, V. M., Hackshaw, K. V., and Stephens Jr., R. L. (2005). Glutamate uptake is attenuated in spinal deep dorsal and ventral horn in the rat spinal nerve ligation model. *Brain Research*, 1041(1):38–47.

Bruno, J. P., Gash, C., Martin, B., Zmarowski, A., Pomerleau, F., Burmeister, J., Huettl, P., and Gerhardt, G. A. (2006). Second-by-second measurement of acetylcholine release in prefrontal cortex. *Eur J Neurosci*, 24(10):2749–2757.

Burmeister, J. J. and Gerhardt, G. A. (2001). Self-referencing ceramic-based multisite microelectrodes for the detection and elimination of interferences from the measurement of l-glutamate and other analytes. *Anal. Chem.*, 73(5):1037–1042.

Burmeister, J. J., Palmer, M., and Gerhardt, G. A. (2003). Ceramic-based multisite microelectrode array for rapid choline measures in brain tissue. *Anal. Chim. Acta*, 481(1):65–74.

Burmeister, J. J., Palmer, M., and Gerhardt, G. A. (2005). L-lactate measures in brain tissue with ceramic-based multisite microelectrodes. *Biosensors & bioelectronics*, 20(9):1772–1779.

Burmeister, J. J., Pomerleau, F., Huettl, P., Gash, C. R., Werner, C. E., Bruno, J. P., and Gerhardt, G. A. (2008). Ceramic-based multisite microelectrode arrays for simultaneous measures of choline and acetylcholine in cns. *Biosensors & bioelectronics*, 23(9):1382–1389.

Burmeister, J. J., Pomerleau, F., Palmer, M., Day, B. K., Huettl, P., and Gerhardt, G. A. (2002). Improved ceramic-based multisite microelectrode for rapid measurements of -glutamate in the cns. *J Neurosci Methods*, 119(2):163–171.

Daws, L. C., Montaez, S., Owens, W. A., Gould, G. G., Frazer, A., Toney, G. M., and Gerhardt, G. A. (2005). Transport mechanisms governing serotonin clearance in

vivo revealed by high-speed chronoamperometry. *J Neurosci Methods*, 143(1):49–62.

Day, B. K., Pomerleau, F., Burmeister, J. J., Huettl, P., and Gerhardt, G. A. (2006). Microelectrode array studies of basal and potassium-evoked release of l-glutamate in the anesthetized rat brain. *J. Neurochem.*, 96(6):1626–1635.

Devonshire, I. M., Grandy, T. H., Dommett, E. J., and Greenfield, S. A. (2010). Effects of urethane anaesthesia on sensory processing in the rat barrel cortex revealed by combined optical imaging and electrophysiology. *European Journal of Neuroscience*, 32(5):786–797.

Frey, O., Holtzman, T., McNamara, R. M., Theobald, D. E. H., van der Wal, P. D., de Rooij, N. F., Dalley, J. W., and Koudelka-Hep, M. (2010). Enzyme-based choline and l-glutamate biosensor electrodes on silicon microprobe arrays. *Biosensors & Bioelectronics*, 26(2):477–484.

Friedberg, M. H., Lee, S. M., and Ebner, F. F. (1999). Modulation of receptive field properties of thalamic somatosensory neurons by the depth of anesthesia. *J Neurophysiol*, 81(5):2243–2252.

Gardner-Medwin, A. R. (1983). A study of the mechanisms by which potassium moves through brain tissue in the rat. *J Physiol*, 335:353–374.

Geise, R. J., Adams, J. M., Barone, N. J., and Yacynych, A. M. (1991). Electropolymerized films to prevent interferences and electrode fouling in biosensors. *Biosensors and Bioelectronics*, 6(2):151–160.

Gusev, A. G. and Uteshev, V. V. (2010). Physiological concentrations of choline activate native alpha7-containing nicotinic acetylcholine receptors in the presence of pnu-120596 [1-(5-chloro-2,4-dimethoxyphenyl)-3-(5-methylisoxazol-3-yl)-urea]. *J Pharmacol Exp Ther*, 332(2):588–598.

Hashemi, P. and Wightman, R. M. (2007). Paying attention with the latest technology. *Neuron*, 56(1):4–5.

Humphrey, D. R. and Schmidt, E. M. (1990). Extracellular single-unit recording methods. In *Neuromethods*, volume 15, pages 1–64. Humana Press, Clifton, NJ.

Johnson, K. W. (1991). Reproducible electrodeposition of biomolecules for the fabrication of miniature electroenzymatic biosensors. *Sensors and Actuators B: Chemical*, 5(1-4):85–89.

Kipke, D. R., Shain, W., Buzski, G., Fetz, E., Henderson, J. M., Hetke, J. F., and Schalk, G. (2008). Advanced neurotechnologies for chronic neural interfaces: new horizons and clinical opportunities. *J Neurosci*, 28(46):11830–11838.

Kovacs, G. T. A. (1994). Introduction to the theory, design and modeling of thin-film microelectrodes for neural interfaces. In Stenger, D. and McKenna, T., editors, *Enabling Technologies for Cultured Neural Networks*, pages 121–166. Academic Press, New York.

Ludwig, K. A., Langhals, N. B., Joseph, M. D., Richardson-Burns, S. M., Hendricks, J. L., and Kipke, D. R. (2011). Poly(3,4-ethylenedioxythiophene) (pedot) polymer coatings facilitate smaller neural recording electrodes. *Journal of neural engineering*, 8(1):014001.

Ludwig, K. A., Uram, J. D., Yang, J., Martin, D. C., and Kipke, D. R. (2006). Chronic neural recordings using silicon microelectrode arrays electrochemically deposited with a poly(3,4-ethylenedioxythiophene) (pedot) film. *J Neural Eng*, 3(1):59–70.

Michael, A. and Borland, L. (2007). *Electrochemical methods for neuroscience*. CRC Press/Taylor & Francis.

Mitchell, K. M. (2004). Acetylcholine and choline amperometric enzyme sensors characterized in vitro and in vivo. *Anal. Chem.*, 76(4):1098–1106.

Nicholson, C. (201). Diffusion and related transport mechanisms in brain tissue. *Reports on Progress in Physics*, 64:815–884.

Oldenziel, W. H., Dijkstra, G., Cremers, T. I. F. H., and Westerink, B. H. C. (2006). In vivo monitoring of extracellular glutamate in the brain with a microsensor. *Brain Res.*, 1118(1):34–42.

Owesson-White, C. A., Cheer, J. F., Beyene, M., Carelli, R. M., and Wightman, R. M. (2008). Dynamic changes in accumbens dopamine correlate with learning during intracranial self-stimulation. *Proc. Natl. Acad. Sci. U. S. A.*, 105(33):11957–11962.

Parikh, V., Ji, J., Decker, M. W., and Sarter, M. (2010). Prefrontal beta2 subunit-containing and alpha7 nicotinic acetylcholine receptors differentially control glutamatergic and cholinergic signaling. *J Neurosci*, 30(9):3518–3530.

Parikh, V., Kozak, R., Martinez, V., and Sarter, M. (2007). Prefrontal acetylcholine release controls cue detection on multiple timescales. *Neuron*, 56(1):141–154.

Parikh, V., Man, K., Decker, M. W., and Sarter, M. (2008). Glutamatergic contributions to nicotinic acetylcholine receptor agonist-evoked cholinergic transients in the prefrontal cortex. *J Neurosci*, 28(14):3769–3780.

Parikh, V., Pomerleau, F., Huettl, P., Gerhardt, G. A., Sarter, M., and Bruno, J. P. (2004). Rapid assessment of in vivo cholinergic transmission by amperometric detection of changes in extracellular choline levels. *Eur. J. Neurosci.*, 20(6):1545–1554.

Parikh, V. and Sarter, M. (2006). Cortical choline transporter function measured in vivo using choline-sensitive microelectrodes: clearance of endogenous and exogenous choline and effects of removal of cholinergic terminals. *J. Neurochem.*, 97(2):488–503.

Paxinos, G. and Watson, C. (2007). *The Rat Brain in Stereotaxic Coordinates, Sixth Edition*. Academic Press, London, UK, 6th edition.

Phillips, P. E. M., Stuber, G. D., Heien, M. L. A. V., Wightman, R. M., and Carelli, R. M. (2003). Subsecond dopamine release promotes cocaine seeking. *Nature*, 422(6932):614–618.

Retterer, S. T., Smith, K. L., Bjornsson, C. S., Neeves, K. B., Spence, A. J. H., Turner, J. N., Shain, W., and Isaacson, M. S. (2004). Model neural prostheses with integrated microfluidics: a potential intervention strategy for controlling reactive cell and tissue responses. *IEEE Trans Biomed Eng*, 51(11):2063–2073.

Rohatgi, P., Langhals, N. B., Kipke, D. R., and Patil, P. G. (2009). In vivo performance of a microelectrode neural probe with integrated drug delivery. *Neurosurgical focus*, 27(1):E8.

Rothwell, S. A., Kinsella, M. E., Zain, Z. M., Serra, P. A., Rocchitta, G., Lowry, J. P., and O'Neill, R. D. (2009). Contributions by a novel edge effect to the permselectivity of an electrosynthesized polymer for microbiosensor applications. *Anal. Chem.*, 81(10):3911–3918.

Sabeti, J., Adams, C. E., Burmeister, J., Gerhardt, G. A., and Zahniser, N. R. (2002). Kinetic analysis of striatal clearance of exogenous dopamine recorded by chronoamperometry in freely-moving rats. *J Neurosci Methods*, 121(1):41–52.

Sarter, M., Bruno, J. P., and Parikh, V. (2007). Abnormal neurotransmitter release underlying behavioral and cognitive disorders: toward concepts of dynamic and function-specific dysregulation. *Neuropsychopharmacology*, 32(7):1452–1461.

Sceniak, M. P. and Maciver, M. B. (2006). Cellular actions of urethane on rat visual cortical neurons in vitro. *J Neurophysiol*, 95(6):3865–3874.

Seymour, J. P., Langhals, N. B., Anderson, D. J., and Kipke, D. R. (2011). Novel multi-sided, microelectrode arrays for implantable neural applications. *Biomed Microdevices*.

Strike, D. J., de Rooij, N. F., and Koudelka-Hep, M. (1995). Electrochemical techniques for the modification of microelectrodes. *Biosens. Bioelectron.*, 10(1-2):61–66.

Uteshev, V. and Knot, H. (2005). Somatic ca2+ dynamics in response to choline-mediated excitation in histaminergic tuberomammillary neurons. *Neuroscience*, 134(1):133–143.

Walker, E., Wang, J., Hamdi, N., Monbouquette, H. G., and Maidment, N. T. (2007). Selective detection of extracellular glutamate in brain tissue using microelectrode arrays coated with over-oxidized polypyrrole. *Analyst*, 132(11):1107–1111.

Ward, M. P., Rajdev, P., Ellison, C., and Irazoqui, P. P. (2009). Toward a comparison of microelectrodes for acute and chronic recordings. *Brain Res.*, 1282:183–200.

Wassum, K., Tolosa, V., Wang, J., Walker, E., Monbouquette, H., and Maidment, N. (2008). Silicon wafer-based platinum microelectrode array biosensor for near real-time measurement of glutamate in vivo. *Sensors*, 8(8):5023–5036.

Wightman, R. M. and Robinson, D. L. (2002). Transient changes in mesolimbic dopamine and their association with 'reward'. *J. Neurochem.*, 82(4):721–735.

CHAPTER IV

Influence of Calibration Media on Performance Characteristics of Amperometric Biosensors: Implications for *in vivo* Measurements

4.1 Introduction

Electrochemical biosensors are in active use and development for the detection of many biological analytes, including glucose, acetylcholine, choline, glutamate, lactate, dopamine, and cholesterol (Wilson and Gifford, 2005; Johnson et al., 2008; Trkarslan et al., 2009; Moatti-Sirat et al., 1992; Aravamudhan et al., 2007; Jena and Raj, 2011; Ryan et al., 1997; McMahon et al., 2006; Hamdi et al., 2006; Mitchell, 2004; Burmeister and Gerhardt, 2003; Burmeister et al., 2005, 2003; Zachek et al., 2010a; Heien et al., 2005; Bowser and Kennedy, 2001; Shou et al., 2004). Frequently, these biosensors measure the concentration of analytes of interest within a physiological environment, such as a fluid sample. In many cases, the biosensor may be implanted directly in tissue for *in vivo* measurements (Johnson et al., 2008; Burmeister and Gerhardt, 2003; Burmeister et al., 2005; Heien et al., 2005). The complex environments of the body pose a significant difficulty for obtaining accurate physiological measurements due to interactions of biological constituents with the sensor that may affect its performance.

Biological sensors are calibrated for sensitivity to the desired analyte and selectivity over potential interferents. These calibration factors are then used to translate raw measurements (typically current) to analyte concentration within the desired physiological system. Ideally, the calibration environment is identical or equivalent to the environment in which recordings will take place (Phillips and Wightman, 2003; Wilson and Gifford, 2005; Webster and Clark, 1998; Periasamy et al., 2011; Moatti-Sirat et al., 1992; Poitout et al., 1993; Abel et al., 1984; Gifford et al., 2005; Updike et al., 2000; Aravamudhan et al., 2007).

Unfortunately, calibration procedures for developing biosensors often vary across the field. These differences may influence the characterization of the sensors and, more importantly, the degree to which the benchtop characterization accurately represents performance within physiological environments. Finding appropriate calibration media and developing robust calibration procedures can be difficult. In some cases, such as for glucose or cholesterol sensors, blood or serum may be used as an *in vitro* media to approximate the recording environment (Updike et al., 2000; Aravamudhan et al., 2007; Poitout et al., 1993). Implantable neural biosensors do not have a readily accessible media analagous to the brain. Typically a buffered electrolyte is used as the calibration media. Common media choices vary, but include artificial cerebrospinal fluid, phophate-buffered saline, and Tris-buffered saline (Mitchell, 2004; Johnson et al., 2008; Hamdi et al., 2005, 2006; Kume-Kick and Rice, 1998; Burmeister et al., 2002; Zachek et al., 2010b; Hashemi et al., 2009). Concentration range and testing of selectivity over potential interferents differ as well.

While appropriate calibration procedures have been encouraged in the literature (as an example, see Phillips and Wightman, 2003), little work has been done to establish common standards. One noteworthy example includes a 1998 study conducted by Kume-Kick and Rice. This studied showed that the presence of divalent cations Mg^{2+} and Ca^{2+}, which are both present in brain tissue, could reduce the sensitivity of

dopamine at carbon fiber electrodes when using fast-scan cyclic voltammetry. Their results suggested a reduction in the active surface of the carbon due to occupation of redox sites by Mg^{2+} and Ca^{2+}. Kume-Kick and Rice appropriately suggested that the effects of cations should be considered for voltammetric techniques using carbon electrodes. This recommendation is typically followed and carbon fiber electrodes are generally calibrated in electrolyte media containing Mg^{2+} and Ca^{2+}.

The Kume-Kick and Rice study did not include other electrode materials, such as platinum, which has since been used as the primary metal for various amperometric neural biosensors. Platinum electrodes are particularly common for enzymatic biosensors that employ H_2O_2 as a reporter molecule for glutamate, choline, or other neurochemicals (Burmeister et al., 2003; Mitchell, 2004; Parikh et al., 2004; Wassum et al., 2008). The following generalized reactions describe these processes ("Ox" represents an oxidase enzyme and "FAD" represents flavin adenine dinucleotide, which becomes $FADH_2$ when oxidized) (Rothwell et al., 2009):

$$\text{Substrate} + \text{Ox/FAD} \rightarrow \text{Products} + \text{Ox/FADH}_2 \tag{4.1}$$

$$\text{Ox/FADH}_2 + \text{O}_2 \rightarrow \text{Ox/FAD} + \text{H}_2\text{O}_2 \tag{4.2}$$

$$\text{H}_2\text{O}_2 \rightarrow \text{O}_2 + 2\mathsf{H}^+ + 2e^- \tag{4.3}$$

Amperometric biosensors commonly utilize a permselective membrane, such as Nafion or phenylenediamine, to provide selectivity over potential interferents (Parikh et al., 2004; Mitchell, 2004; Frey et al., 2010; Kirwan et al., 2007; Burmeister et al., 2008).

This work investigates the effects of calibration media, analyte concentration range, and functional coatings on the characterization of platinum electrode amperometric biosensors. While amperometric biosensors are widely used for a variety

sensors, this work focuses on applications in neural biosensors, such as those for recording choline, glutamate, glucose, and dopamine.

4.2 Materials and methods

4.2.1 Fabrication of microsensors

The microelectrode arrays used in this work were designed for benchtop testing, and are non-implantable devices. They consisted of six round microelectrodes sites with diameters of 50μm (area = 1963μm^2) or 55μm (area = 2376μm^2). Only electrodes of identical dimensions were used within each group or for comparison between groups.

Arrays were fabricated on silicon wafers using standard planar photolithography microfabrication techniques with photoresist patterning. The devices consisted of four layers: silicon substrate, sputtered gold traces for connecting the electrode sites, sputtered platinum electrode sites, and silicon nitride deposited by plasma-enhanced chemical vapor deposition. The silicon nitride served as a dielectric insulation layer. The probes were dice cut and wire bonded to custom printed circuit boards. Each electrode was independent of other electrode sites and could be accessed individually.

4.2.2 Chemicals

Choline oxidase (ChOx) (EC 1.1.3.17) from arthrobacter globiformis, bovine serum albumin (BSA), glutaraldehyde, m-phenylenediamine, hydrogen peroxide (H_2O_2), choline, ascorbic acid (AA), dopamine (DA), potassium chloride (KCl), sodium chloride (NaCl), sodium dihydrogen phosphate (NaH_2PO_4), disodium hydrogen phosphate (Na_2HPO_4), monopotassium phosphate (KH_2PO_4), sodium bicarbonate ($NaHCO_3$), glucose, calcium chloride ($CaCl_2$), magnesium chloride ($MgCl_2$) were purchased from Sigma-Aldrich (St. Louis, MO). All chemicals were prepared in ultra pure filtered

water (Millipore, Billerica, MA).

We conducted calibrations in four electrolyte solutions: 0.01M phosphate buffered saline ("0.01M PBS": 137mM NaCl, 2.7mM KCl, 1.9mM KH_2PO_4, 10mM Na_2HPO_4), 0.05M phosphate buffered saline ("0.05M PBS": 100mM NaCl, 10mM NaH_2PO_4, 40mM Na_2HPO_4), artificial cerebrospinal fluid ("aCSF": 126mM NaCl, 3.5mM KCl, 1.2mM NaH_2PO_4, 25mM $NaHCO_3$, 2mM glucose, 2mM $CaCl_2$, 1.3mM $MgCl_2$), and a tris-buffered electrolyte ("TBE" 15mM Tris, 140mM NaCl, 3.25mM KCl, 1.25mM NaH_2PO_4, 1.2mM $CaCl_2$, 1.2mM $MgCl_2$, 2 $NaSO_4$). Each calbration media was pH balanced to 7.3-7.4. The aCSF was bubbled with a gas mixture of 95% O_2, 5% CO_2 to maintain constant CO_2 levels for proper buffering.

4.2.3 Preparation of Sensors

Electrodes were divided into four groups for testing: bare/unmodified, Nafion-coated, m-phenylenediamine (mPD) coated, or choline oxidase and mPD (ChOx+mPD). Nafion was deposited by dip-coating, followed by oven drying at 175°C for 3 minutes (Burmeister et al., 2002). mPD was deposited by electrodeposition (Geise et al., 1991; Mitchell, 2004; Burmeister et al., 2008; Frey et al., 2010). A solution of 5mM m-phenylenediamine and 5mM resorcinol in 0.01M PBS was mixed and immediately purged of oxygen by bubbling N_2 for 30 minutes. After placement in the mPD/resorcinol solution, the electrode bias was cycled between 0.0V and 0.7V versus Ag/AgCl at 2mV/sec twice followed by a ramp back up to 0.7V where the potential was held for 15 minutes.

Choline sensitive electrodes (ChOx+mPD) were modified by depositing a droplet of a mixture consisting of 1% choline oxidase, 1% BSA, and 0.125% glutaraldehyde in water (Burmeister et al., 2003). This mixture was allowed to cure on the electrode sites for approximately 48 hours. After the curing period, mPD was deposited on the electrode sites as described above.

4.2.4 Calibrations

Calibration procedures were conducted by immersing the electrodes in a stirred solution of an electrolyte solution (0.01M PBS, 0.05M PBS, aCSF, TBE) at 37°C. Electrode sites were biased with a constant potential of +0.7V versus an Ag/AgCl reference electrode (Bioanalytical Systems, Inc., West Lafayette, IN) using multichannel potentiostat systems (BioStat, Discovery Technology International, LLLP, Sarasota FL) and sampled at 60Hz, the maximum rate of the potentiostat system. After reaching a stable baseline, the electrodes were calibrated with increasing concentrations of H_2O_2, dopamine, ascorbic acid, and/or choline.

H_2O_2 calibrations were performed from 0-40μM using the following steps: 1μM, 2μM, 3μM, 4μM, 5μM, 10μM, 15μM, 20μM, 30μM, 40μM. H_2O_2 calibrations were performed on bare, Nafion, and mPD electrodes. Choline sensitive sites were similarly calibrated with the same concentration steps, but with choline instead of H_2O_2: The different calibration step sizes allowed us have increased resolution to determine whether or not the sensors had any concentration-dependent sensitivity. A subset of Nafion-coated electrodes was calibrated for dopamine from 0-40μM using 10μM steps. Amperometric sensing of dopamine has also been reported in the literature and this measurement also provided more direct connection to the Kume-Kick and Rice (1998) report (Johnson et al., 2008). Each sensor was calibrated in each buffer 3 times. The order of calibration was randomized to avoid skewing results from possible changes in the electrode performance over time.

Sensitivity calculations were calculated with custom automated MATLAB software (The MathWorks, Inc., Natick, MA). Repeated measures ANOVA followed by pairwise t-tests with a Bonferroni correction were conducted in SPSS software (IBM Corporation, Armonk, NY) to determine statistical significance of sensitivity differences between the calibration media. For purposes of this study, p–values less than 0.01 were considered significant. A second level of functional significance was also

defined as $p<0.01$ and a percent difference greater than 30%. This additional level of significance was chosen for two reasons. First, electrode sensitivities have some inherent variability in the calibration results. Second, while in several incidences a p–value may indicate significance, functionally that difference may have little relevance. The 30% level was chosen as a conservative measure of statistical significance and functional relevance.

4.3 Results

H_2O_2 was chosen as a baseline calibration molecule due to its role in the sensing mechanisms of many amperometric biosensors. Figure 4.1 shows the results of H_2O_2 calibrations on bare electrodes, Nafion coated electrodes, and mPD coated electrodes in each of the four calibration electrolytes. In general the phosphate-buffered solutions perform similarly. Likewise, the aCSF and TBE typically perform quite similarly. For bare electrodes, the calibration differences are both statistically ($p<0.01$) and functionally different ($\geq 30\%$) between either of the phosphate buffers and each of the aCSF and TBE solutions. This difference is most pronounced for the bare electrodes and mPD-coated electrodes, while at the Nafion electrodes the difference is statistically significant, but less pronounced. The effect may be mitigated by the overall reduced sensitivity that occured with the Nafion coatings.

In order to determine the cause of the significant differences in calibration performance among the calibration solutions from Figure 4.1, we tested parts of aCSF to build the entire solution stepwise. We began by testing the electrodes in various components of the electrolye buffer (BC = buffer components, BC1 = 126mM NaCl, 3.5mM KCl, 1.2mM; BC2 = BC1 + NaH_2PO_4, 25mM $NaHCO_3$; BC3 = BC2 + 2mM $CaCl_2$; BC4 = BC2 + 2mM $MgCl_2$)

When calibrated piecewise in this manner, we determined that the decrease in sensitivity was directly attributed to the presence of Ca^{2+} or Mg^{2+} (see Figure 4.2)

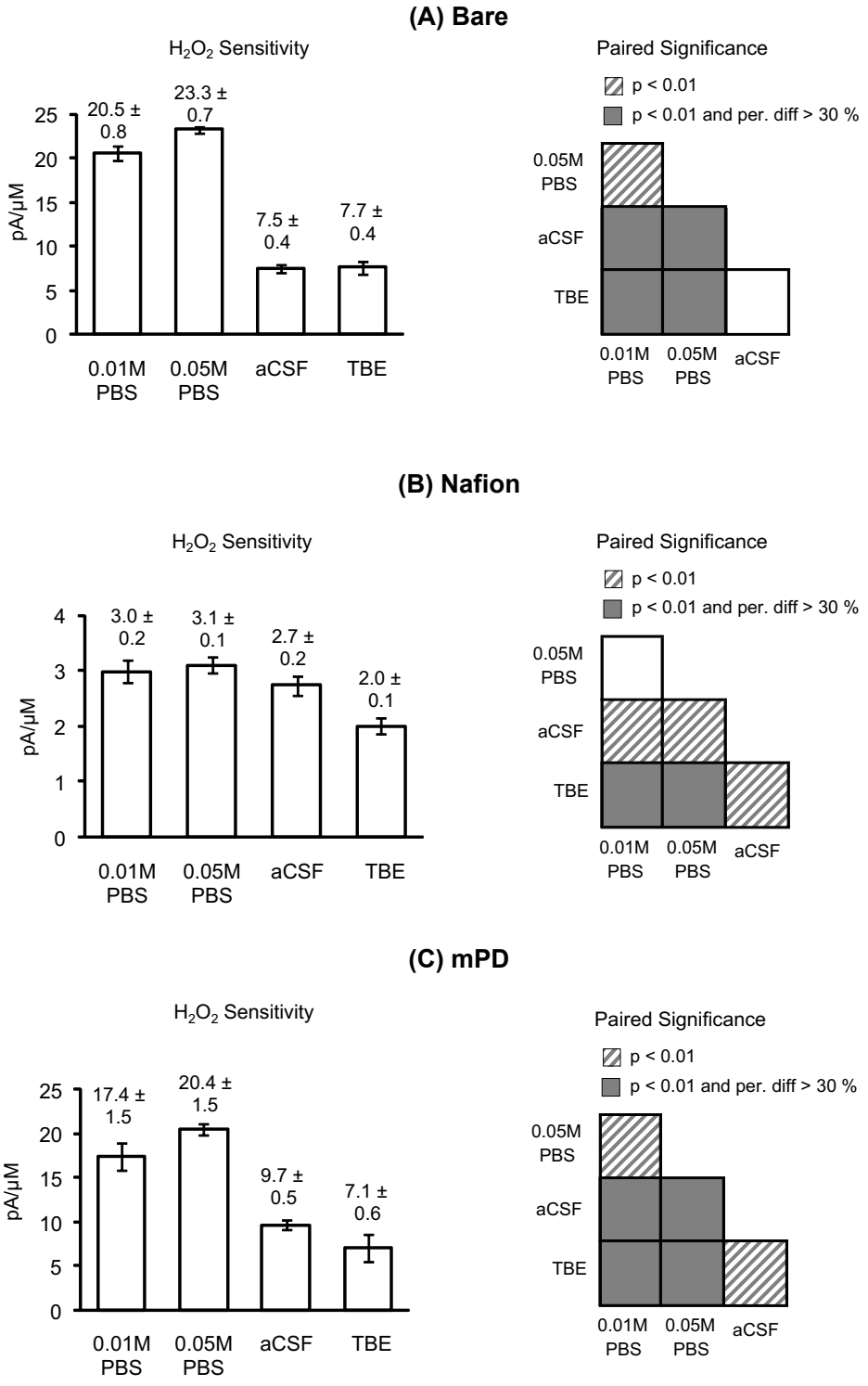

Figure 4.1: H_2O_2 Calibrations at (A) Bare electrodes (n = 84 in each calibration solution), (B) Nafion coated electrodes(n = 33), and (C) mPD coated electrodes (n = 21).

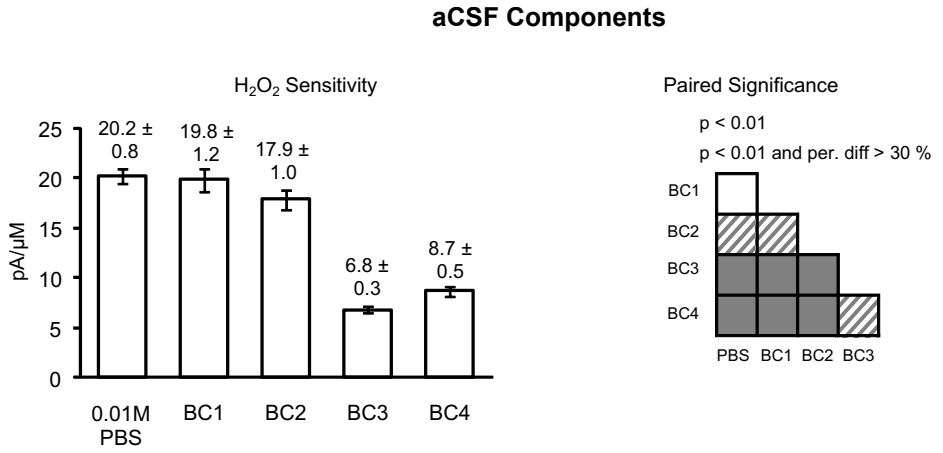

Figure 4.2: Calibration in Components of aCSF. The various buffer compositions are described in the text, but most importantly, BC3 contains Ca^{2+} and BC4 contains Mg^{2+} (n = 6).

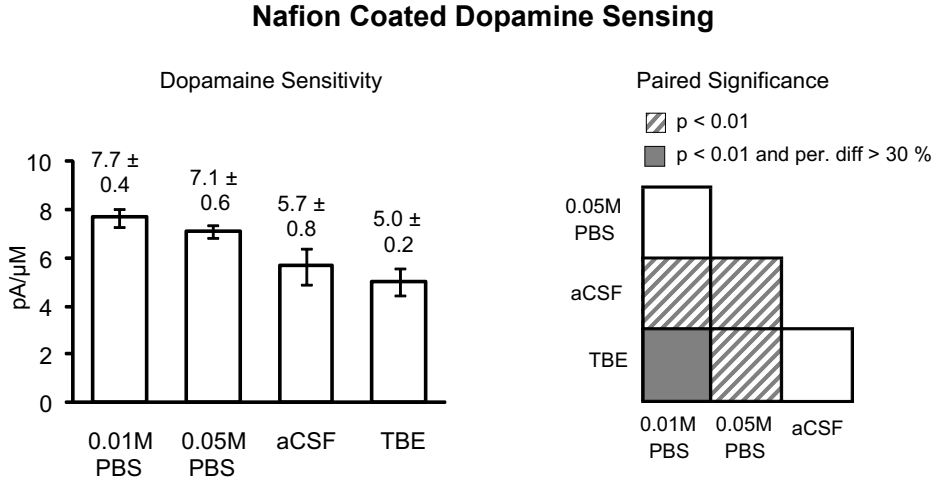

Figure 4.3: Nafion Coated Dopamine Calibrations in each of the calibration media (n = 12).

In addition to H_2O_2 calibrations, we also performed dopamine calibrations on a subset of the Nafion coated electrodes (see Figure 4.3). The dopamine sensing showed a similar response pattern as the H_2O_2 testing, thus indicating the changes in the sensitivity are primarily due to the effects at the electrode that interfere with the oxidation processes, and not due to specifically to the H_2O_2.

Fully functionalized enzyme-based biosensors generate H_2O_2 locally, and may have different diffusion characteristics. Additionally, the measured H_2O_2 has not circulated in the builk solution. In order to determine whether the oxidation processes would

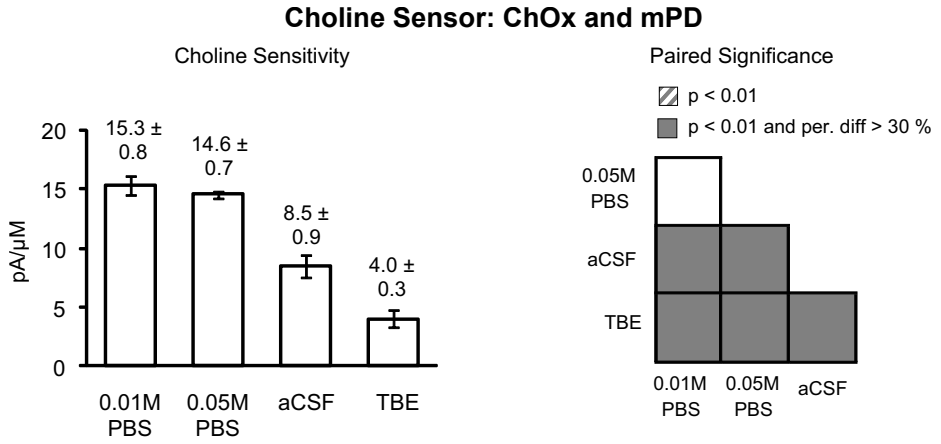

Figure 4.4: Choline sensor calibrations in each of the calibration media (n = 62)

be similarly affected with these differences, we calibrated fully functionalized (choline oxidase and mPD) choline biosensors. As seen in Figure 4.4, the responses to choline also showed significant reductions in aCSF and TBE.

By calibrating across a wide range (0-40μM) and using many concentration steps, were were able to determine the concentration of the sensor at various concentration points. We were specifically interested in the differences at the lower (0-2μM) and upper (20-40μM) ranges. Figure 4.5 shows the results for H_2O_2 at bare electrodes. Differences in the sensitivity at 0-2μM compared to 20-40μM were found in 0.01M PBS, 0.05M PBS, and aCSF. It should be noted that the sensors had very linear responses ($R^2 \geq 0.98$) for the entire range (0-40μM) as well as the upper and lower components, thus these changes in sensitivity are not entirely obvious, and are impossible to see with large concentration steps.

We conducted a similar sensitivity-concentration comparision for the fully functionalized choline sensors (Figure 4.6). In this case, differences in the sensitivity at 0-2μM compared to 20-40μM were found in 0.01M PBS, 0.05M PBS, and TBE, but not in the aCSF.

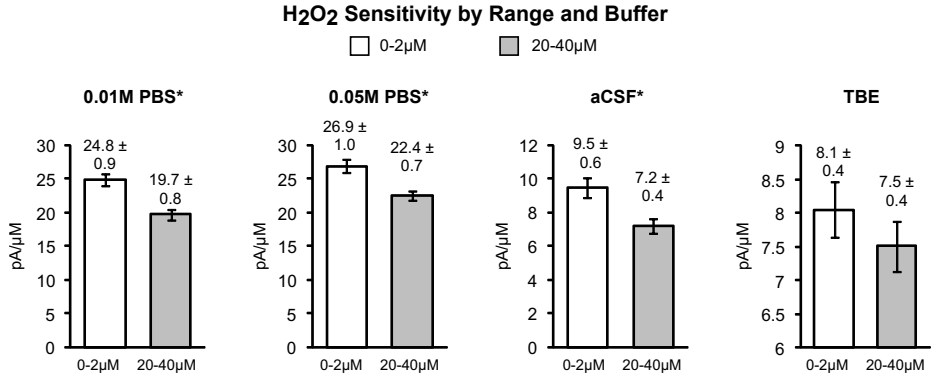

Figure 4.5: H_2O_2 Sensitivity on Bare Electrodes by Concentration and Calibration Media (n = 84)
*p < 0.01

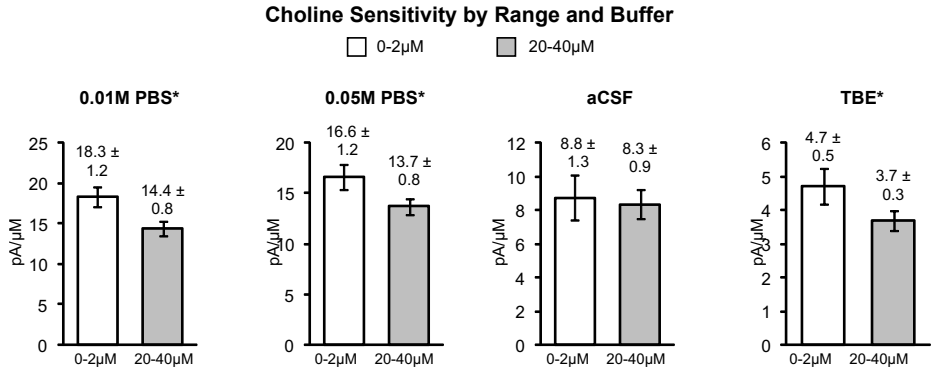

Figure 4.6: Choline Sensitivity on Bare Electrodes by Concentration and Calibration Media (n = 62)
*p < 0.01

4.4 Discussion and Conclusion

The results presented here demonstrate that various commonly used calibration media can significantly alter reported sensor performance. This effect is similarly seen on carbon microelectrodes (Kume-Kick and Rice, 1998). Specifically we determined that the presence of Mg^{2+} and Ca^{2+} reduce sensitivity compared to standard phosphate buffered saline solutions. These effects were seen on electrodes modified with functional coatings of Nafion, mPD, and choline oxidase with mPD. The finding that these cations similarly affect H_2O_2, dopamine, and choline-derived H_2O_2 oxidation processes indicates that the effect is not molecule dependent. It strongly suggests that the interaction occurs at the electrode interface, and not in the bulk solution since choline-derived H_2O_2 takes place locally at the electrode.

We additionally found sensitivity differences at different parts of the calibration range related to concentration, with slightly higher sensitivities at lower concentrations. Functionally, these differences may vary by sensor type, and may not affect the integrity of measurements in all situations; however, these data suggest that calibrations within the physiological range are more relevant to *in vivo* measurements than tests for expansive linearity ranges. For example, it is common practice to test choline sensors up to 80μM concentrations and above, even when physiological recordings show responses in the range of 1-10μM. The differences in sensitivity across a broad range may be averaged out and appear fairly linear, particularly if large concentration steps are used during calibration, which would adversely affect the accuracy of measurements.

Electrochemical sensors are commonly used to report absolute concentration levels of neurotransmitters *in vivo* (Frey et al., 2010; Parikh et al., 2004; Johnson et al., 2008; Rutherford et al., 2007; Burmeister et al., 2008). In some cases, they have been used to determine basal concentration levels (Day et al., 2006) In general, the ability to record concentration is generally considered a primary advantage of electrochemical

sensors. These data suggest that the relationship between benchtop calibrations, *in vivo* performance, and the conversion of raw data to concentration is not yet well defined. Clearly, since the neural recording environment contains both Mg^{2+} and Ca^{2+}, a model calibration media should include those molecules as well. A decrease in sensitivity when implanted would, in fact, result in underestimating the concentration levels; however, it is undetermined to what extent other molecules and proteins in the extracellular matrix may affect *in vivo* measurements. In fact, Mg^{2+} and Ca^{2+} levels can change due to tissue damage, electrical stimulation, or normal physiological responses (Jones et al., 1994; Rice et al., 1997; Kume-Kick and Rice, 1998; Torreano and Cohan, 1997; Berridge, 1998; Lee et al., 2010). Importantly, implantation of a sensor disrupts the blood brain barrier, which results in albumin diffusing into brain tissue. Albumin has been shown to directly increase Ca^{2+} levels in the brain (Nadal et al., 1995, 1998). This disruption has the effect of further obfuscating physiological recordings both within a single session if those changes are transient, and between recording sessions if those changes have significant variability. The magnitude and time course of those effects must be further verified *in vivo*, but this work serves as a foundation point for characterizing their impact on sensor performance.

Although reporting concentrations is desirable and convenient, the present data suggest that this practice may be inappropriate for various biological sensors. Alternatives to reporting concentration may include including the raw data values with *in vitro* calibration values, or calculating percent change as is commonly done with other methods, including microdialysis.

Continued analysis will be required to more closely mimic *in vivo* conditions during calibrations to accurately establish the relationship between benchtop characterization and physiological measurements.

Acknowledgements

I would like to thank Karen Schroeder and Bob Kennedy for assistance with this work.

This work was supported by a National Science Foundation Graduate Fellowship and the Center for Neural Communication Technology. The Center for Neural Communication Technology is a P41 Resource Center funded by the National Institute of Biomedical Imaging and Bioengineering (NIBIB, P41 EB002030) and supported by the National Institutes of Health (NIH).

References

Abel, P., Mller, A., and Fischer, U. (1984). Experience with an implantable glucose sensor as a prerequisite of an artificial beta cell. *Biomed Biochim Acta*, 43(5):577–584.

Aravamudhan, S., Kumar, A., Mohapatra, S., and Bhansali, S. (2007). Sensitive estimation of total cholesterol in blood using au nanowires based micro-fluidic platform. *Biosens Bioelectron*, 22(9-10):2289–2294.

Berridge, M. J. (1998). Neuronal calcium signaling. *Neuron*, 21(1):13–26.

Bowser, M. T. and Kennedy, R. T. (2001). In vivo monitoring of amine neurotransmitters using microdialysis with on-line capillary electrophoresis. *Electrophoresis*, 22(17):3668–3676.

Burmeister, J. J. and Gerhardt, G. A. (2003). Ceramic-based multisite microelectrode arrays for in vivo electrochemical recordings of glutamate and other neurochemicals. *TrAC Trends in Analytical Chemistry*, 22(8):498–502.

Burmeister, J. J., Palmer, M., and Gerhardt, G. A. (2003). Ceramic-based multisite microelectrode array for rapid choline measures in brain tissue. *Anal. Chim. Acta*, 481(1):65–74.

Burmeister, J. J., Palmer, M., and Gerhardt, G. A. (2005). L-lactate measures in brain tissue with ceramic-based multisite microelectrodes. *Biosensors & bioelectronics*, 20(9):1772–1779.

Burmeister, J. J., Pomerleau, F., Huettl, P., Gash, C. R., Werner, C. E., Bruno, J. P., and Gerhardt, G. A. (2008). Ceramic-based multisite microelectrode arrays for simultaneous measures of choline and acetylcholine in cns. *Biosensors & bioelectronics*, 23(9):1382–1389.

Burmeister, J. J., Pomerleau, F., Palmer, M., Day, B. K., Huettl, P., and Gerhardt, G. A. (2002). Improved ceramic-based multisite microelectrode for rapid measurements of -glutamate in the cns. *J Neurosci Methods*, 119(2):163–171.

Day, B. K., Pomerleau, F., Burmeister, J. J., Huettl, P., and Gerhardt, G. A. (2006). Microelectrode array studies of basal and potassium-evoked release of l-glutamate in the anesthetized rat brain. *J. Neurochem.*, 96(6):1626–1635.

Frey, O., Holtzman, T., McNamara, R. M., Theobald, D. E. H., van der Wal, P. D., de Rooij, N. F., Dalley, J. W., and Koudelka-Hep, M. (2010). Enzyme-based choline and l-glutamate biosensor electrodes on silicon microprobe arrays. *Biosensors & Bioelectronics*, 26(2):477–484.

Geise, R. J., Adams, J. M., Barone, N. J., and Yacynych, A. M. (1991). Electropolymerized films to prevent interferences and electrode fouling in biosensors. *Biosensors and Bioelectronics*, 6(2):151–160.

Gifford, R., Batchelor, M. M., Lee, Y., Gokulrangan, G., Meyerhoff, M. E., and Wilson, G. S. (2005). Mediation of in vivo glucose sensor inflammatory response via nitric oxide release. *J Biomed Mater Res A*, 75(4):755–766.

Hamdi, N., Wang, J., and Monbouquette, H. G. (2005). Polymer films as permselective coatings for h2o2-sensing electrodes. *J. Electroanal. Chem.*, 581(2):258–264.

Hamdi, N., Wang, J., Walker, E., Maidment, N. T., and Monbouquette, H. G. (2006). An electroenzymatic l-glutamate microbiosensor selective against dopamine. *J. Electroanal. Chem.*, 591(1):33–40.

Hashemi, P., Dankoski, E. C., Petrovic, J., Keithley, R. B., and Wightman, R. M. (2009). Voltammetric detection of 5-hydroxytryptamine release in the rat brain. *Anal Chem*, 81(22):9462–9471.

Heien, M. L. A. V., Khan, A. S., Ariansen, J. L., Cheer, J. F., Phillips, P. E. M., Wassum, K. M., and Wightman, R. M. (2005). Real-time measurement of dopamine fluctuations after cocaine in the brain of behaving rats. *Proc. Natl. Acad. Sci. U. S. A.*, 102(29):10023–10028.

Jena, B. K. and Raj, C. R. (2011). Enzyme integrated silicate-pt nanoparticle architecture: a versatile biosensing platform. *Biosens Bioelectron*, 26(6):2960–2966.

Johnson, M. D., Franklin, R. K., Gibson, M. D., Brown, R. B., and Kipke, D. R. (2008). Implantable microelectrode arrays for simultaneous electrophysiological and neurochemical recordings. *J Neurosci Methods*, 174(1):62–70.

Jones, S. R., Mickelson, G. E., Collins, L. B., Kawagoe, K. T., and Wightman, R. M. (1994). Interference by ph and ca2+ ions during measurements of catecholamine release in slices of rat amygdala with fast-scan cyclic voltammetry. *J Neurosci Methods*, 52(1):1–10.

Kirwan, S., Rocchitta, G., McMahon, C., Craig, J., Killoran, S., O'Brien, K., Serra, P., Lowry, J., and O'Neill, R. (2007). Modifications of poly(o-phenylenediamine) permselective layer on pt-ir for biosensor application in neurochemical monitoring. *Sensors*, 7(4):420–437.

Kume-Kick, J. and Rice, M. E. (1998). Dependence of dopamine calibration factors on media ca2+ and mg2+ at carbon-fiber microelectrodes used with fast-scan cyclic voltammetry. *J Neurosci Methods*, 84(1-2):55–62.

Lee, K., Duan, W., Sneyd, J., and Herbison, A. E. (2010). Two slow calcium-activated afterhyperpolarization currents control burst firing dynamics in gonadotropin-releasing hormone neurons. *J Neurosci*, 30(18):6214–6224.

McMahon, C. P., Rocchitta, G., Serra, P. A., Kirwan, S. M., Lowry, J. P., and O'Neill, R. D. (2006). The efficiency of immobilised glutamate oxidase decreases with surface enzyme loading: an electrostatic effect, and reversal by a polycation significantly enhances biosensor sensitivity. *Analyst*, 131(1):68–72.

Mitchell, K. M. (2004). Acetylcholine and choline amperometric enzyme sensors characterized in vitro and in vivo. *Anal. Chem.*, 76(4):1098–1106.

Moatti-Sirat, D., Capron, F., Poitout, V., Reach, G., Bindra, D. S., Zhang, Y., Wilson, G. S., and Thvenot, D. R. (1992). Towards continuous glucose monitoring: in vivo evaluation of a miniaturized glucose sensor implanted for several days in rat subcutaneous tissue. *Diabetologia*, 35(3):224–230.

Nadal, A., Fuentes, E., Pastor, J., and McNaughton, P. A. (1995). Plasma albumin is a potent trigger of calcium signals and dna synthesis in astrocytes. *Proc Natl Acad Sci U S A*, 92(5):1426–1430.

Nadal, A., Sul, J. Y., Valdeolmillos, M., and McNaughton, P. A. (1998). Albumin elicits calcium signals from astrocytes in brain slices from neonatal rat cortex. *J Physiol*, 509 (Pt 3):711–716.

Parikh, V., Pomerleau, F., Huettl, P., Gerhardt, G. A., Sarter, M., and Bruno, J. P. (2004). Rapid assessment of in vivo cholinergic transmission by amperometric detection of changes in extracellular choline levels. *Eur. J. Neurosci.*, 20(6):1545–1554.

Periasamy, A. P., Chang, Y.-J., and Chen, S.-M. (2011). Amperometric glucose sensor based on glucose oxidase immobilized on gelatin-multiwalled carbon nanotube modified glassy carbon electrode. *Bioelectrochemistry*, 80(2):114–120.

Phillips, P. E. M. and Wightman, R. M. (2003). Critical guidelines for validation of the selectivity of in-vivo chemical microsensors. *TrAC Trends in Analytical Chemistry*, 22(8):509–514.

Poitout, V., Moattisirat, D., Thome, V., Gangnerau, M., Zhang, Y., Wilson, G., and Reach, G. (1993). Evaluation in rats and man of a glucose sensor insensitive to acetaminophen. *Diabetologia*, 36:A152–A152.

Rice, M. E., Cragg, S. J., and Greenfield, S. A. (1997). Characteristics of electrically evoked somatodendritic dopamine release in substantia nigra and ventral tegmental area in vitro. *J Neurophysiol*, 77(2):853–862.

Rothwell, S. A., Kinsella, M. E., Zain, Z. M., Serra, P. A., Rocchitta, G., Lowry, J. P., and O'Neill, R. D. (2009). Contributions by a novel edge effect to the permselectivity of an electrosynthesized polymer for microbiosensor applications. *Anal. Chem.*, 81(10):3911–3918.

Rutherford, E. C., Pomerleau, F., Huettl, P., Strmberg, I., and Gerhardt, G. A. (2007). Chronic second-by-second measures of l-glutamate in the central nervous system of freely moving rats. *J. Neurochem.*, 102(3):712–722.

Ryan, M. R., Lowry, J. P., and O'Neill, R. D. (1997). Biosensor for neurotransmitter l-glutamic acid designed for efficient use of l-glutamate oxidase and effective rejection of interference. *Analyst*, 122(11):1419–1424.

Shou, M., Smith, A. D., Shackman, J. G., Peris, J., and Kennedy, R. T. (2004). In vivo monitoring of amino acids by microdialysis sampling with on-line derivatization by naphthalene-2,3-dicarboxyaldehyde and rapid micellar electrokinetic capillary chromatography. *J Neurosci Methods*, 138(1-2):189–197.

Torreano, P. J. and Cohan, C. S. (1997). Electrically induced changes in ca2+ in helisoma neurons: regional and neuron-specific differences and implications for neurite outgrowth. *J Neurobiol*, 32(2):150–162.

Trkarslan, z., Kayahan, S. K., and Toppare, L. (2009). A new amperometric cholesterol biosensor based on poly(3,4-ethylenedioxypyrrole). *Sensors and Actuators B: Chemical*, 136(2):484–488.

Updike, S. J., Shults, M. C., Gilligan, B. J., and Rhodes, R. K. (2000). A subcutaneous glucose sensor with improved longevity, dynamic range, and stability of calibration. *Diabetes Care*, 23(2):208–214.

Wassum, K., Tolosa, V., Wang, J., Walker, E., Monbouquette, H., and Maidment, N. (2008). Silicon wafer-based platinum microelectrode array biosensor for near real-time measurement of glutamate in vivo. *Sensors*, 8(8):5023–5036.

Webster, J. and Clark, J. (1998). *Medical instrumentation: application and design*. Wiley.

Wilson, G. S. and Gifford, R. (2005). Biosensors for real-time in vivo measurements. *Biosens. Bioelectron.*, 20(12):2388–2403.

Zachek, M. K., Park, J., Takmakov, P., Wightman, R. M., and McCarty, G. S. (2010a). Microfabricated fscv-compatible microelectrode array for real-time monitoring of heterogeneous dopamine release. *Analyst*, 135(7):1556–1563.

Zachek, M. K., Takmakov, P., Park, J., Wightman, R. M., and McCarty, G. S. (2010b). Simultaneous monitoring of dopamine concentration at spatially different brain locations in vivo. *Biosens Bioelectron*, 25(5):1179–1185.

CHAPTER V

Conclusion and Future Directions

The primary outcome of this work has been the development and validation of multimodal neural probes with the ability to record rapid dynamics of choline, glutamate, and electrophysiology combined with local drug delivery.

Chapter II presented the first step in this process: a multimodal probe that enables concurrent detection of choline, recording of electrophysiology, and localized drug delivery. Key to the success of this work was the development of precise, selective electrodeposition methods for enzyme immobilization and polymerization of permselective membrane on individual microelectrode sites.

The developments of Chapter III further extended these capabilities to include glutamate sensing concurrent with choline sensing, electrophysiology recordings, and drug delivery, thus establishing a multi-analyte interface. As multiple neurotransmitter systems are involved in virtually all neurological functions and disorders, the ability to simultaneously monitor multiple chemical signals concurrently with electrophysiology and integrated pharmacological manipulation can serve as a useful tool to further advances in understanding and treating these disorders.

Finally, the work presented in Chapter IV aims to improve our ability to interpret *in vivo* neurochemical recordings by investigating the influence of calibration media on performance characteristics of amperometric biosensors. We demonstrated that

differences in calibration procedures can impact reported performance making the interpretation of both *in vitro* and *in vivo* difficult. This work has provided insight to improve our ability to obtain and interpret physiological neurochemical recordings.

5.1 Suggestions for Future Directions

The multimodal neural sensors presented in this work have potential applications in a wide range of application areas. Within areas of basic science, many neurological disorders are not well understood. A multi-dimensional interface may enable novel investigations into the interactions among neural systems. For example, the glutamatergic, dopaminergic, and cholinergic systems are all implicated in the pathophysiology of schizophrenia and other disorders, yet the direct relationships remain unclear (Sarter et al., 1999; Arco and Mora, 2005). The ability to simultaneously monitor multiple chemical signals concurrent with unit activity and local field potentials can provide significant insights into neurophysiology, neuropharmacology, and neuropathology.

One important area of continued development is the validation of these, or similar, neural probes in behavioral experiments. As discussed in previous chapters, the purpose of the current experimental set was the validation of these probes. The fundamental neurophysiology will prove to be even more exciting, with potential for significant scientific and clinical impact.

One hurdle to this work is developing the ability for long-term sensing. Multimodal recording in chronic experiments for extended periods is essentially non-existent. It is unclear whether the currently developed coatings are sufficiently stable to enable long-term recordings, although other single-molecule biosensors with enzyme-glutaraldehyde-BSA coatings have been used for periods of weeks in the brain (Rutherford et al., 2007; Parikh et al., 2007). Polymer coatings, including forms of phenylenediamine, have also been used for longer-term recording (O'Neill et al., 2008). Chronic

biosensors will require high stability and low noise. Ideally, they will also have a well-established relationship between sensor performance and recorded responses, as discussed in Chapter IV.

While the current work has focused on choline and glutamate sensing, many other potential molecules are of interest for neural recordings. For example, we have recently piloted a multi-analyte sensing system with choline and dopamine. We were successful in having three independently sensitive electrode sites—choline, dopamine, and a reference—as illustrated in Figure 5.1. This sensor uses a combination of a Nafion coating, choline oxidase coating, and phenylenediamine to enable amperometric sensing of choline and dopamine. Other sensing modalities may continue to increase the power of technology presented here.

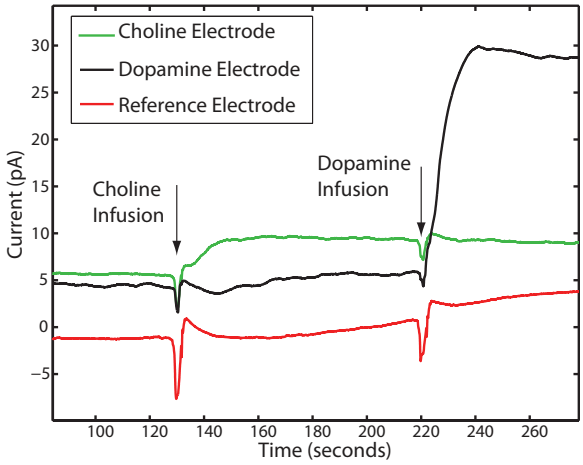

Figure 5.1: Preliminary testing of Choline-Dopamine probe. Site 1 (green) was modified for selective sensitivity to choline, site 2 (black) for dopamine, and site 3 (red) for chemical referencing and noise reduction. The arrows indicate infusions of choline and dopamine.

Multimodal neural biosensors also have potential clinical relevance. For example, the devices presented in this work were intentially designed to record across multiple brain regions. This ability may prove useful in providing improved verification of electrode placement during deep brain stimulation procedures for the treatment of Parkinson's disease, essential tremor, and depression.

5.2 Concluding Remarks

Neural technologies are an exciting and important area of development. Advancements in our ability to interface with the brain offer new hope as they bring us closer to treatments for neurological disorders. We, as individuals and a society, are directly impacted by these debilitating diseases. In many ways, diseases of the brain represent the most frightening and difficult diseases to face. It is my hope that this work may contribute, even in some small way, to our ability to understand, manage, and more effectively treat these disorders.

References

Arco, A. D. and Mora, F. (2005). Glutamate-dopamine in vivo interaction in the prefrontal cortex modulates the release of dopamine and acetylcholine in the nucleus accumbens of the awake rat. *J Neural Transm*, 112(1):97–109.

O'Neill, R. D., Rocchitta, G., McMahon, C. P., Serra, P. A., and Lowry, J. P. (2008). Designing sensitive and selective polymer/enzyme composite biosensors for brain monitoring in vivo. *TrAC Trends in Analytical Chemistry*, 27(1):78–88.

Parikh, H., Marzullo, T. C., Yazdan-Shahmorad, A., Gage, G. J., and Kipke, D. (2007). Laminar characterization of spiking activity in the rat motor cortex. *Conf Proc IEEE Eng Med Biol Soc*, 2007:4735–4738.

Rutherford, E. C., Pomerleau, F., Huettl, P., Strmberg, I., and Gerhardt, G. A. (2007). Chronic second-by-second measures of l-glutamate in the central nervous system of freely moving rats. *J. Neurochem.*, 102(3):712–722.

Sarter, M., Bruno, J. P., and Turchi, J. (1999). Basal forebrain afferent projections modulating cortical acetylcholine, attention, and implications for neuropsychiatric disorders. *Ann N Y Acad Sci*, 877:368–382.

APPENDIX

APPENDIX A

Early Development

There is a story commonly told that when Thomas Edison was asked about his failed attempts to develop the light bulb, he replied, "I haven't failed 1000 times. I found 1000 ways not to invent the light bulb." Difficult engineering problems frequently require many iterations. The purpose of this appendix is simply to highlight some of the precursor work in the development process for the neural probes described in the main body.

A.1 Droplet Methods

Much of the early development work attempted to deposit droplets of the enzyme solution onto electrodes. The typical enzyme immobilization recipe was similar to that found in the literature, consisting of 1% choline oxidase, 1% BSA, and 0.125% glutaraldehyde in water (Burmeister et al., 2003; Mitchell, 2004). Sometimes ascorbate oxidase was used in the mixture. Ascorbate oxidase should reduce the potential interference of ascorbic acid, but phenylenediamine has proven to be sufficient as a permselective membrane to block ascorbic acid. The typical device used was a non-implantable silicon "test structure" with electrode sizes similar to future electrode sizes. This allowed us to show proof of concept. Figure A.1 shows a test structure and the enzyme droplet over a set of sites.

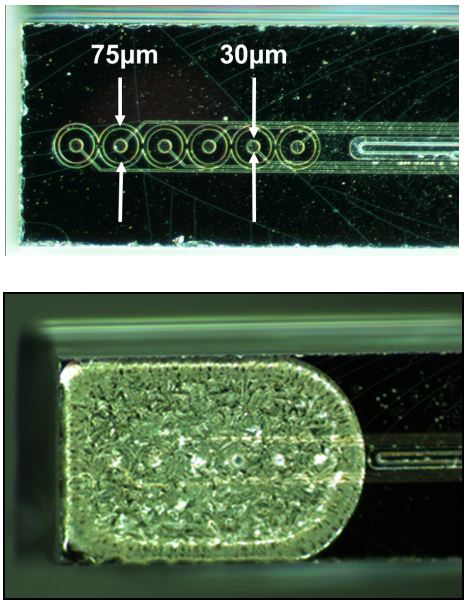

Figure A.1: Test Structure and Droplet Immobilization. The top figure shows a typical test structure design used for early prototyping. The outer circle is a raised SU-8 edge to create a well around the electrode site. The bottom figure shows a cured droplet of the immobilized choline oxidase solution

Using the droplet method, we were able to show that the coatings worked to create functional sensors. The primary limitation of the droplet method is the size of the droplet. It proved difficult to impossible to selectively coat individual sites or even groups of sites. One attempt to overcome this was to use a micropipette with a pressure injection system. In general, the droplets were still too large to coat just one site or a few sites. The tip of the pipette clogged very readily due to the nature of the enzyme-BSA-glutaraldehyde solution. Attempts at forming the droplets with the probes immersed in oil to assist in droplet formation and placement were also met with limited success.

One set of test devices had wells, designed with the intention of containing the enzyme solution to one electrode (Figure A.1). While occasionally this was successful, the results were inconsistent and clogging occurred frequently, thus overall this strategy did not work well. Figure A.2 shows one successful attempt of containing a fluorescent test solution.

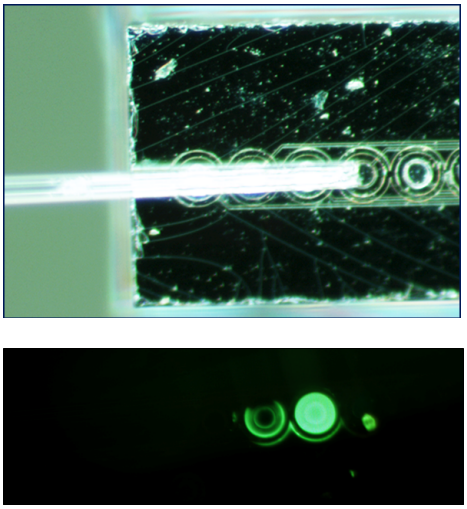

Figure A.2: Use of Wells for Enzyme Immobilization. The top figure shows the micropipette at the electrode site injecting a fluorescent test solution. The bottom figure shows the solution in the well

While coating individual sites with droplets did not seem to be particularly feasible or reproducible, it was possible to coat one or two sites near the tip separate from the rest of the electrodes on the tip. This was done by forming a droplet and using a micromanipulator to slowly immerse only the tip into the solution. After that step was complete, a second droplet was placed on the electrode much more distally so that it did not mix with the other coating. One coating was a choline oxidase immobilization layer, while the other coating was the reference layer (Figure A.3). This method was tedious and suffered from very low yield. It was successful enough to coat several probes and pilot *in vivo* experiments.

The pilot *in vivo* experiments were conducted by implanting the neural biosensor probe in the prefrontal cortex and implanting a stimulation electrode in the substantia innominata. Stimulation resulted in choline release and LFP responses as seen in Figure A.4 and Figure A.5.

These early attempts were encouraging in terms of the feasibility of microelectrode biosensors with adequate performance specifications, but it became clear that a different technique would necessary to make the processes robust and achieve the

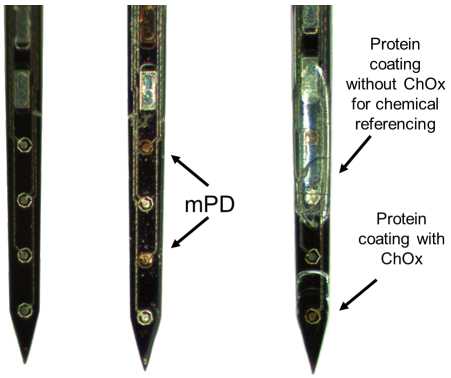

Figure A.3: Multiple Droplet Coatings. On the left is an uncoated probe. In the center is a probe coated with mPD. On the right is a probe differentially coated with a choline oxidase solution and a reference solution

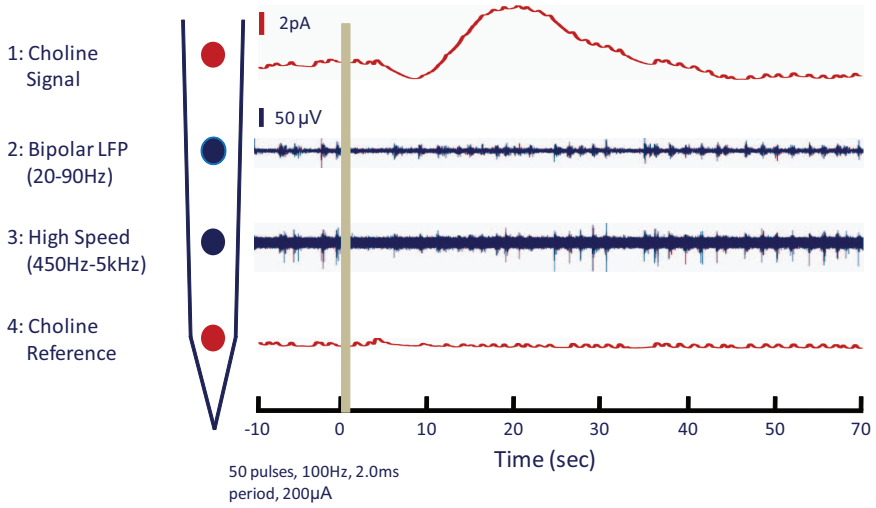

Figure A.4: Choline-Electrophysiology Recordings During Stimulation. Probes were implanted in prefrontal-prelimbic cortex. A stimulation probe was implanted into substantia innominata. Site 1 was used to record cholinergic activity and Site 4 served as a choline reference. Sites 2 and 3 record electrophysiological activity. Shown here are the local field potentials (20-90Hz) and unit activity (450Hz-5KHz). Stimulation (50 biphasic pulses, 100Hz, 2.0ms period, 200A) occurred at time 0. The signal from site 4 was subtracted from the signal from site 1 to identify the choline-specific activity.

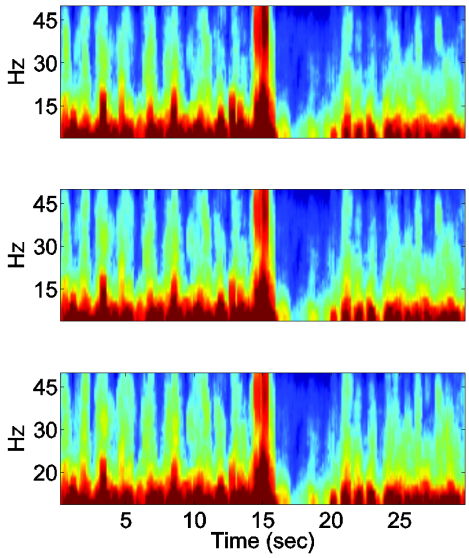

Figure A.5: LFP Response to Stimulation. Local field potentials were recorded in prefrontal-prelimbic cortex before, during, and after stimulation of substantia innominata (50 pluses, 100Hz, 1 ms/phase, 200μA). Stimulation at t = 15 sec. Changes occurred in Theta (4-7Hz), Alpha (8-12Hz), Beta (12-30Hz) bands immediately after stimulation.

objective of developing multi-analyte interfaces described in the main text. After exploring these techniques, searching the literature, and considering the nature of our electrodes, enzyme, and functional coatings, my focus turned to the development of electrodeposition techniques.

A.2 Electrodeposition

Two papers in particular served as the starting point for the electrodeposition techniques: Johnson, 1991; Strike et al., 1995. In the early stages of the development of electrodeposition techniques, we also used the test structures to show proof of concept; however, we found that it was best to pursue development on the same devices we would use. The transition from one style of device to another could affect the immobilization procedure. In that process we were able to show successful sensor function on several types of devices. Usha Ramkrishna was particularly helpful in the first parts of this process.

One of the first steps was testing current pulses of various magnitude and duration (Figure A.6). We also looked at different concentrations of the solution, including some that did not include BSA and were not sensitive, even though a coating was visible. BSA appears to provide spacing for optimal enzyme function (Figure A.7).

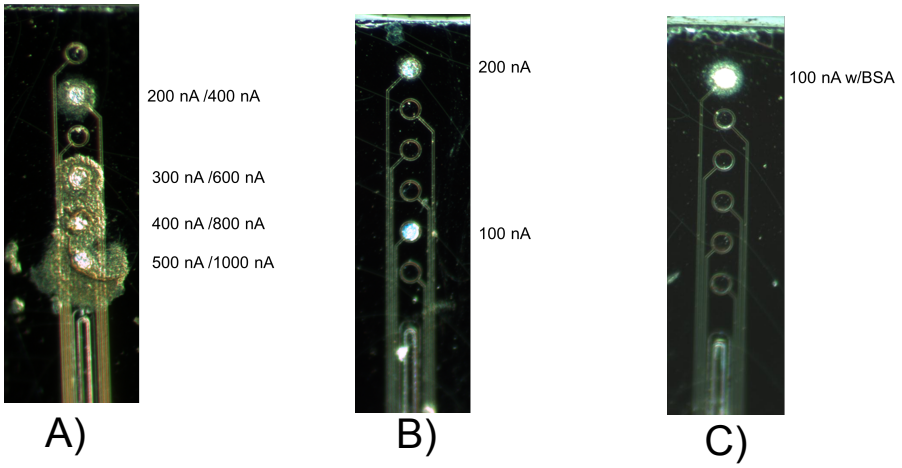

Figure A.6: Electrodeposition on Test Structures. (A)Probes were placed in a solution of ChOx (0.34% w/v) and glutaraldehyde (1% v/v). A pulse train of 1 second pulses followed by 5 seconds open was applied for 7 minutes followed by a second higher current pulse train of 1 second pulses followed by 5 seconds open was applied for 14 minutes. Current amplitude significantly affected spatial deposition. (B) Probes were placed in a solution of ChOx (0.34% w/v) and glutaraldehyde (1% v/v). A pulse train of 1 second pulses followed by 5 seconds open was applied for 30 minutes. Lower currents over longer times produce even, localized deposition at electrode sites. (C) Probes were placed in a solution of ChOx (0.5% w/v), BSA (0.5% w/v) and glutaraldehyde (0.5% v/v). A pulse train of 1 second pulses of 100nA followed by 5 seconds open was applied for 25 minutes. BSA increased deposition and choline sensitivity.

At one point we began work on using the electrochemically aided immobilization technique on the ceramic substrate probes and showed good progress. For example, using a solution of 0.5% w/v Choline Oxidase, 1% w/v BSA, and 1% v/v Glutaraldehyde and a pulse train of 30 pulses of 175 nA for 5 seconds per pulse and 5 second resting phase, we selectively coated a site 15μm by 333μm (area = 4995μm^2) to have choline sensitivity of 12-14pA/μM choline before phenylenediamine deposition (Figure A.8). Sometimes neighboring sites showed some choline sensitivity, perhaps due

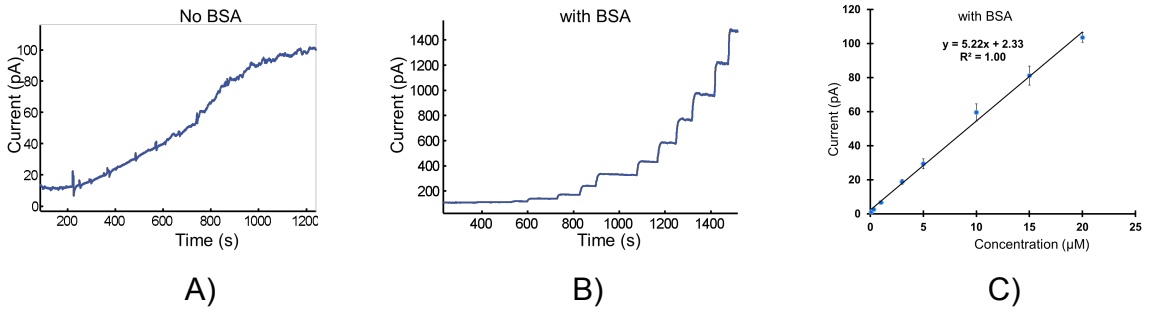

Figure A.7: Calibration of Electrodeposited Test Structures. Biosensor probes were calibrated at increasing chemical concentrations of choline. (A) Calibration of the probe shown in Figure A.6B. When the enzyme deposition solution did not include BSA, the sensors performed poorly. (B) Calibration of the probe shown in Figure A.6C. When BSA was included in the enzyme deposition solution, the sensors performed very well. The BSA is thought to provide spacing for optimal enzyme function. (C) Sensitivity plot of the probe in (B).

to diffusion or a coating that extended beyond the site to some degree.

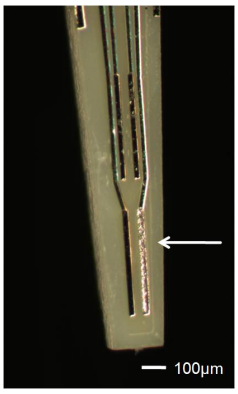

Figure A.8: Electrodeposition on a Ceramic Substrate Probe. The coating is confined to a single site and showed good sensitivity. Site size is 15μm by 333μm.

The electrodeposition techniques proved to be very robust and repeatable with high sensitivity on a variety of electrode designs. We were able to design probes for the work in the main text and successfully functionalize multimodal neural biosensor probes.

References

Burmeister, J. J., Palmer, M., and Gerhardt, G. A. (2003). Ceramic-based multisite microelectrode array for rapid choline measures in brain tissue. *Anal. Chim. Acta*, 481(1):65–74.

Johnson, K. W. (1991). Reproducible electrodeposition of biomolecules for the fabrication of miniature electroenzymatic biosensors. *Sensors and Actuators B: Chemical*, 5(1-4):85–89.

Mitchell, K. M. (2004). Acetylcholine and choline amperometric enzyme sensors characterized in vitro and in vivo. *Anal. Chem.*, 76(4):1098–1106.

Strike, D. J., de Rooij, N. F., and Koudelka-Hep, M. (1995). Electrochemical techniques for the modification of microelectrodes. *Biosens. Bioelectron.*, 10(1-2):61–66.